ruhr.paD
UA Ruhr Zentrum für
partielle Differentialgleichungen

Effective description of anisotropic wave dispersion in mechanical band-gap metamaterials via the relaxed micromorphic model

M.V. d'Agostino, G. Barbagallo, I.D. Ghiba, B. Eidel, P. Neff and A. Madeo

Preprint 2018-14

Effective description of anisotropic wave dispersion in mechanical band-gap metamaterials via the relaxed micromorphic model

Marco Valerio d'Agostino[1], Gabriele Barbagallo[2], Ionel-Dumitrel Ghiba[3], Bernhard Eidel[4], Patrizio Neff[5] and Angela Madeo[6]

January 19, 2018

Abstract

In this paper the relaxed micromorphic material model for anisotropic elasticity is used to describe the dynamical behavior of a band-gap metamaterial with tetragonal symmetry. Unlike other continuum models (Cauchy, Cosserat, second gradient, classical Mindlin-Eringen micromorphic etc.), the relaxed micromorphic model is endowed to capture all the main microscopic and macroscopic characteristics of the targeted metamaterial, namely, stiffness, anisotropy, dispersion and band-gaps.

The simple structure of our material model, which simultaneously lives on a micro-, a meso- and a macroscopic scale, requires only the identification of a limited number of frequency-independent and thus truly constitutive parameters, valid for both static and wave-propagation analyses in the plane. The static macro- and micro-parameters are identified by numerical homogenization in static tests on the unit-cell level. The 3 macro-parameters are obtained by imposing periodic boundary conditions thus mimicking the structure at large. The 3 micro-parameters can be uniquely identified from unit-cells, which (i) represent the unit-cells with maximal stiffness and (ii) preserve its tetragonal symmetry. Both conditions (i) and (ii) are built on the inherent rationale of the relaxed micromorphic model. The missing mesoscopic elastic parameters directly follow from a recently developed harmonic-mean type micro-macro homogenization rule, which establishes the general relation between the elasticities in the micromorphic model on its three scales. The remaining inertia parameters for dynamical analyses are calibrated on the dispersion curves of the same metamaterial as obtained by a classical Bloch-Floquet analysis for two wave directions.

We demonstrate via polar plots that the obtained material parameters describe very well the response of the structural material for all wave directions in the plane, thus covering the complete panorama of anisotropy of the targeted metamaterial. Our findings suggest that a deeper understanding of micromorphic continuum models for anisotropic elasticity can pave the way towards future developments such as the conception of morphologically complex (meta-) structures by finite element analyses.

Keywords: anisotropy, dispersion, planar harmonic waves, relaxed micromorphic model, enriched continua, dynamic problems, micro-elasticity, size effects, wave propagation, band-gaps, parameter identification, periodic homogenization, effective properties, unit-cell, micro-macro transition, Löwner matrix supremum.

AMS 2010 subject classification: 74A10 (stress), 74A30 (nonsimple materials), 74A35 (polar materials), 74A60 (micromechanical theories), 74B05 (classical linear elasticity), 74M25 (micromechanics), 74Q15 (effective constitutive equations), 74J05 (linear waves).

[1]Marco Valerio d'Agostino, corresponding author, marco-valerio.dagostino@insa-lyon.fr, SMS-ID, INSA-Lyon, Université de Lyon, 20 avenue Albert Einstein, 69621, Villeurbanne cedex, France

[2]Gabriele Barbagallo, gabriele.barbagallo@insa-lyon.fr, LaMCoS-CNRS & SMS-ID, INSA-Lyon, Universitité de Lyon, 20 avenue Albert Einstein, 69621, Villeurbanne cedex, France

[3]Ionel-Dumitrel Ghiba, dumitrel.ghiba@uaic.ro, Alexandru Ioan Cuza University of Iaşi, Department of Mathematics, Blvd. Carol I, no. 11, 700506 Iaşi, Romania; and Octav Mayer Institute of Mathematics of the Romanian Academy, Iaşi Branch, 700505 Iaşi.

[4]Bernhard Eidel, bernhard.eidel@uni-siegen.de, Universität Siegen, Institut für Mechanik, Heisenberg-group, Paul-Bonatz-Straße 9-11 57076 Siegen, Germany

[5]Patrizio Neff, patrizio.neff@uni-due.de, Head of Chair for Nonlinear Analysis and Modelling, Fakultät für Mathematik, Universität Duisburg-Essen, Mathematik-Carrée, Thea-Leymann-Straße 9, 45127 Essen, Germany

[6]Angela Madeo, angela.madeo@insa-lyon.fr, SMS-ID, INSA-Lyon, Université de Lyon, 20 avenue Albert Einstein, 69621, Villeurbanne cedex, France

Contents

1 Introduction

1.1 Describing metamaterials as generalized continua

Engineering metamaterials showing exotic behaviors with respect to both mechanical and electromagnetic wave propagation are recently attracting growing attention for their numerous possible astonishing applications [4,24,37, 66]. Actually, materials which are able to "stop" or "bend" the propagation of waves of light or sound with no energetic cost could suddenly disclose rapid and unimaginable technological advancements. Metamaterials exhibiting such unorthodox behaviors are obtained by suitably assembling different microstructural components in such a way that the resulting macroscopic material possesses completely new properties with respect to the original one.

By their intrinsic nature, metamaterials show strong heterogeneities at the level of the microstructure and, except for few particular cases, their mechanical behavior is definitely anisotropic. Depending on their degree of anisotropy, band-gap metamaterials can exhibit one or both of the following behaviors:

- anisotropic behavior with respect to deformation (the deformation patterns vary when varying the direction of application of the externally applied loads),
- anisotropic behavior with respect to band-gap properties (the width of the band-gap varies when varying the direction of propagation of the travelling wave).

Thus, the description of anisotropy in metamaterials is a challenging issue, given that extra innovative applications could be conceived. In fact, a metamaterial in which different modes propagate with different speeds when changing the direction of propagation could be fruitfully employed as wave-guides or wave filters.

The need of a homogenized model which is able to account for anisotropy in band-gap metamaterials at large scale is of great concern for the engineering scientific community. Indeed, the ultimate task of an engineer is that of dealing with models which are able to describe the overall macroscopic behavior of (meta-)materials in the most simplified possible way in order to proceed towards the conception of morphologically complex engineering (meta-)structures.

As Green abandoned any attempt to relate the elastic behavior of materials to their molecular arrangements, we abandon any effort to connect "a priori" the elastic behavior of metamaterials to the arrangement of their constituting elements (cf. our discussion in the Appendix11.5). Nevertheless, when the best macroscopic model for the description of the mechanical behavior of metamaterials will be selected it will be easy to connect "a posteriori" some of its elastic parameters to the specific properties of the unit-cell. Hence our primary goal is that of establishing which continuum model has to be used to describe the mechanical behavior of (isotropic and anisotropic) metamaterials at the macroscopic scale.

To this aim, we want to start from the easiest possible "experimental" evidence and then try to build macroscopic strain and kinetic energy densities which are able to account for the phenomena we are interested in.

Our macroscopic primary observation is the typical behavior of the dispersion curves in a metamaterial (see e.g. Fig. 2). Since the considered metamaterial is not isotropic, such dispersion curves vary when changing the direction of propagation of the travelling wave (Fig. 2(a) and (b)).

We start from the observation that the typical dispersion curves of a given metamaterial show different branches that can be classified roughly as follows:

1. acoustic branches (starting from the origin) which, very close to the origin, are well approximated by straight lines that coincide with the straight lines obtained by classical linear elasticity. Such branches, at least for small wavenumbers (large wavelengths) are related to the macroscopic modes of vibration of the unit-cell,
2. optic branches (starting from cut-off values of the frequency) which are related to the modes of vibration of the microstructure inside the unit-cell.

We then proceed trying to find the simplest possible continuum model which allows us to account for the behavior of all such dispersion curves. It is clear that classical elasticity is too restrictive to accomplish this task. Indeed, in the fully anisotropic case, classical elasticity features at most 3 different acoustic dispersion curves which are straight lines the slopes of which gives the speed of propagation of compression and shear waves inside the material. In other words, in classical elastic solids waves propagate with the same speed for any wavelength: a classical elastic solid is said to be "non-dispersive".

To proceed in the right direction and find a good candidate for the "best" continuum model for metamaterials, we need to introduce in the model two fundamental things:

1. the ability of describing dispersive behaviors (the acoustic curves are not straight lines but curves),
2. the ability of introducing extra "optic" curves related to the vibration of the microstructure (often these curves show dispersive behaviors).

As we anticipated, none of these two features can be obtained by classical elasticity, but the answer must be found in the realm of so-called "enriched" continuum models. Nevertheless, the choice of the "best" enriched continuum model is not a trivial task, considering that a huge variety of such models is present in the literature.

A way to approach point 1. (i.e. introducing dispersive behavior for acoustic modes in the picture) could be that of using so-called higher-gradient theories. Indeed, it is known that considering a strain energy density which depends not only on $\varepsilon = \operatorname{sym} \nabla u$, but also on its gradient $\nabla \varepsilon$ allows for obtaining governing equations of higher order than those of classical elasticity. This, in terms of dispersion curves, means that the acoustic lines are not straight, but can show some dispersion (see e.g. [20, 60, 62]).

Moreover, generalizing the constitutive form of the strain energy density to account for anisotropic behaviors not only on the first gradient, but also on the second gradient terms, qualitative anisotropic patterns for the wave speeds associated to the acoustic compression and shear waves can be obtained (see [61]).

Approaching the modeling of metamaterials through second (or higher) order theories has, at least, two limitations, namely:

- no optic branches can be described, but only some dispersion in the acoustic curves,
- the treatment of anisotropy in the framework of higher gradient continua quickly becomes uselessly complicated. Indeed, the need of introducing non-classical elastic tensors (of the sixth order against the fourth order of classical elasticity) arises and the study of the class of symmetries of such tensors introduces non-trivial technical difficulties. On the other hand, the introduced complexity is not justified by a true advantage in terms of enhanced description of the physical phenomena concerning metamaterials: the only improvements with respect to classical elasticity are the description of the dispersion for acoustic curves and the description of anisotropy only for the first two (acoustic) modes.

We will show in the remainder of this paper that both such informations, as well as many extra features such as the description of optic modes, anisotropy (also at higher frequencies) and band-gaps, can be obtained in a much more simple fashion which does not need to invoke any new theoretical framework with respect to the classical treatment of classes of symmetries for classical elasticity.

1.2 Isotropic modelling of metamaterials via relaxed micromorphic model

Having shown that second gradient models are not the right way to answer to the need of an optimal enriched continuum material model for metamaterials, the attention has to be shifted on so-called micromorphic models. Micromorphic models feature an enriched kinematics with respect to classical elasticity in the sense that extra degrees of freedom are added to the continuum. The enriched kinematics thus consists of the macroscopic displacement vector u plus a second order tensor (generally not symmetric) P which is known as micro-distortion tensor. The simple fact of enriching the kinematics allows for the possibility of describing extra (optic) dispersion curves, and thus for including the effect of microstructure on the dynamical behavior of heterogeneous materials (see, e.g., [15, 16]). The properties and the shape of such curves then depend on the constitutive choice that one makes for the strain energy and kinetic energy densities. The true difficulty is thus that of making a "smart" selection of such constitutive choices so that:

- the expressions of both the strain energy and the kinetic energy densities are the easiest possible, avoiding any unuseful complexification,
- such expressions still allow to describe the macroscopic phenomena we are interested in (dispersion and anisotropy for acoustic and optic modes, band-gaps,...).

We have already addressed the problem of selecting the possible model for description of metamaterials' elasticity for the isotropic case (see [19,39,42,44,45]). The answer we found is that this optimal choice is given by the so-called **relaxed micromorphic model** whose kinetic and strain energy densities respectively take the form

$$\begin{aligned} J\left(u_{,t}, P_{,t}\right) = & \frac{1}{2}\rho\left\|u_{,t}\right\|^2 + \frac{1}{2}\left(\eta_1\left\|\operatorname{dev}\operatorname{sym}P_{,t}\right\|^2 + \eta_2\left\|\operatorname{skew}P_{,t}\right\|^2 + \frac{1}{3}\eta_3\left(\operatorname{tr}P_{,t}\right)^2\right) \\ & + \frac{1}{2}\left(\overline{\eta}_1\left\|\operatorname{dev}\operatorname{sym}\nabla u_{,t}\right\|^2 + \overline{\eta}_2\left\|\operatorname{skew}\nabla u_{,t}\right\|^2 + \frac{1}{3}\overline{\eta}_3\left(\operatorname{tr}\nabla u_{,t}\right)^2\right), \end{aligned} \tag{1}$$

$$\begin{aligned} W\left(\nabla u, P, \operatorname{Curl}P\right) = & \mu_e\left\|\operatorname{sym}\left(\nabla u - P\right)\right\|^2 + \frac{\lambda_e}{2}\left(\operatorname{tr}\left(\nabla u - P\right)\right)^2 + \mu_{\text{micro}}\left\|\operatorname{sym}P\right\|^2 + \frac{\lambda_{\text{micro}}}{2}\left(\operatorname{tr}P\right)^2 \\ & + \mu_c\left\|\operatorname{skew}\left(\nabla u - P\right)\right\|^2 + \frac{L_c^2}{2}\left(\alpha_1\left\|\operatorname{dev}\operatorname{sym}\operatorname{Curl}P\right\|^2 + \alpha_2\left\|\operatorname{skew}\operatorname{Curl}P\right\|^2 + \frac{1}{3}\alpha_3\left(\operatorname{tr}\operatorname{Curl}P\right)^2\right). \end{aligned} \tag{2}$$

The characteristic length scale of the model is denoted by $L_c \geq 0$. We showed that this model has the following advantages:

- it produces the smallest possible number of elastic parameters in the strain energy density with respect to classical isotropic elasticity,

- all the introduced homogenized parameters are true material constants (exactly as the averaged Young's modulus and Poisson's ratio) since they do not depend on frequency, as it is instead the case for classical dynamic homogenization results (see e.g. [3, 54, 55]),

- the splitting of the displacement gradient ∇u and the micro-distortion P in their sym and skew part allows from one side, to naturally extend classical elasticity and, from the other side, to isolate macro and micro deformation modes related to distortions and rotations, respectively,

- it allows the description of dispersion (wave speed varying with the considered wavelength) not only for the acoustic modes, but also for the optic modes at higher frequencies,

- it allows, when desired, the description of non-localities in metamaterials thanks to the term $\operatorname{Curl} P$ which includes combinations of space derivatives of the micro-distortion P. In this respect, we have to remember that such a constitutive choice is much less restrictive compared to classical Mindlin-Eringen micromorphic models featuring the whole gradient ∇P of P in the strain energy density [23,48]. We indeed showed (see [39–45,52,53]) that the non-localities introduced by ∇P are so strong that sometimes they preclude the micromorphic model from describing essential features such as band-gaps. We found the relaxed micromorphic model to be the best compromise between the description of non-localities and the possibility of allowing realistic band-gap behaviors,

- when treating the limiting case $L_c \to 0$, the considered relaxed micromorphic continuum tends to a classical Cauchy continuum with stiffness λ_{macro} and μ_{macro}. Such macro stiffness can be experimentally determined by using standard mechanical tests on specimens which are large enough that the influence of the underlying microstructure can be neglected. As a replacement of the true experimental tests on sufficiently large specimens, finite element methods can be used (at least for periodic media) which feature the introduction of so-called periodic boundary conditions applied on the unit-cell[1]. This is indeed the method that we will use in order to derive the macroscopic coefficients of the metamaterial considered in this paper. In the framework of the isotropic relaxed micromorphic model, the macroscopic coefficients of the equivalent continuum are related to the parameters of the relaxed micromorphic model through the homogenization formulas (see [8, 49, 50])

$$\mu_{\text{macro}} = \frac{\mu_e\, \mu_{\text{micro}}}{\mu_e + \mu_{\text{micro}}}, \qquad 2\mu_{\text{macro}} + 3\lambda_{\text{macro}} = \frac{(2\mu_e + 3\lambda_e)\,(2\mu_{\text{micro}} + 3\lambda_{\text{micro}})}{2\,(\mu_e + \mu_{\text{micro}}) + 3\,(\lambda_e + \lambda_{\text{micro}})}. \tag{3}$$

  These formulas are strongly reminiscent of putting two springs with stiffness μ_e and μ_{micro} in series, resulting in the combined stiffness $(3)_1$. Such formulas, as we will show in this paper for the anisotropic case, are essential to characterize the mechanical behavior of heterogeneous metamaterials. In classical micromorphic media of Mindlin-Eringen type, formulas which are analogous to (3) can also be found ([8, Section 7]), but they do not have the simple and transparent expression peculiar to the relaxed micromorphic model,

- in the limiting case $L_c \to \infty$ (zoom on the microstructure) the isotropic relaxed micromorphic model reduces to an equivalent continuum of the Cauchy type with elastic stiffnesses μ_{micro} and λ_{micro} (see [8]). Such micro stiffnesses can be interpreted as the stiffnesses of the unit-cell which could be determined by performing classical mechanical tests on a specimen which is made up of a single unit-cell. It is clear that such stiffnesses, as issued by the described mechanical tests, would have a finite value, albeit larger than the macroscopic stiffnesses associated to a large specimen ("smaller is stiffer"). Unlike the relaxed micromorphic model, classical micromorphic models of the Mindlin-Eringen type do not provide bounded stiffness when considering inhomogeneous deformations and letting $L_c \to \infty$, which is equivalent to saying that the mechanical properties of the unit-cell are grossly overestimated by such models. The relaxed micromorphic model is the only possible model of the micromorphic type which allows for modeling a finite stiffness on the unit-cell level. In this paper, we propose to replace the true experiments on the unit-cell by finite element simulations on the unit-cell with Dirichlet boundary conditions (assigning a displacement on the boundary of the unit-cell is in fact what we would do performing the experimental tests). It is indeed known (see [33, 58]) that finite element simulations

[1] It is indeed well known in the field of homogenization techniques (see e.g. [22, 58]) that the homogenization of a unit-cell on which one imposes periodic boundary conditions mimics the behavior of a very large specimen of the associated equivalent Cauchy continuum. Usually, homogenization techniques only provide a direct transition from the micro to the macro scale without considering the intermediate (transition) scale in which all relevant microstructure-related phenomena are manifest. Some attempts to introduce a transition scale via the homogenization towards a micromorphic continuum are made in [36, 69], even if it is clear that a definitive answer is far from being provided (see [36, 69] and references cited there). Our relaxed micromorphic model naturally provides the bridge between the micro and macro behavior of the considered homogenized material with the simple and transparent homogenization formulas (3).

on the unit-cell with Dirichlet boundary conditions give a stiffer response than equivalent simulations with periodic boundary conditions. Once the micro stiffnesses are known according to the aforementioned procedure and once the macro stiffnesses of the equivalent continuum are measured via the methods described previously, the static behavior of the considered metamaterial results to be almost uniquely determined. In fact the coefficients μ_e and λ_e can be derived using the homogenization formulas

$$\mu_e = \frac{\mu_{\text{macro}}\,\mu_{\text{micro}}}{\mu_{\text{micro}} - \mu_{\text{macro}}}, \qquad 2\mu_e + 3\lambda_e = \frac{(2\mu_{\text{macro}} + 3\lambda_{\text{macro}})\,(2\mu_{\text{micro}} + 3\lambda_{\text{micro}})}{(2\mu_{\text{micro}} + 3\lambda_{\text{micro}}) - (2\mu_{\text{macro}} + 3\lambda_{\text{macro}})}. \tag{4}$$

The only elastic parameter which is not yet determined by the presented arguments is the Cosserat couple modulus μ_c, but it can be evaluated when considering the dynamical analysis of the proposed metamaterial.

1.3 Anisotropic modelling approach in this work

At this point, the remaining fundamental question is "how to select the optimal model for the description of anisotropy in metamaterials"?

We started answering this question in [8] where the generalization of the relaxed micromorphic model to the anisotropic case was presented. One of the main advantages of this model, as we will see in the remainder of this paper, is that of describing the anisotropy related to the microstructure. To this aim, no cumbersome treatment related to the classes of symmetries of higher order tensors is needed since, in our model, everything can be recast in the classical study of the classes of symmetry of the classical fourth order elasticity tensor.

We end up with the simplest possible continuum model which is able to describe simultaneously:

- macro and micro anisotropies in metamaterials,
- dispersion and band-gaps,
- non-local effects.

We prove the efficacy of this relatively simplified model by superimposing the dispersion curves of our model with the "phenomenological evidence" which in this paper we suppose to be the dispersion curves of a given anisotropic (tetragonal) metamaterial obtained by so-called Bloch-Floquet analysis [10, 25].

We will also show that our model is able to recover the behavior of the phase velocity as a function of the direction of propagation of the travelling wave not only for the first two acoustic modes, but also for the optic modes.

We find an excellent agreement with the phenomenological evidence, often not only for large wavelengths, but also for wavelengths which become relatively close to the size of the unit-cell.

In the present paper, while developing a relaxed micromorphic theoretical framework which is capable to generally treat full anisotropy in metamaterials (also based on the results obtained in [8]), we will present a first application to an actual metamaterial with a low degree of anisotropy. More specifically, we select a metamaterial with a particular microstructure for which the band-gap is almost isotropic (not varying with the direction of propagation of the traveling wave), but which has an anisotropic (tetragonal) elastic behavior. As a second step, we use the anisotropic relaxed micromorphic model to reproduce both the patterns of the dispersion curves and of the phase velocity as function of the angle giving the direction of propagation of the travelling wave.

We compare the obtained results with the analogous ones issued by a classical Bloch wave analysis of the same metamaterial, showing that the relaxed micromorphic model is able to catch the main features of the mechanical behavior of such metamaterial, namely:

- the overall patterns of the dispersion curves as function of the direction of propagation,
- the polar plots of the phase velocity,
- the band-gap characteristics.

In order to accomplish this task, we will make strong use of a generalization of the procedure proposed before for the identification of the micro and macro coefficients for the isotropic case. More particularly we will use the fundamental results derived in [8] according to which

- for $L_c \to 0$ the homogenization formula takes the form

$$\mathbb{C}_{\text{macro}} = \mathbb{C}_{\text{micro}}\left(\mathbb{C}_{\text{micro}} + \mathbb{C}_e\right)^{-1}\mathbb{C}_e,$$

- for $L_c \to \infty$ the equivalent continuum (microscopic scale) has stiffness $\mathbb{C}_{\text{micro}}$.

As explained before, the elastic tensors $\mathbb{C}_{\text{macro}}$ and $\mathbb{C}_{\text{micro}}$ will be determined by using finite element simulations on the unit-cell with periodic and Dirichlet boundary conditions, respectively. This paper is now organized as follows:

- in Section 2 we introduce the notation used in the paper,
- in Section 3 we present the general anisotropic relaxed micromorphic model in a variational format and we derive the PDEs governing the system by performing the first variation of the introduced action functional,
- in Section 4 we introduce the plane wave ansatz on the unknown kinematical fields in order to show how it is possible to reduce the system of governing PDEs to an algebraic problem, describing the procedures to derive the dispersion curves,
- in Section 5 we consider a particular periodic microstructure which has tetragonal symmetry and we perform the Bloch-Floquet analysis in order to derive the dispersion curves associated to the equivalent continuum. The dispersion curves obtained with this method will be used in following sections to calibrate the parameters of the relaxed micromorphic model,
- in Section 6 we particularize the general framework of the anisotropic relaxed micromorphic model presented in Section 3 to the particular case of the tetragonal material symmetry,
- in Section 7 we show how almost all of the static elastic coefficients of the relaxed micromorphic model (except the Cosserat couple modulus μ_c) can be determined on the basis of purely static tests on very large specimens of metamaterial and on suitable unit-cells of the metamaterial itself. To this aim, finite element simulations on the unit-cell with periodic and Dirichlet boundary conditions are used, respectively,
- in Section 8 we present in detail the fitting procedure that we used to obtain the remaining parameters of the relaxed micromorphic model which have not been determined by static arguments. This will be done via the superposition of the dispersion curves obtained from our model to those obtained via Bloch-Floquet analysis,
- in Section 9 we show how the proposed anisotropic relaxed model is able to catch the anisotropic behavior of the considered tetragonal metamaterial. This is done by comparing the polar plots of the phase velocity as obtained with the relaxed micromorphic model to those obtained via Bloch-Floquet analysis. We show that a very good agreement exists for all directions of propagation and for wavelength which can become very small, even comparable to the size of the unit-cell.

Since in this paper we present many novel concepts we strive for maximal clarity and have kept the paper as self-contained as possible, for the convenience of the reader.

2 Notation

Throughout this paper the Einstein convention of summation over repeated indexes is used unless stated otherwise. We denote by $\mathbb{R}^{3\times3}$ the set of real 3×3 second order tensors and by $\mathbb{R}^{3\times3\times3}$ the set of real $3\times3\times3$ third order tensors. The standard Euclidean scalar product on $\mathbb{R}^{3\times3}$ is given by $\langle X, Y\rangle_{\mathbb{R}^{3\times3}} = \text{tr}(X \cdot Y^T)$ and, thus, the Frobenius tensor norm is $\|X\|^2 = \langle X, X\rangle_{\mathbb{R}^{3\times3}}$. Moreover, the identity tensor on $\mathbb{R}^{3\times3}$ will be denoted by $\mathbb{1}$, so that $\text{tr}(X) = \langle X, \mathbb{1}\rangle$. We adopt the usual abbreviations of Lie-algebra theory, i.e.:

- $\text{Sym}(3) := \{X \in \mathbb{R}^{3\times3} \,|X^T = X\}$ denotes the vector-space of all symmetric 3×3 matrices,
- $\mathfrak{so}(3) := \{X \in \mathbb{R}^{3\times3} \,|X^T = -X\}$ is the Lie-algebra of skew symmetric tensors,
- $\mathfrak{sl}(3) := \{X \in \mathbb{R}^{3\times3} \,|\text{tr}(X) = 0\}$ is the Lie-algebra of traceless tensors,
- $\mathbb{R}^{3\times3} \simeq \mathfrak{gl}(3) = \{\mathfrak{sl}(3) \cap \text{Sym}(3)\} \oplus \mathfrak{so}(3) \oplus \mathbb{R}\cdot\mathbb{1}$ is the *orthogonal Cartan-decomposition of the Lie-algebra* $\mathfrak{gl}(3)$.

In other words, for all $X \in \mathbb{R}^{3\times3}$, we consider the orthogonal decomposition

$$X = \text{dev sym}X + \text{skew}X + \frac{1}{3}\text{tr}(X)\,\mathbb{1}, \tag{5}$$

where:

- $\operatorname{sym} X = \frac{1}{2}(X^T + X) \in \operatorname{Sym}(3)$ is the symmetric part of X,
- $\operatorname{skew} X = \frac{1}{2}(X - X^T) \in \mathfrak{so}(3)$ is the skew-symmetric part of X,
- $\operatorname{dev} X = X - \frac{1}{3}\operatorname{tr}(X)\,\mathbb{1} \in \mathfrak{sl}(3)$ is the deviatoric (trace-free) part of X.

Throughout all the paper we indicate:

- without superscripts, i.e. $\mathbb{C}$, a classical fourth order tensor acting only on symmetric matrices ($\mathbb{C} : \operatorname{Sym}(3) \to \operatorname{Sym}(3)$) or skew-symmetric ones ($\mathbb{C}_c : \mathfrak{so}(3) \to \mathfrak{so}(3)$) ,
- with tilde, i.e. $\widetilde{\mathbb{C}}_c$, a second order tensor $\widetilde{\mathbb{C}}_c : \mathbb{R}^3 \to \mathbb{R}^3$ appearing as elastic stiffness of certain coupling terms.

The operation of simple contraction between tensors of suitable order is denoted by $\cdot$; for example,

$$\left(\widetilde{\mathbb{C}} \cdot v\right)_i = \widetilde{\mathbb{C}}_{ij} v_j\,, \qquad \left(\widetilde{\mathbb{C}} \cdot X\right)_{ij} = \widetilde{\mathbb{C}}_{ih} X_{hj}\,. \tag{6}$$

Typical conventions for differential operations are used, such as a comma followed by a subscript to denote the partial derivative with respect to the corresponding Cartesian coordinate, i.e. $(\cdot)_{,j} = \frac{\partial(\cdot)}{\partial x_j}$.
The curl of a vector field v is defined as

$$(\operatorname{curl} v)_i = \varepsilon_{ijk}\, v_{k,j},$$

where ε_{ijk} is the Levi-Civita third order permutation tensor. Let $X \in \mathbb{R}^{3\times 3}$ be a second order tensor field and $X_1, X_2, X_3 \in \mathbb{R}^3$ three vector fields such that

$$X = \begin{pmatrix} X_1^T \\ X_2^T \\ X_3^T \end{pmatrix}.$$

The Curl of a smooth matrix field X is defined as follows:

$$\operatorname{Curl} X = \begin{pmatrix} (\operatorname{curl} X_1)^T \\ (\operatorname{curl} X_2)^T \\ (\operatorname{curl} X_3)^T \end{pmatrix}$$

or in index notation,

$$(\operatorname{Curl} X)_{ij} = \varepsilon_{jmn}\, X_{in,m}.$$

For the iterated Curl we find

$$\begin{aligned}(\operatorname{Curl}\operatorname{Curl} P)_{ij} &= \varepsilon_{jmn}\,(\operatorname{Curl} P)_{in,m} = \varepsilon_{jmn}\,(\varepsilon_{nab} P_{ib,a})_{,m} = \varepsilon_{jmn}\varepsilon_{nab} P_{ib,am} \\ &= -\,\varepsilon_{nmj}\varepsilon_{nab} P_{ib,am} = -\,(\delta_{ma}\delta_{jb} - \delta_{mb}\delta_{ja})\, P_{ib,am} = P_{im,jm} - P_{ij,mm}.\end{aligned}$$

The divergence $\operatorname{div} v$ of a smooth vector field v is defined as $\operatorname{div} v = v_{i,i}$ and the divergence $\operatorname{Div} X$ of a tensor field $X \in \mathbb{R}^{3\times 3}$ as

$$\operatorname{Div} X = \begin{pmatrix} \operatorname{div} X_1 \\ \operatorname{div} X_2 \\ \operatorname{div} X_3 \end{pmatrix}$$

or, in index notation, $(\operatorname{Div} X)_i = X_{ij,j}$. Given two differentiable vector fields $u, v : \Omega \subseteq \mathbb{R}^3 \to \mathbb{R}^3$, we find[2]

$$\operatorname{div}(u \times v) = \langle \operatorname{curl} u, v\rangle - \langle u, \operatorname{curl} v\rangle\,, \tag{7}$$

since

$$\operatorname{div}(u \times v) = (\varepsilon_{ijk} u_j v_k)_{,i} = \varepsilon_{ijk} u_{j,i} v_k + \varepsilon_{ijk} u_j v_{k,i} = \varepsilon_{kij} u_{j,i} v_k - u_j \varepsilon_{jik} v_{k,i} = \langle \operatorname{curl} u, v\rangle - \langle u, \operatorname{curl} v\rangle\,.$$

We also introduce the Sobolev spaces

$$H^1(\Omega) = \left\{u \in L^2(\Omega) \mid \nabla u \in L^2(\Omega)\right\},$$

with norm $\|u\|^2_{H^1(\Omega)} = \|u\|^2_{L^2(\Omega)} + \|\nabla u\|^2_{L^2(\Omega)}$, and

$$H(\operatorname{Curl};\Omega) = \left\{P \in L^2(\Omega) \mid \operatorname{Curl} P \in L^2(\Omega)\right\},$$

with norm $\|P\|^2_{H(\operatorname{Curl};\Omega)} = \|P\|^2_{L^2(\Omega)} + \|\operatorname{Curl} P\|^2_{L^2(\Omega)}$.

[2] We denote by $u \times v$ the cross product of two vectors u, v.

3 Variational formulation of the relaxed micromorphic model

The kinematical fields of the problem are the displacement field u and the micro-distortion tensor P, where

$$u : \overline{\Omega} \times [0,T] \to \mathbb{R}^3, \quad (x,t) \mapsto u(x,t), \qquad P : \overline{\Omega} \times [0,T] \to \mathbb{R}^{3\times 3}, \quad (x,t) \mapsto P(x,t),$$

Ω is an open bounded domain in $\mathbb{R}^3$ with a piecewise smooth boundary $\partial\Omega$ and closure $\overline{\Omega}$ and $[0,T] \subseteq \mathbb{R}$ is the time interval. The mechanical model is formulated in the variational context. This means that we have to consider an action functional on an appropriate space of functions. Setting $\Omega_0 = \Omega \times \{0\}$, the space of configurations of the problem is

$$\mathcal{Q} := \left\{ (u,P) \in \mathscr{C}^1\left(\overline{\Omega} \times I, \mathbb{R}^3\right) \times \mathscr{C}^1\left(\overline{\Omega} \times I, \mathbb{R}^{3\times 3}\right) : (u,P) \text{ verifies conditions } (\mathsf{B}_1) \text{ and } (\mathsf{B}_2) \right\}$$

where

- (B_1) is the imposition of the boundary conditions $u(x,t) = \varphi(x,t)$ and $P_i(x,t) \times n = \psi_i(x,t)$, $i = 1,2,3$, $(x,t) \in \partial\Omega \times [0,T]$, where n is the unit outward normal vector at $\partial\Omega \times [0,T]$, P_i, $i = 1,2,3$ are the rows of P and φ, ψ_i are prescribed functions,
- (B_2) is the imposition of the initial conditions $u|_{\Omega_0} = u_0$, $u_{,t}|_{\Omega_0} = \underline{u}_0$, $P|_{\Omega_0} = P_0$, $P_{,t}|_{\Omega_0} = \underline{P}_0$ in Ω_0, where $u_0(x), \underline{u}_0(x), P_0(x), \underline{P}_0(x)$ are prescribed functions,

The action functional $\mathscr{A} : \mathcal{Q} \to \mathbb{R}$ is the sum of the internal and external action functionals $\mathscr{A}^{int}_{\mathscr{L}}, \mathscr{A}^{ext} : \mathcal{Q} \to \mathbb{R}$ defined by

$$\begin{aligned} \mathscr{A}^{int}_{\mathscr{L}}[(u,P)] &:= \int_0^T \int_\Omega \mathscr{L}(u_{,t}, \nabla u_{,t}, P_{,t}, \nabla u, P, \operatorname{Curl} P)\, dm\, dt, \\ \mathscr{A}^{ext}[(u,P)] &:= \int_0^T \int_\Omega \left(\left\langle f^{ext}, u \right\rangle + \left\langle M^{ext}, P \right\rangle \right) dm\, dt, \end{aligned} \tag{8}$$

where $\mathscr{L}$ is the Lagrangian density of the system and f^{ext}, M^{ext} are the body force and body double force, respectively. In this work we will consider $f^{ext} = 0$, $M^{ext} = 0$ and the derivatives have to be understood in the sense of distributions. In order to find the stationary points of the action functional, we have to calculate its first variation:

$$\delta\mathscr{A} = \delta\mathscr{A}^{int}_{\mathscr{L}} = \delta \int_0^T \int_\Omega \mathscr{L}(u_{,t}, \nabla u_{,t}, P_{,t}, \nabla u, P, \operatorname{Curl} P)\, dm\, dt.$$

Results of well-posedness for variational problems of this type (existence, uniqueness and stability of solution) have been proved in [29, 51, 52]. In order to effectively compute this first variation, a specific form for the Lagrangian has to be specified.

3.1 Constitutive assumptions on the Lagrangian and equations of motion

For the Lagrangian energy density we assume the standard split into kinetic minus potential energy:

$$\mathscr{L}(u_{,t}, \nabla u_{,t}, P_{,t}, \nabla u, P, \operatorname{Curl} P) = J(u_{,t}, \nabla u_{,t}, P_{,t}) - W(\nabla u, P, \operatorname{Curl} P). \tag{9}$$

When considering anisotropic linear elastic micromorphic media, as reported in [8, 52], the kinetic energy density and the potential one may take on the form

$$J\left(u_{,t}, \nabla u_{,t}, P_{,t}\right) = \frac{1}{2}\left\langle \rho\, u_{,t}, u_{,t}\right\rangle + \frac{1}{2}\left\langle \mathbb{J}_{\text{micro}}\,\operatorname{sym} P_{,t}, \operatorname{sym} P_{,t}\right\rangle + \frac{1}{2}\left\langle \mathbb{J}_c\,\operatorname{skew} P_{,t}, \operatorname{skew} P_{,t}\right\rangle \tag{10}$$
$$+ \frac{1}{2}\left\langle \mathbb{T}\operatorname{sym}\nabla u_{,t}, \operatorname{sym}\nabla u_{,t}\right\rangle + \frac{1}{2}\left\langle \mathbb{T}_c\operatorname{skew}\nabla u_{,t}, \operatorname{skew}\nabla u_{,t}\right\rangle,$$

$$W\left(\nabla u, P, \operatorname{Curl} P\right) = \underbrace{\frac{1}{2}\left\langle \mathbb{C}_e\operatorname{sym}\left(\nabla u - P\right), \operatorname{sym}\left(\nabla u - P\right)\right\rangle_{\mathbb{R}^{3\times 3}}}_{\text{anisotropic elastic - energy}} + \underbrace{\frac{1}{2}\left\langle \mathbb{C}_{\text{micro}}\operatorname{sym} P, \operatorname{sym} P\right\rangle_{\mathbb{R}^{3\times 3}}}_{\text{micro - self - energy}} \tag{11}$$
$$+ \underbrace{\frac{1}{2}\left\langle \mathbb{C}_c\operatorname{skew}\left(\nabla u - P\right), \operatorname{skew}\left(\nabla u - P\right)\right\rangle_{\mathbb{R}^{3\times 3}}}_{\text{invariant local anisotropic rotational elastic coupling}}$$
$$+ \underbrace{\frac{L_c^2}{2}\left(\left\langle \mathbb{L}\operatorname{sym}\operatorname{Curl} P, \operatorname{sym}\operatorname{Curl} P\right\rangle_{\mathbb{R}^{3\times 3}} + \left\langle \mathbb{L}_c\operatorname{skew}\operatorname{Curl} P, \operatorname{skew}\operatorname{Curl} P\right\rangle_{\mathbb{R}^{3\times 3}}\right)}_{\text{curvature}}$$

with

$$\begin{cases} \rho : \Omega \to \mathbb{R}^+ & \text{macro-inertia mass density,} \\ \mathbb{J}_{\text{micro}} : \operatorname{Sym}(3) \to \operatorname{Sym}(3) & \text{classical } 4^{th}\text{order free micro-inertia density tensor,} \\ \mathbb{T} : \operatorname{Sym}(3) \to \operatorname{Sym}(3) & \text{classical } 4^{th}\text{order gradient micro-inertia density tensor,} \\ \mathbb{J}_c, \mathbb{T}_c : \mathfrak{so}(3) \to \mathfrak{so}(3) & 4^{th}\text{order coupling tensors with 6 independent components,} \\ \\ \mathbb{C}_e, \mathbb{C}_{\text{micro}}, \mathbb{L} : \operatorname{Sym}(3) \to \operatorname{Sym}(3) & \text{classical } 4^{th}\text{order elasticity tensors with 21 independent components,} \\ \mathbb{C}_c, \mathbb{L}_c : \mathfrak{so}(3) \to \mathfrak{so}(3) & 4^{th} \text{ order coupling tensors with 6 independent components,} \end{cases}$$

where L_c is the characteristic length of the relaxed micromorphic model. We demand that the bilinear forms induced by $\mathbb{J}_{\text{micro}}, \mathbb{T}, \mathbb{C}_e, \mathbb{C}_{\text{micro}}, \mathbb{L}$ are positive definite, i.e.,

$$\exists\, c^+, \tau^+, c_e^+, c_m^+, c_l^+ > 0;\ \forall S \in \operatorname{Sym}(3): \quad \begin{cases} \left\langle \mathbb{J}_{\text{micro}}\, S, S\right\rangle_{\mathbb{R}^{3\times 3}} & \geq c^+\|S\|^2_{\mathbb{R}^{3\times 3}}, \\ \left\langle \mathbb{T}\, S, S\right\rangle_{\mathbb{R}^{3\times 3}} & \geq \tau^+\|S\|^2_{\mathbb{R}^{3\times 3}}, \\ \left\langle \mathbb{C}_e\, S, S\right\rangle_{\mathbb{R}^{3\times 3}} & \geq c_e^+\|S\|^2_{\mathbb{R}^{3\times 3}}, \\ \left\langle \mathbb{C}_{\text{micro}}\, S, S\right\rangle_{\mathbb{R}^{3\times 3}} & \geq c_m^+\|S\|^2_{\mathbb{R}^{3\times 3}}, \\ \left\langle \mathbb{L}\, S, S\right\rangle_{\mathbb{R}^{3\times 3}} & \geq c_l^+\|S\|^2_{\mathbb{R}^{3\times 3}}, \end{cases} \tag{12}$$

while the bilinear forms induced by $\mathbb{J}_c, \mathbb{T}_c, \mathbb{C}_c, \mathbb{L}_c$ are only required to be positive semi-definite, i.e.

$$\forall \overline{A} \in \mathfrak{so}(3): \quad \begin{cases} \left\langle \mathbb{J}_c\, \overline{A}, \overline{A}\right\rangle_{\mathbb{R}^{3\times 3}} \geq 0, \\ \left\langle \mathbb{T}_c\, \overline{A}, \overline{A}\right\rangle_{\mathbb{R}^{3\times 3}} \geq 0, \\ \left\langle \mathbb{C}_c\, \overline{A}, \overline{A}\right\rangle_{\mathbb{R}^{3\times 3}} \geq 0, \\ \left\langle \mathbb{L}_c\, \overline{A}, \overline{A}\right\rangle_{\mathbb{R}^{3\times 3}} \geq 0. \end{cases} \tag{13}$$

The equations of motion[3] are given as a set of 3 coupled PDE-systems for u, $\operatorname{sym} P$ and $\operatorname{skew} P$:

$$\begin{aligned} &\rho\, u_{,tt} - \operatorname{Div}\left(\mathbb{T}\operatorname{sym}\nabla u_{,tt}\right) \\ &\quad -\operatorname{Div}\left(\mathbb{T}_c\operatorname{skew}\nabla u_{,tt}\right) = \operatorname{Div}\left(\mathbb{C}_e\operatorname{sym}\left(\nabla u - P\right) + \mathbb{C}_c\operatorname{skew}\left(\nabla u - P\right)\right), \\ &\qquad \mathbb{J}_{\text{micro}}\operatorname{sym} P_{,tt} = \mathbb{C}_e\operatorname{sym}\left(\nabla u - P\right) - \mathbb{C}_{\text{micro}}\operatorname{sym} P - L_c^2\operatorname{sym}\operatorname{Curl}\left(\mathbb{L}\operatorname{sym}\operatorname{Curl} P + \mathbb{L}_c\operatorname{skew}\operatorname{Curl} P\right), \\ &\qquad \mathbb{J}_c\operatorname{skew} P_{,tt} = \mathbb{C}_c\operatorname{skew}\left(\nabla u - P\right) - L_c^2\operatorname{skew}\operatorname{Curl}\left(\mathbb{L}\operatorname{sym}\operatorname{Curl} P + \mathbb{L}_c\operatorname{skew}\operatorname{Curl} P\right). \end{aligned} \tag{14}$$

[3] For the explicit derivation of these equations, see Appendix (11.1).

4 Plane wave propagation in anisotropic relaxed micromorphic media

As it is known in the context of dynamical analysis, a particular class of solutions of the system of partial differential equations (14) can be found considering the monochromatic plane wave form for the kinematics fields, i.e.

$$u(x,t) = \widehat{u}\cos\left(\langle \boldsymbol{k}, x\rangle - \omega t\right), \qquad P = \widehat{P}\sin\left(\langle \boldsymbol{k}, x\rangle - \omega t\right), \qquad \boldsymbol{k} = k\,\widehat{\boldsymbol{k}}, \tag{15}$$

where $\widehat{u} = (\widehat{u}_1, \widehat{u}_2, \widehat{u}_3)$ is the so-called polarization vector in $\mathbb{R}^3$, $\widehat{\boldsymbol{k}} = (k_1, k_2, k_3) \in \mathbb{R}^3$, $\left\|\widehat{\boldsymbol{k}}\right\| = 1$ is the direction of wave propagation and $\widehat{P} \in \mathbb{R}^{3\times 3}$. Under this hypothesis, when replacing (15) in (14), the search of solutions to (14) turns into an algebraic problem. Indeed, the system of partial differential equations (14) becomes the following one:

$$D(k,\omega)\cdot v = 0, \tag{16}$$

where, in this specific case, $D(k,\omega)$ is a 12×12 matrix with real-valued entries, whose components are functions of the constitutive tensors[4] and of (k,ω). Moreover, we set

$$v = \left(\widehat{u}_1, \widehat{P}^D, \widehat{P}^S, \widehat{u}_2, \widehat{P}_{(12)}, \widehat{P}_{[12]}, \widehat{u}_3, \widehat{P}_{(13)}, \widehat{P}_{[13]}, \widehat{P}_{(23)}, \widehat{P}_{[23]}, \widehat{P}^V\right) \in \mathbb{R}^{12}, \tag{17}$$

in which $\widehat{P}^D, \widehat{P}^S, \widehat{P}^V, \widehat{P}_{(12)}, \widehat{P}_{(13)}, \widehat{P}_{(23)}, \widehat{P}_{[12]}, \widehat{P}_{[13]}, \widehat{P}_{[23]}$, are defined, following [19, 44], as

$$\widehat{P}^D = \frac{2}{3}\widehat{P}_{11} - \frac{1}{3}\left(\widehat{P}_{22} + \widehat{P}_{33}\right), \qquad \widehat{P}_{(rl)} = \widehat{P}_{(rl)} = \frac{1}{2}\left(\widehat{P}_{rl} + \widehat{P}_{lr}\right) \text{ if } r \neq l, \qquad \widehat{P}_{[rl]} = \frac{1}{2}\left(\widehat{P}_{rl} - \widehat{P}_{lr}\right) = -\widehat{P}_{[lr]},$$
$$\widehat{P}^S = \frac{1}{3}\left(\widehat{P}_{11} + \widehat{P}_{22} + \widehat{P}_{33}\right), \qquad \widehat{P}^V = \widehat{P}_{22} - \widehat{P}_{33} \qquad 2\,\widehat{P}^S - \widehat{P}^D = \widehat{P}_{22} + \widehat{P}_{33}.$$

Clearly, the algebraic problem (16) admits non-trivial solutions if and only if the determinant of the matrix D is zero. The equation $\det D = 0$ allows to calculate the eigenvalues $\omega = \omega(k)$. The curves $\omega = \omega(k)$ plotted in the (ω, k) plane are called **dispersion curves**. The nature of the solutions to this specific algebraic problem is hard to investigate and at the moment, a rigorous mathematical description of the behavior of the dispersion curves is missing. For example, for the general relaxed micromorphic model, we need

(C1) to show that under the hypothesis of positive definiteness of the Lagrangian density[5] we have real wave velocity (i.e. real ω) and to find conditions that characterize this phenomenon (this kind of analysis has already been performed for the isotropic case: in [53] the authors showed that the rank one convexity condition does not imply real wave propagation and they found another characterizing condition),

(C2) to prove that under the hypothesis of positive definiteness of the Lagrangian the problem (16) admits as solutions a finite set of regular dispersion curves $\{\widehat{\omega}_i(k)\}_{i=1}^{n\in\mathbb{N}}$.

At the moment, we simply assume the validity of the two conjectures C1 and C2 (postponing to future works the aim to rigorously prove them) and will only numerically check that, for our choice of the material parameters, we have only real wave propagation. Due to the complicated form of the components of the matrix $D(k,\omega)$ as a function of the constitutive parameters in the fully anisotropic case, we will not explicitly write them here but, we can say that, in general, the matrix $D(k,\omega)$ has the structure $D(k,\omega) = A_2\,k^2 + B_2\,\omega^2 + A_1 k + C_0$, where A_2, B_2, A_1, C_0 are matrices in $\mathbb{R}^{12\times 12}$ depending on the material parameters.

4.1 Reduction to the 2D plain strain case

It is noteworthy that the anisotropic relaxed micromorphic model (more precisely, the model with tetragonal symmetry), supports purely in-plane wave solutions in plain strain, provided we use the simplification that $\mathbb{L} = \mathbb{1}$, $\mathbb{L}_c = \mathbb{1}$ in (14). This is due to the fact that for $\mathbb{L}, \mathbb{L}_c = \mathbb{1}$ we have that

$$\mathbb{L}\,\mathrm{symCurl}\,P + \mathbb{L}_c\,\mathrm{skewCurl}\,P = \mathrm{sym}\,\mathrm{Curl}\,P + \mathrm{skew}\,\mathrm{Curl}\,P = \mathrm{Curl}\,P$$

[4] This means that the components D_{ij} of the matrix D are functions $D_{ij}(k,\omega,\mathbb{T},\mathbb{T}_c,\mathbb{J}_{\mathrm{micro}},\mathbb{J}_c,\mathbb{C}_e,\mathbb{C}_c,\mathbb{C}_{\mathrm{micro}},\mathbb{L},\mathbb{L}_c,L_c)$. In the following, we will explicitly state only the dependence on (k,ω) if not differently specified.

[5] With positive definiteness of the Lagrangian density we mean that all the 4-order symmetric tensors present in $\mathscr{L}$ are positive definite (i.e. the associated bilinear forms are positive definite). On the other hand we say that $\mathscr{L}$ verifies the Legendre-Hadamard strong ellipticity condition if letting $z = (u,P) \in \mathbb{R}^{12}$ and $Z = (\nabla u, \nabla P)$ we have that $\nabla^2_Z \mathscr{L}(z,Z)(\xi\otimes A, \xi\otimes A)\ \forall\,\xi\in\mathbb{R}^3,\ A\in\mathbb{R}^{3\times 3}$. It is well known (for example see [18]) that if $\mathscr{L}$ is $\mathcal{C}^2$ with respect to Z, then the Legendre-Hadamard strong ellipticity condition is equivalent to rank-one convexity, i.e. to the convexity in θ of the function $\theta \mapsto \mathscr{L}(z, Z + \theta(\xi\otimes A))$ at all (z,Z) (see [53]).

in (14) and then the operation Curl Curl respects the plain strain format, i.e.

$$\operatorname{Curl}\operatorname{Curl}\begin{pmatrix}\star & \star & 0\\ \star & \star & 0\\ 0 & 0 & 0\end{pmatrix}=\begin{pmatrix}\star & \star & 0\\ \star & \star & 0\\ 0 & 0 & 0\end{pmatrix}. \tag{18}$$

We take advantage of this simplification and we will be interested (for simplicity of the computational task) only in the study of the wave propagation with $\widehat{\boldsymbol{k}}$ in the plane $(x_1, x_2, 0)$. In this way, setting the amplitudes out of the plane, $\widehat{u}_3, \widehat{P}_{13}, \widehat{P}_{23}, \widehat{P}_{33}, \widehat{P}_{31}, \widehat{P}_{32}$, equal to zero, the vector of the unknown amplitudes v given in (17) reduces to[6]

$$\widetilde{v}=\left(\widehat{u}_1, \widehat{P}^D, \widehat{P}^S, \widehat{u}_2, \widehat{P}_{(12)}, \widehat{P}_{[12]}\right).$$

The system of algebraic equations (16) simplifies to

$$\widetilde{D}\left(k,\omega\right)\cdot\widetilde{v}=0, \tag{19}$$

where the explicit expression of the 6×6 matrix $\widetilde{D}$ is given in Appendix 11.3. The dispersion curves $\omega=\omega\left(k\right)$ that we will show in the following are then the solutions of the algebraic equation

$$\det\widetilde{D}\left(k,\omega\right)=0.$$

5 Unit-cell and discrete numerical simulations via classical Bloch-Floquet analysis

In this section, we perform some discrete numerical simulations of wave dispersion in a precise metamaterial which will be further used to suitably show how the proposed relaxed micromorphic model can describe its (effective) homogenized behavior. Chosen the microstructure, we perform a Bloch-Floquet analysis of the wave propagation in the generated periodic infinite medium thanks to the FEM code COMSOL®. This kind of analysis can be easily implemented using the Bloch-Floquet boundary conditions which are built in the code. The microstructure Ω_c (see Fig.1(b)) we account for is realized as follows: given the plane structure Σ_c shown in Fig.1(a), with dimensions specified in Table 1, we define $\Omega_c=\Sigma_c\times[0,1]$ in which the unit is in meters. The grey region of Σ_c is filled by aluminum while the white one is empty. The group symmetry of the introduced microstructure is the tetragonal one (i.e., in the language of group theory, the generated solid is invariant under the action of the discrete subgroup[7] $\mathbb{D}_4$ of SO(3)).

The geometric dimensions and the mechanical parameters (Young's modulus and Poisson's ratio) of the presented microstructure are given in Table 1.

a	b	c	d	E	ν	μ	λ
[mm]	[mm]	[mm]	[m]	[GPa]	–	[GPa]	[GPa]
1	0.9	0.3	1	70	0.33	26.32	51.08

Table 1: Geometry of the unit-cell (Fig. 1) and elastic parameters of Aluminum.

We can now determine the apparent density ρ of the unit-cell Ω_c. In order to do this, denoting with V_{al} the volume occupied by the aluminum in the unit-cell (55%), we find that

$$M_{\text{al}}=\rho_{\text{al}}V_{\text{al}}=2.7\times10^3\times5.5\times10^{-7}\left[\frac{\text{kg}}{\text{m}^3}\right]\left[\text{m}^3\right]=14.85\times10^{-4}\left[\text{kg}\right],$$

where M_{al} is the mass of the volume occupied by the aluminum and $\rho_{\text{al}}=2.7\times10^3\left[\frac{\text{kg}}{\text{m}^3}\right]$ is the aluminum mass density. Having that the volume of the unit-cell is $Vol\left(\Omega_c\right)=10^{-6}\left[\text{m}^3\right]$ we find that

$$\rho=\frac{M_{\text{al}}}{Vol\left(\Omega_c\right)}\left[\frac{\text{kg}}{\text{m}^3}\right]=1485\left[\frac{\text{kg}}{\text{m}^3}\right]. \tag{20}$$

[6]Note that once $\widehat{P}^D$ and $\widehat{P}^S$ are known then $\widehat{P}^V$ is automatically determined and, in general, not vanishing.
[7]$\mathbb{D}_4$ is the dihedral group of order 4. It counts 8 elements.

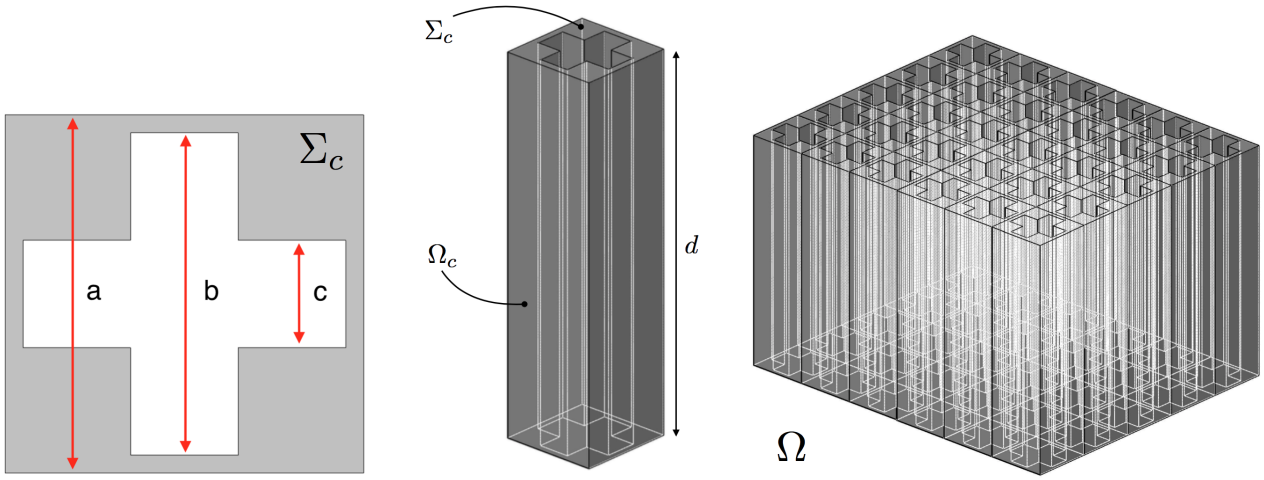

(a) (b) (c)

Figure 1: Microstructure implemented in COMSOL®: (a) Plane cell Σ_c, (b) 3D tetragonal cell Ω_c, (c) infinite periodic medium Ω.

When fixing the parameters of the unit-cell as in Table 1 and when performing a Bloch-Floquet analysis on the considered periodic structure, the dispersion curves shown in Fig.2 are obtained.

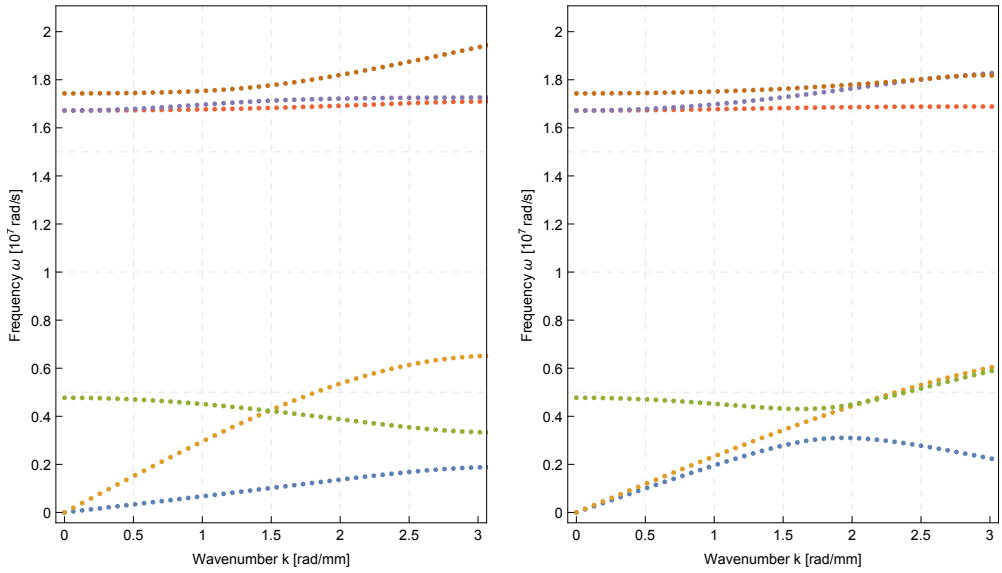

(a) (b)

Figure 2: COMSOL® model (plane strain Bloch-Floquet analysis). In (a) we plot the dispersion branches for $\widehat{\boldsymbol{k}} = (1, 0, 0)$ (horizontal wave propagation) and in (b) for $\widehat{\boldsymbol{k}} = \left(\sqrt{2}/2, \sqrt{2}/2, 0\right)$ (wave propagation at 45°). We observe a band-gap.

These curves for the two directions will be used in Section 8 to fit the dynamical parameters of the relaxed micromorphic model.

6 The tetragonal case in the relaxed micromorphic model

In this section we are able to show one of the main interests of using the proposed relaxed micromorphic model for the description of the homogenized mechanical behavior of anisotropic metamaterials. Indeed, classical elastic tensors of linear elasticity can be used once the symmetry class of the material is identified. This avoids unnecessary

complexifications related to the study of the symmetry classes of higher order tensors as happens e.g. in gradient elasticity (see, e.g., [5, 62]).

Having remarked that the crystallographic symmetry group of Ω_c is $\mathbb{D}_4$, we specify the general anisotropic model of a continuum which has the tetragonal symmetry property. This means that all involved structural tensors $\mathbb{C}$ have to respect the invariance condition

$$Q_{ai}Q_{bj}Q_{ch}Q_{dk}\mathbb{C}_{abcd} = \mathbb{C}_{ijhk}, \qquad \forall Q \in \mathbb{D}_4. \tag{21}$$

In order to express the constitutive tensors as 6×6 matrices, we use the following identification $\mathbb{C} \to \widetilde{\mathbb{C}} \in \mathbb{R}^{6\times 6}$ (see [8]), where

$$\widetilde{\mathbb{C}} = \begin{pmatrix} \mathbb{C}_{1111} & \mathbb{C}_{1122} & \mathbb{C}_{1133} & \frac{2}{c}\mathbb{C}_{1123} & \frac{2}{c}\mathbb{C}_{1113} & \frac{2}{c}\mathbb{C}_{1112} \\ \mathbb{C}_{2211} & \mathbb{C}_{2222} & \mathbb{C}_{2233} & \frac{2}{c}\mathbb{C}_{2223} & \frac{2}{c}\mathbb{C}_{2213} & \frac{2}{c}\mathbb{C}_{2212} \\ \mathbb{C}_{3311} & \mathbb{C}_{3322} & \mathbb{C}_{3333} & \frac{2}{c}\mathbb{C}_{3323} & \frac{2}{c}\mathbb{C}_{3313} & \frac{2}{c}\mathbb{C}_{3312} \\ \frac{2}{c}\mathbb{C}_{2311} & \frac{2}{c}\mathbb{C}_{2322} & \frac{2}{c}\mathbb{C}_{2333} & \frac{4}{c^2}\mathbb{C}_{2323} & \frac{4}{c^2}\mathbb{C}_{2313} & \frac{4}{c^2}\mathbb{C}_{2312} \\ \frac{2}{c}\mathbb{C}_{1311} & \frac{2}{c}\mathbb{C}_{1322} & \frac{2}{c}\mathbb{C}_{1333} & \frac{4}{c^2}\mathbb{C}_{1323} & \frac{4}{c^2}\mathbb{C}_{1313} & \frac{4}{c^2}\mathbb{C}_{1312} \\ \frac{2}{c}\mathbb{C}_{1211} & \frac{2}{c}\mathbb{C}_{1222} & \frac{2}{c}\mathbb{C}_{1233} & \frac{4}{c^2}\mathbb{C}_{1223} & \frac{4}{c^2}\mathbb{C}_{1213} & \frac{4}{c^2}\mathbb{C}_{1212} \end{pmatrix} \tag{22}$$

and $c \in \mathbb{R}$. According to the considered transformation, the strain tensor $\varepsilon \in \mathrm{Sym}\,(3)$ transforms in the vector $\widetilde{\varepsilon} \in \mathbb{R}^6$ according to:

$$\widetilde{\varepsilon} = \begin{pmatrix} \varepsilon_{11}, & \varepsilon_{22}, & \varepsilon_{33}, & c\,\varepsilon_{23}, & c\,\varepsilon_{13}, & c\,\varepsilon_{12} \end{pmatrix}^T. \tag{23}$$

On the other hand, the stress tensor $\sigma \in \mathrm{Sym}\,(3)$ is transformed into the vector $\widetilde{\sigma} \in \mathbb{R}^6$ as

$$\widetilde{\sigma} = \begin{pmatrix} \sigma_{11}, & \sigma_{22}, & \sigma_{33}, & \frac{2}{c}\,\sigma_{23}, & \frac{2}{c}\,\sigma_{13}, & \frac{2}{c}\,\sigma_{12} \end{pmatrix}^T = \widetilde{\mathbb{C}} \cdot \widetilde{\varepsilon}. \tag{24}$$

According to this notation, the classical tensorial stress-strain relation $\sigma_{ij} = \mathbb{C}_{ijhk}\,\varepsilon_{hk}$ can be written in compact vector form as

$$\widetilde{\sigma} = \widetilde{\mathbb{C}} \cdot \widetilde{\varepsilon}. \tag{25}$$

In the following, all the elastic tensors $\mathbb{C}_e, \mathbb{C}_c, \mathbb{C}_{\mathrm{micro}}, \mathbb{L}, \mathbb{L}_c, \mathbb{J}_{\mathrm{micro}}, \mathbb{J}_c, \mathbb{T}, \mathbb{T}_c$ appearing in eqs. (10), (11) will be written in compact form according to the transformation (25) and considering $c = 2$ (Voigt notation). This means that all the introduced second order elastic tensors and the associates stress and strain vectors $\widetilde{\sigma}$ and $\widetilde{\epsilon}$ will take the particular (Voigt) form[8]

$$\widetilde{\mathbb{C}} = \begin{pmatrix} \mathbb{C}_{1111} & \mathbb{C}_{1122} & \mathbb{C}_{1133} & \mathbb{C}_{1123} & \mathbb{C}_{1113} & \mathbb{C}_{1112} \\ \mathbb{C}_{2211} & \mathbb{C}_{2222} & \mathbb{C}_{2233} & \mathbb{C}_{2223} & \mathbb{C}_{2213} & \mathbb{C}_{2212} \\ \mathbb{C}_{3311} & \mathbb{C}_{3322} & \mathbb{C}_{3333} & \mathbb{C}_{3323} & \mathbb{C}_{3313} & \mathbb{C}_{3312} \\ \mathbb{C}_{2311} & \mathbb{C}_{2322} & \mathbb{C}_{2333} & \mathbb{C}_{2323} & \mathbb{C}_{2313} & \mathbb{C}_{2312} \\ \mathbb{C}_{1311} & \mathbb{C}_{1322} & \mathbb{C}_{1333} & \mathbb{C}_{1323} & \mathbb{C}_{1313} & \mathbb{C}_{1312} \\ \mathbb{C}_{1211} & \mathbb{C}_{1222} & \mathbb{C}_{1233} & \mathbb{C}_{1223} & \mathbb{C}_{1213} & \mathbb{C}_{1212} \end{pmatrix}, \qquad \widetilde{\sigma} = \begin{pmatrix} \sigma_{11} \\ \sigma_{22} \\ \sigma_{33} \\ \sigma_{23} \\ \sigma_{13} \\ \sigma_{12} \end{pmatrix}, \quad \widetilde{\varepsilon} = \begin{pmatrix} \varepsilon_{11} \\ \varepsilon_{22} \\ \varepsilon_{33} \\ 2\,\varepsilon_{23} \\ 2\,\varepsilon_{13} \\ 2\,\varepsilon_{12} \end{pmatrix}. \tag{26}$$

In the considered tetragonal case, the matrices corresponding to the considered tensors have the following structure

[8] Many different other choices exist in literature, for example $c = \sqrt{2}$ is known as Mandel notation. Nevertheless, it has to be remarked that changing the values of c changes not only the elastic tensor, but also the way in which the tensors σ and ε transform in the corresponding vectors $\widetilde{\sigma}$ and $\widetilde{\varepsilon}$ (see eq. (25)).

(see e.g. [8]):

$$\widetilde{\mathbb{C}}_e = \begin{pmatrix} 2\mu_e+\lambda_e & \lambda_e & \lambda_e^* & 0 & 0 & 0 \\ \lambda_e & 2\mu_e+\lambda_e & \lambda_e^* & 0 & 0 & 0 \\ \lambda_e^* & \lambda_e^* & (\widetilde{\mathbb{C}}_e)_{33} & 0 & 0 & 0 \\ 0 & 0 & 0 & (\widetilde{\mathbb{C}}_e)_{44} & 0 & 0 \\ 0 & 0 & 0 & 0 & (\widetilde{\mathbb{C}}_e)_{44} & 0 \\ 0 & 0 & 0 & 0 & 0 & \mu_e^* \end{pmatrix}, \qquad \widetilde{\mathbb{C}}_c = \begin{pmatrix} 4\mu_c^* & 0 & 0 \\ 0 & 4\mu_c^* & 0 \\ 0 & 0 & 4\mu_c \end{pmatrix},$$

$$\widetilde{\mathbb{L}} = \begin{pmatrix} 2\alpha_1+\alpha_3 & \alpha_3 & \alpha_3^* & 0 & 0 & 0 \\ \alpha_3 & 2\alpha_1+\alpha_3 & \alpha_3^* & 0 & 0 & 0 \\ \alpha_3^* & \alpha_3^* & \widetilde{\mathbb{L}}_{33} & 0 & 0 & 0 \\ 0 & 0 & 0 & \widetilde{\mathbb{L}}_{44} & 0 & 0 \\ 0 & 0 & 0 & 0 & \widetilde{\mathbb{L}}_{44} & 0 \\ 0 & 0 & 0 & 0 & 0 & \alpha_1^* \end{pmatrix}, \qquad \widetilde{\mathbb{L}}_c = \begin{pmatrix} 4\alpha_2^* & 0 & 0 \\ 0 & 4\alpha_2^* & 0 \\ 0 & 0 & 4\alpha_2 \end{pmatrix},$$

$$\widetilde{\mathbb{T}} = \begin{pmatrix} 2\overline{\eta}_1+\overline{\eta}_3 & \overline{\eta}_3 & \overline{\eta}_3^* & 0 & 0 & 0 \\ \overline{\eta}_3 & 2\overline{\eta}_1+\overline{\eta}_3 & \overline{\eta}_3^* & 0 & 0 & 0 \\ \overline{\eta}_3^* & \overline{\eta}_3^* & \widetilde{\mathbb{T}}_{33} & 0 & 0 & 0 \\ 0 & 0 & 0 & \widetilde{\mathbb{T}}_{44} & 0 & 0 \\ 0 & 0 & 0 & 0 & \widetilde{\mathbb{T}}_{44} & 0 \\ 0 & 0 & 0 & 0 & 0 & \overline{\eta}_1^* \end{pmatrix}, \qquad \widetilde{\mathbb{T}}_c = \begin{pmatrix} 4\overline{\eta}_2^* & 0 & 0 \\ 0 & 4\overline{\eta}_2^* & 0 \\ 0 & 0 & 4\overline{\eta}_2 \end{pmatrix},$$

$$\widetilde{\mathbb{J}}_{\text{micro}} = \begin{pmatrix} 2\eta_1+\eta_3 & \eta_3 & \eta_3^* & 0 & 0 & 0 \\ \eta_3 & 2\eta_1+\eta_3 & \eta_3^* & 0 & 0 & 0 \\ \eta_3^* & \eta_3^* & (\widetilde{\mathbb{J}}_{\text{micro}})_{33} & 0 & 0 & 0 \\ 0 & 0 & 0 & (\widetilde{\mathbb{J}}_{\text{micro}})_{44} & 0 & 0 \\ 0 & 0 & 0 & 0 & (\widetilde{\mathbb{J}}_{\text{micro}})_{44} & 0 \\ 0 & 0 & 0 & 0 & 0 & \eta_1^* \end{pmatrix}, \qquad \widetilde{\mathbb{J}}_c = \begin{pmatrix} 4\eta_2^* & 0 & 0 \\ 0 & 4\eta_2^* & 0 \\ 0 & 0 & 4\eta_2 \end{pmatrix}, \tag{27}$$

$$\widetilde{\mathbb{C}}_{\text{micro}} = \begin{pmatrix} 2\,\mu_{\text{micro}}+\lambda_{\text{micro}} & \lambda_{\text{micro}} & \lambda_{\text{micro}}^* & 0 & 0 & 0 \\ \lambda_{\text{micro}} & 2\,\mu_{\text{micro}}+\lambda_{\text{micro}} & \lambda_{\text{micro}}^* & 0 & 0 & 0 \\ \lambda_{\text{micro}}^* & \lambda_{\text{micro}}^* & (\widetilde{\mathbb{C}}_{\text{micro}})_{33} & 0 & 0 & 0 \\ 0 & 0 & 0 & (\widetilde{\mathbb{C}}_{\text{micro}})_{44} & 0 & 0 \\ 0 & 0 & 0 & 0 & (\widetilde{\mathbb{C}}_{\text{micro}})_{44} & 0 \\ 0 & 0 & 0 & 0 & 0 & \mu_{\text{micro}}^* \end{pmatrix}.$$

Remark 1. We explicitly remark that in the considered plane strain 2D case (no micro and macro motion in the 3-direction) some of the components of the elastic tensors do not explicitly appear neither in the PDEs (14) nor in the algebraic system (19). This is equivalent to say that, in the considered 2D tetragonal case, the only active components of the involved elastic tensors can be identified as follows:

$$\widetilde{\mathbb{C}}_e = \begin{pmatrix} 2\mu_e+\lambda_e & \lambda_e & \star & 0 & 0 & 0 \\ \lambda_e & 2\mu_e+\lambda_e & \star & 0 & 0 & 0 \\ \star & \star & \star & 0 & 0 & 0 \\ 0 & 0 & 0 & \star & 0 & 0 \\ 0 & 0 & 0 & 0 & \star & 0 \\ 0 & 0 & 0 & 0 & 0 & \mu_e^* \end{pmatrix}, \qquad \widetilde{\mathbb{C}}_c = \begin{pmatrix} \star & 0 & 0 \\ 0 & \star & 0 \\ 0 & 0 & 4\mu_c \end{pmatrix}. \tag{28}$$

Thus, we may arrange the elasticity tensor for our purpose as

$$\begin{pmatrix} 2\mu_e+\lambda_e & \lambda_e & 0 \\ \lambda_e & 2\mu_e+\lambda_e & 0 \\ 0 & 0 & \mu_e^* \end{pmatrix} \tag{29}$$

acting only on $(\varepsilon_{11}, \varepsilon_{22}, \varepsilon_{12})$. A similar reducibility holds for the other involved tensors.

7 Elastic parameter identification by numerical homogenization

The main task which has to be accomplished to successfully apply constitutive laws to the real material world is the identification of their parameters. For the present relaxed micromorphic model there are three sets of material parameters $\mathbb{C}_{\text{micro}}$, $\mathbb{C}_e$ and $\mathbb{C}_{\text{macro}}$ describing the size-independent static response. By virtue of the recently established harmonic mean-type micro-macro homogenization rule (59), the elasticities of the three scales are connected such that the determination of two sets is enough to infer on the third one. Only the micro $\mathbb{C}_{\text{micro}}$ as well as mesoscale-elastic parameters $\mathbb{C}_e$ appear directly in the relaxed micromorphic energy (11), while $\mathbb{C}_{\text{macro}}$ refers to a macroscopic, energetically equivalent, linear elastic surrogate model. In view of these characteristics, the coefficients of $\mathbb{C}_{\text{macro}}$ can be identified by standard homogenization on the periodic unit-cell level. However the identification of the micro parameters $\mathbb{C}_{\text{micro}}$ through homogenization is completely non-standard, since novel criteria have to be established to identify an appropriate unit-cell and boundary conditions.

For analyses of the considered tetragonal metamaterial in the plane, the number of independent material constants in linear elasticity is three for each of the scales (see (29)). Both the macro- as well as the microscopic elasticity parameters are computed by numerical homogenization on the unit-cell level. To that aim we employ the Finite-Element Heterogeneous Multiscale Method FE-HMM [22], a two-level finite element method, which is based on asymptotic homogenization and on the most general Heterogeneous Multiscale Method HMM [21]. A mathematical analysis of FE-HMM for linear elasticity is provided in [1], an overview of the method is given in [2].

A key advantage of FE-HMM is its sound mathematical foundation. In [1] error estimates for the fully discrete case are derived, which cover the micro and the macro error in a unified manner. The error introduced by approximating the exact elasticity tensor $\mathbb{C}^0_{ij}$ by its numerical counterpart $\mathbb{C}^{0,h}_{ij}$ follows for sufficiently regular problems

$$|\mathbb{C}^{0,h}_{ij} - \mathbb{C}^0_{ij}| \leq C(h/\delta)^{2q}\,, \tag{30}$$

where h is the characteristic mesh-size, δ is the side length of the unit-cell, and q is the polynomial degree of the finite element shape functions. Here, it holds $\delta = a$ (see Table 1) whereas for linear shape functions $q = 1$.

7.1 Determination of the macroscopic parameters $\mathbb{C}_{\text{macro}}$ - periodic homogenization

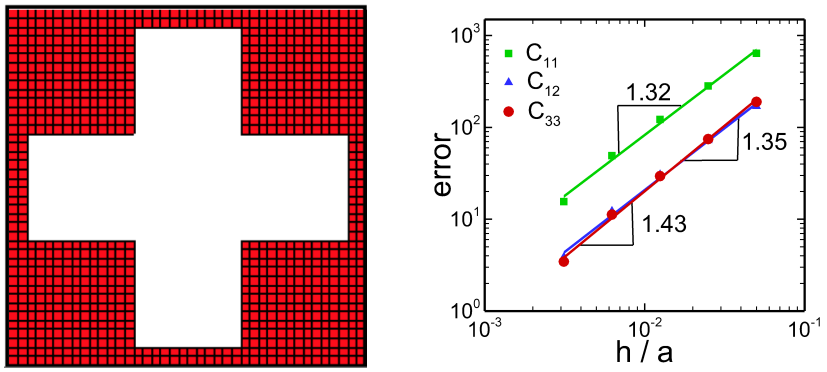

Figure 3: The Finite Element Heterogeneous Multiscale Method: a computational strategy for multiscale PDEs. Discretization of the unit cell (left) and error (right) .

Since periodic boundary conditions (PBCs) mimic an infinite number of unit-cells, they are employed to compute the macroscopic parameters of the relaxed micromorphic model. A uniform discretization of the unit-cell is shown in the left of Fig. 3. The Lamé constants for the converged solution are obtained for mesh-size $h = 1/2560$ mm; they are displayed in Table 2.

$\mathbb{C}_{\text{macro}}$	geometry Fig.6	boundary conditions in x-y-dir./loading	elasticity parameters λ_{macro} [GPa]	μ_{macro} [GPa]	μ^*_{macro} [GPa]
	(a)–(d)	periodic	1.738	5.895	0.620

Table 2: Homogenized macroscopic Lamé constants identified under plane strain and PBCs. Results of the Finite Element simulation.

On the right of Fig. 3 the convergence diagram for the error in the coefficients of $\mathbb{C}_{ij}^{0,h}$ is displayed, where the fully converged solution served as reference. Due to the low regularity of the problem – reentrant corners along with the infinite stiffness contrast between the phases – the observed convergence order is in the range of 1.32 to 1.43 and therefore far behind the nominal convergence order of $2q = 2$ according to (30).

In mathematical terms, the macroscopic stiffness $\mathbb{C}_{\text{macro}}$ is obtained by using the classical result of periodic homogenization (see e.g. [9, 12, 13]):

$$\frac{1}{2}\langle \mathbb{C}_{\text{macro}}\,\overline{E},\overline{E}\rangle := \inf\left\{ \frac{1}{|V(x)|}\int_{\xi\in V(x)} \frac{1}{2}\left\langle \mathbb{C}\left(\xi\right)\,\text{sym}\left(\nabla_\xi v\left(\xi\right)+\overline{E}\right),\text{sym}\left(\nabla_\xi v\left(\xi\right)+\overline{E}\right)\right\rangle d\xi \;\middle|\; v\in\mathcal{C}^\infty\left(V(x),\mathbb{R}^3\right)\right\}, \tag{31}$$

where $\mathbb{C}(\xi)$ is the elasticity tensor of the aluminum phase or air depending on the position of ξ in the unit-cell[9] and $\overline{E} = \text{sym}\nabla u\left(x\right)$ is the applied straining at the macroscopic point x, where the unit cell $V(x)$ is centered at x. For the computation of these macroscopic elasticity coefficients we use the two-scale finite element method FE-HMM [22] (see also [47, 67, 68]) and we assume that the microproblem is driven under macroscopic plane strain conditions.

The transition from a heterogeneous unit-cell of tetragonal symmetry to the case of homogeneous isotropy is shown in Fig. 4, which, for a cross-shaped pore of vanishing size, results in the Lamé constants of aluminum, see Table 3.

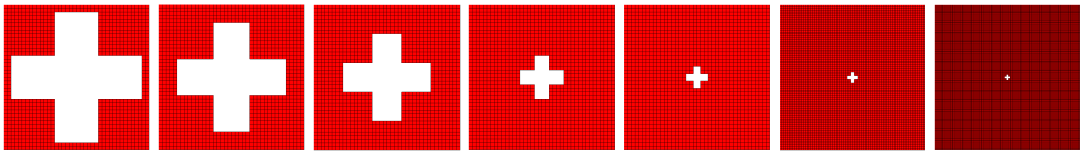

Figure 4: Consistency check of the method: decreasing the cross size recovers the homogeneous case of isotropic elasticity.

[9]Here, x is the macro space variable of the continuum, while ξ is the micro-variable spanning inside the unit-cell.

7.2 Determination of the microscopic parameters $\mathbb{C}_{\text{micro}}$ – nonstandard criteria imposed on homogenization by the relaxed micromorphic model

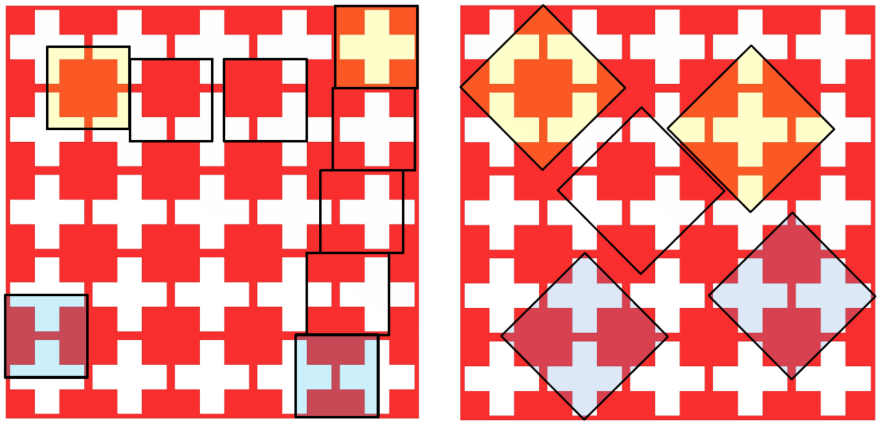

(a) (b)

Figure 5: Identification of the (a) standard square unit-cells of sidelenght a and (b) rotated square unit-cells of sidelength $a\sqrt{2}$. Yellow/blue shading indicates tetragonal/orthorhombic symmetries. No shading for cells with only one symmetry axis. Note that the metamaterial obtained by the infinite repetition of all these different unit-cells is the same tetragonal metamaterial.

As has been shown in previous works [58], $\mathbb{C}_{\text{micro}}$ represents the stiffness of an equivalent microscopic problem when letting the characteristic length $L_c \to \infty$, i.e., a maximal zoom on the microstructure. The relaxed micromorphic model is the only micromorphic type model so far that features a bounded micro-stiffness in the limit of $L_c \to \infty$; in fact, classical Mindlin-Eringen micromorphic models or even higher gradient models always provide an infinite stiffness when letting $L_c \to \infty$ and assuming inhomogeneous loading. By its very construction, the relaxed model is endowed to treat the class of heterogeneous metamaterials as a singularity free problem both at macro and micro scales.

Similar to the macro parameters, the micro set $\mathbb{C}_{\text{micro}}$ shall be identified by numerical homogenization. In contrast to the macroscopic scale, the relaxed micromorphic model imposes conditions at the micro-scale, which are non-standard, and in particular, in their combination, very selective as far as the choice of the unit-cells is concerned. The conditions which are imposed by the relaxed micromorphic model on choice of the unit-cells and on the boundary conditions read:

(i) they correspond to the case $L_c \to \infty$, a maximal zoom into the material,
(ii) they represent the maximal stiffness response of the (meta)material at the micro-scale,
(iii) they reflect the material's (tetragonal) symmetry.

The first condition $L_c \to \infty$ is rather vague and not very selective. The zoom into the single solid phase of the material however can be ruled out, since the resultant isotropy of aluminum violates condition (iii).

Condition (ii) alone suggests to consider constant strain conditions, since they yield the upper bound of stiffness, the Voigt-bound. Under constant strain assumption however, symmetry information of the microstructure is lost; numerical homogenization results in an isotropic material response, $\mu = \mu^*$, see Table 3, which again violates condition (iii). The conclusion is, that conditions (ii) and (iii) cannot be fulfilled by the constant strain assumption except for the trivial case of isotropy.

Among the boundary and loading conditions fulfilling the Hill-Mandel postulate (see footnote 20), linear Dirichlet boundary conditions (KUBC) are the candidate to estimate the maximal stiffness while preserving material symmetries. It is well known, that periodic boundary conditions (PBCs) yield less stiff results, and the constant stress assumption defines the lower bound of stiffness, the Reuss-bound.

There is an infinite number of valid, hence "equivalent" unit-cell variants for the homogenization of periodic media, if PBCs are applied[10]. Figure 5 shows some of them for the case of periodic tessellation based on squares of side length a and based on rotated squares of sidelength $a\sqrt{2}$. Additionally, other quadrilaterals like rectangles and

[10]For a discussion of the non-uniqueness of the unit-cell, see [63].

parallelograms can be used for valid periodic tessellation as well. They all result in the same material macroscopic stiffness and they all preserve the tetragonal symmetry, if PBCs are applied to the unit-cell.

The application of linear Dirichlet BCs (kinematically uniform boundary conditions KUBC) drastically reduces the above set of periodically "equivalent" unit-cells of sidelenghts a and $a\sqrt{2}$, since only four of them capture the tetragonal symmetry under these boundary conditions. These cells are highlighted in yellow color in Fig. 5, those with two symmetry axes of orthorhombic materials appear in blue shading. The rest of the displayed unit-cells exhibit only one symmetry axis. The KUBC render the symmetry criterion (iii) very selective for unit-cells.

The requirement for maximal stiffness on top of that condition, however, does not determine without ambiguity any variant in Fig. 6 as the single stiffest unit-cell.

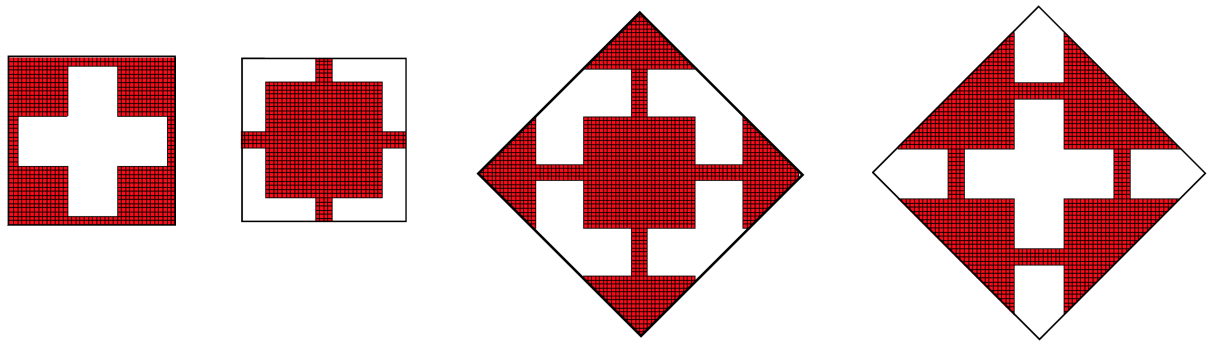

Figure 6: The four regular square unit-cells respecting tetragonal symmetry.

Nevertheless, from Table 3 we will distill an upper estimate for the stiffness of the microstructural response. This is done as follows. For each unit cell (a), (b), (c), (d) in Figure 6, we have calculated the corresponding stiffness tensor $\mathbb{C}^V_{\text{KUBC}}$. We will then determine that positive definite tensor $\mathbb{C}_{\text{micro}}$ which has tetragonal symmetry and which satisfies

$$\forall\, \overline{E} \in \text{Sym}\,(3)\ :\ \left\langle \mathbb{C}_{\text{micro}}\, \overline{E}, \overline{E} \right\rangle \geq \left\langle \mathbb{C}^V_{\text{KUBC}}\, \overline{E}, \overline{E} \right\rangle \tag{32}$$

for all 4 unit cells and in addition, any other possible tensor $\mathbb{C}^*_{\text{micro}}$, satisfying (32) will satisfy

$$\left\langle \mathbb{C}^*_{\text{micro}}\, \overline{E}, \overline{E} \right\rangle \geq \left\langle \mathbb{C}_{\text{micro}}\, \overline{E}, \overline{E} \right\rangle .$$

In this sense $\mathbb{C}_{\text{micro}}$ is optimal. It turns out that $\mathbb{C}_{\text{micro}}$ is a matrix supremum in the so called Löwner-half-order [14]. The mathematical reasoning behind (32) will be explained in the next subsection. Note that identifying $\mathbb{C}_{\text{micro}}$ as the Löwner supremum is an entirely new approach unique to the relaxed micromorphic model.

geometry	boundary conditions	elasticity parameters			
Fig.6	in x-y-dir./loading	λ_{hom}	μ_{hom}	μ^*_{hom}	
(a) – (d)	PBCs	1.738	5.895	0.620	
(a)	KUBC	4.37	6.242	**8.332**	
(b)		2.125	5.899	2.264	$\mathbb{C}_{\textbf{micro}}$
(c)		**5.270**	**8.927**	4.042	
(d)		5.981	6.254	4.96	
(a) – (d)	constant strain - Voigt	28.10	14.47	14.47	
aluminum full	KUBC and PBCs	51.08	26.32	26.32	

Table 3: Elastic parameter values in Voigt notation and restricted to the planar case. Homogenized material parameters [GPa] for tetragonal unit-cell variants (a)–(d) in Fig. 6 for KUBC and PBCs, for constant strain assumption (Voigt-bound), and the case of single phase aluminum.

In Table 3, we also report the computed values of the unit-cell stiffnesses using constant-strain conditions, as well as the stiffness of a unit-cell completely filled by aluminum computed both with KUBC and PBCs.

We repeat again that constant-strain conditions cannot be retained to compute $\mathbb{C}_{\text{micro}}$ because they are not compatible with the fact of considering a microstructure with a given symmetry (note that the obtained result is that of an isotropic material). Finally, we remark that in the case of an isotropic unit-cell (full aluminum) the homogenization results for KUBC and PBCs coincide.

The entries of the Löwner matrix supremum $\mathbb{C}_{\text{micro}}$ are obtained from Table 3 as follows

$$\lambda_{\text{micro}} = \mathbf{5.270}, \qquad \mu_{\text{micro}} = \mathbf{8.927}, \qquad \mu^*_{\text{micro}} = \mathbf{8.332}. \tag{33}$$

In conclusion, the homogenization requirements (i) – (iii) for the microparameter set along with the Hill-Mandel condition lead without ambiguity to KUBC and uniquely identify the stiffest microscopic response in terms of a function of the Lamé-parameters. With $\mathbb{C}_{\text{micro}}$ and $\mathbb{C}_{\text{macro}}$ in hand, we are able to compute $\mathbb{C}_e$ with formula (58).

Conditions (i)–(iii) shall be underpinned by mathematical arguments in the next Section 7.3.

Remark 2. The restriction to a and $a\sqrt{2}$ as the sidelength of quadratic unit-cells is based on the observation that for KUBC, increasing the size of the selection window decreases stiffness and, for an $N \times N$ ensemble of unit-cells, leads for $N \to \infty$ to the stiffness of a unit-cell subject to PBCs.

7.3 Rigorous justification of $\mathbb{C}_{\text{micro}}$ as representing the "maximal stiffness" on the microscale - the Löwner matrix supremum.

In this section we describe the mathematical underpinning towards determining the stiffness $\mathbb{C}_{\text{micro}}$ in the relaxed micromorphic model. We do this in the static case, in which the equilibrium problem (14) can be obtained as the energy minimization problem

$$I(u,P) := \int_\Omega W(\nabla u, P, \operatorname{Curl} P)\, dm \quad \longrightarrow \quad \min\ (u,P) \in H^1(\Omega) \times H(\operatorname{Curl};\Omega), \tag{34}$$

under suitable boundary conditions, with

$$\begin{aligned} W(\nabla u, P, \operatorname{Curl} P) = {} & \underbrace{\frac{1}{2}\left\langle \mathbb{C}_e \operatorname{sym}(\nabla u - P), \operatorname{sym}(\nabla u - P)\right\rangle_{\mathbb{R}^{3\times 3}}}_{\text{anisotropic elastic - energy}} + \underbrace{\frac{1}{2}\left\langle \mathbb{C}_{\text{micro}} \operatorname{sym} P, \operatorname{sym} P\right\rangle_{\mathbb{R}^{3\times 3}}}_{\text{micro - self - energy}} \\ & + \underbrace{\frac{1}{2}\left\langle \mathbb{C}_c \operatorname{skew}(\nabla u - P), \operatorname{skew}(\nabla u - P)\right\rangle_{\mathbb{R}^{3\times 3}}}_{\text{invariant local anisotropic rotational elastic coupling}} \\ & + \underbrace{\frac{L_c^2}{2}\left(\left\langle \mathbb{L} \operatorname{sym}\operatorname{Curl} P, \operatorname{sym}\operatorname{Curl} P\right\rangle_{\mathbb{R}^{3\times 3}} + \left\langle \mathbb{L}_c \operatorname{skew}\operatorname{Curl} P, \operatorname{skew}\operatorname{Curl} P\right\rangle_{\mathbb{R}^{3\times 3}}\right)}_{\text{curvature}}. \end{aligned} \tag{35}$$

For the displacement field u we apply overall affine Dirichlet boundary conditions

$$u|_{\partial\Omega}(x) = \overline{B} \cdot x, \qquad \overline{B} \in \mathbb{R}^{3\times 3} \tag{36}$$

and the microdistortion P has to satisfy the compatible boundary condition

$$\nabla u|_{\partial\Omega}(x) \cdot \tau_{1,2} = P|_{\partial\Omega}(x) \cdot \tau_{1,2}, \tag{37}$$

where $\tau_{1,2}$ are tangent vectors to $\partial\Omega$. One then observes that the minimal energy content of a solution (u,P) to the minimization problem (34), (35), (36),(37) is easily bounded above by choosing the macroscopic fields such that

$$\nabla u(x) = P(x) \qquad \text{in } \Omega. \tag{38}$$

This gives

$$\inf_{(u,P)} \int_{x\in\Omega} W(\nabla u, P, \operatorname{Curl} P)\, dx \le \inf_u \int_{x\in\Omega} W(\nabla u, \nabla u, 0)\, dx = \inf_u \int_{x\in\Omega} \frac{1}{2}\left\langle \mathbb{C}_{\text{micro}} \operatorname{sym}\nabla u(x), \operatorname{sym}\nabla u(x)\right\rangle dx. \tag{39}$$

Therefore, the maximal possible stored elastic energy of the relaxed micromorphic model over an arbitrary window $\widetilde{\Omega} \subset \Omega$ is

$$\inf_{u} \int_{x\in\widetilde{\Omega}} \frac{1}{2} \left\langle \mathbb{C}_{\text{micro}} \operatorname{sym} \nabla u\left(x\right), \operatorname{sym} \nabla u\left(x\right)\right\rangle dx, \qquad u|_{\partial\Omega}\left(x\right) = \overline{B}\cdot x, \tag{40}$$

and this value is attained for $\nabla u\left(x\right) = P\left(x\right)$ for all $x \in \Omega$. Below, we will evaluate the latter condition over a given unit-cell $V(x) = \widetilde{\Omega}$ attached at the macroscopic point $x \in \Omega$. Since ∇u and P are still macroscopic variables[11] (where P is supposed to transport some information from the micro-scale to the macro-scale in the point $x \in \Omega$) we may assume that they are approximately constant over the unit-cell $V(x)$. The average displacement gradient over the unit cell satisfies [72, 3.1, $u \in \mathcal{C}^{\infty}$]

$$\begin{aligned}
\frac{1}{|V(x)|}\int_{\xi\in V(x)} \nabla_{\xi} u\left(x+\xi\right) d\xi &= \frac{1}{|V(x)|}\int_{\xi\in\partial V(x)} u\left(x+\xi\right)\otimes n\left(\xi\right)\, dS_{\xi} \\
&= \frac{1}{|V(x)|}\int_{\xi\in\partial V(x)} \left(\overline{B}\cdot\xi\right)\otimes n\left(\xi\right)\, dS_{\xi} + \frac{\varepsilon^2}{|V(x)|}\underbrace{\int_{\xi\in\partial V(x)} \widetilde{u}\left(\frac{\xi}{\varepsilon}\right)\otimes n\left(\xi\right)\, dS_{\xi}}_{=0 \text{ since } \widetilde{u}\in\mathcal{C}_0^{\infty}(\varepsilon\, V(x),\mathbb{R}^3)} \\
&= \frac{1}{|V(x)|}\int_{\xi\in V(x)} \overline{B}\, d\xi = \overline{B}.
\end{aligned} \tag{41}$$

Symmetrization yields as well for the average strain tensor

$$\overline{\varepsilon} = \frac{1}{|V|}\int_{\xi\in V(x)} \varepsilon\left(x+\xi\right) d\xi = \operatorname{sym}\overline{B} = \overline{E}. \tag{42}$$

Since the integrand in (40) is convex (quasiconvex) and $\mathbb{C}_{\text{micro}}$ is constant by assumption, the maximal storage of elastic energy in $V(x)$, according to the relaxed micromorphic model is realized by the homogeneous displacement $\overline{B}\cdot\xi$ which yields

$$\begin{aligned}
&\inf\left\{\int_{\xi\in V(x)} \frac{1}{2}\left\langle \mathbb{C}_{\text{micro}} \operatorname{sym}\nabla_{\xi}\overline{v}\left(\xi\right), \operatorname{sym}\nabla_{\xi}\overline{v}\left(\xi\right)\right\rangle d\xi \;\middle|\; \overline{v}: V(x)\to\mathbb{R}^3,\ \overline{v}|_{\partial V(x)}\left(\xi\right) = \overline{B}\cdot\xi\right\} \\
&\qquad = \frac{1}{2}\left\langle \mathbb{C}_{\text{micro}} \operatorname{sym}\overline{B}, \operatorname{sym}\overline{B}\right\rangle |V(x)| = \frac{1}{2}\left\langle \mathbb{C}_{\text{micro}}\,\overline{E},\overline{E}\right\rangle |V(x)|, \qquad \overline{E} = \operatorname{sym}\overline{B},
\end{aligned} \tag{43}$$

for the relaxed micromorphic model.

Now we switch to considering the unit cell as described by classical linear elasticity. Macroscopic variables are conceptionally some "averages" over the microscale. Hence the attached unit-cell $V(x)$ must be considered to be loaded such that it produces the given superposed macroscopic average $\nabla u\left(x\right)$. There are several choices satisfying this requirement; prominently KUBC and PBCs. It is well known that affine Dirichlet conditions generate stiffer response than PBCs [35, 58]. Under affine Dirichlet conditions (KUBC) the classical linear elastic stored energy of the unit-cell is given by

$$\begin{aligned}
&\inf\left\{\int_{\xi\in V(x)} \frac{1}{2}\left\langle \mathbb{C}\left(\xi\right)\operatorname{sym}\nabla_{\xi}\widetilde{v}\left(\xi\right), \operatorname{sym}\nabla_{\xi}\widetilde{v}\left(\xi\right)\right\rangle d\xi \;\middle|\; \widetilde{v}: V(x)\to\mathbb{R}^3,\ \widetilde{v}|_{\partial V(x)}\left(\xi\right) = \overline{B}\cdot\xi\right\} \\
&\quad = \inf\left\{\int_{\xi\in V(x)} \frac{1}{2}\left\langle \mathbb{C}\left(\xi\right)\operatorname{sym}\left(\nabla_{\xi}\left[v\left(\xi\right)+\overline{B}\cdot\xi\right]\right), \operatorname{sym}\left(\nabla_{\xi}\left[v\left(\xi\right)+\overline{B}\cdot\xi\right]\right)\right\rangle d\xi \;\middle|\; v\in\mathcal{C}_0^{\infty}\left(V(x),\mathbb{R}^3\right)\right\} \\
&\qquad = \inf\left\{\int_{\xi\in V(x)} \frac{1}{2}\left\langle \mathbb{C}\left(\xi\right)\left(\operatorname{sym}\nabla_{\xi}v\left(\xi\right)+\overline{E}\right), \operatorname{sym}\nabla_{\xi}v\left(\xi\right)+\overline{E}\right\rangle d\xi \;\middle|\; v\in\mathcal{C}_0^{\infty}\left(V(x),\mathbb{R}^3\right)\right\} \\
&\qquad\quad = \int_{\xi\in V(x)} \frac{1}{2}\left\langle \mathbb{C}\left(\xi\right)\left(\operatorname{sym}\nabla_{\xi}\widehat{v}_{\overline{E}}\left(\xi\right)+\overline{E}\right), \operatorname{sym}\nabla_{\xi}\widehat{v}_{\overline{E}}\left(\xi\right)+\overline{E}\right\rangle d\xi,
\end{aligned} \tag{44}$$

where (the corrector) $\widehat{v}_{\overline{E}}\in\mathcal{C}_0^{\infty}\left(V(x),\mathbb{R}^3\right)$ is the realizing minimizer (which is not known a priori).

In the context of homogenization, we now demand that the (fully resolved linear elastic) fine-scale energy (44) should equal the (relaxed micromorphic) coarse-scale energy $(39)_{\text{left}}$ over the same domain $V(x)$, under the same affine boundary conditions $\overline{B}\cdot\xi$ and for the same material. This means we require that for all $\overline{B}\in\mathbb{R}^{3\times3}$:

[11] Despite the name micromorphic model.

$$\inf_{(u,P)} \left\{ \int_{\xi\in V(x)} W\left(\nabla_\xi u\left(x+\xi\right), P\left(x+\xi\right), \operatorname{Curl} P\left(x+\xi\right)\right) d\xi \,\middle|\, u|_{\xi\in\partial V}\left(x+\xi\right) = \overline{B}\cdot\xi,\ \overline{B}\cdot\tau_{1,2} = P|_{\xi\in\partial V}\left(x+\xi\right)\cdot\tau_{1,2} \right\}$$
$$\stackrel{!}{=} \inf_{v} \left\{ \int_{\xi\in V(x)} \frac{1}{2}\left\langle \mathbb{C}\left(\xi\right)\left(\operatorname{sym}\nabla_\xi v + \overline{E}\right), \operatorname{sym}\nabla_\xi v + \overline{E}\right\rangle d\xi \,\middle|\, v\in\mathcal{C}_0^\infty\left(V(x),\mathbb{R}^3\right),\ \overline{E} = \operatorname{sym}\overline{B} \right\}. \tag{45}$$

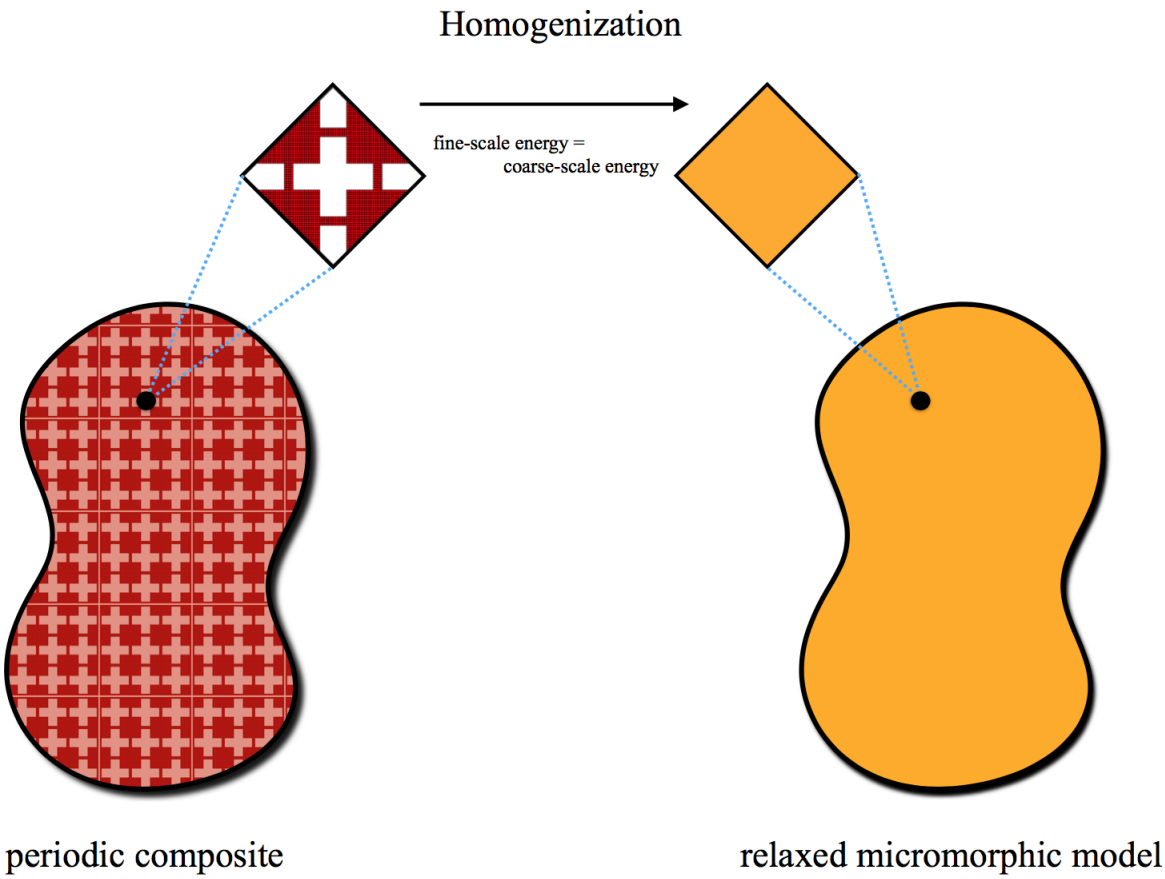

Figure 7: The process of homogenization. We need to demand energy equivalence of the fine-scale linear elastic energy (left) with the coarse-scale relaxed micromorphic energy (right) over the same domain $V(x)$, under the same affine boundary conditions and for the same material that is to be described.

With estimate (39) and (43), taking (45) into account, we obtain the inequality

$$\underbrace{\frac{1}{2}\left\langle \mathbb{C}_{\text{micro}}\,\overline{E},\overline{E}\right\rangle |V(x)|}_{\substack{\text{coarse scale micromorphic}\\ \text{upper energy limit}}} \geq \underbrace{\inf\left\{ \int_{\xi\in V(x)} \frac{1}{2}\left\langle \mathbb{C}\left(\xi\right)\left(\operatorname{sym}\nabla_\xi v\left(\xi\right) + \overline{E}\right), \operatorname{sym}\nabla_\xi v\left(\xi\right) + \overline{E}\right\rangle d\xi \,\middle|\, v\in\mathcal{C}_0^\infty\left(V(x),\mathbb{R}^3\right)\right\}}_{\text{fine-scale linear elastic energy}}. \tag{46}$$

On the other hand, according to the classical[12] Hill-Mandel[13] lemma [31, 32, 34, 46, 72] we can define a unique

[12] And not any of the ambiguous extended versions for generalized continua [26–28].

[13] The Hill-Mandel energy equivalence for KUBC can be obtained easily. We provide it for the convenience of the reader. On the one hand we have in mechanical equilibrium

apparent [35] stiffness tensor[14] $\mathbb{C}^V_{\mathrm{KUBC}}$, independent of $\overline{E}$, but depending on the unit-cell V, by setting

$$\frac{1}{2}\left|V\left(x\right)\right|\left\langle \mathbb{C}^V_{\mathrm{KUBC}}\,\overline{E},\overline{E}\right\rangle =\inf\left\{ \int_{\xi\in V(x)}\frac{1}{2}\left\langle \mathbb{C}\left(\xi\right)\left(\mathrm{sym}\nabla_\xi v\left(\xi\right)+\overline{E}\right),\mathrm{sym}\nabla_\xi v\left(\xi\right)+\overline{E}\right\rangle d\xi\;\Big|\; v\in\mathcal{C}^\infty_0\left(V(x),\mathbb{R}^3\right)\right\}. \tag{49}$$

Combining this with (46) we must have for all $\overline{E}\in\mathrm{Sym}\left(3\right)$:

$$\frac{1}{2}\left\langle \mathbb{C}_{\mathrm{micro}}\,\overline{E},\overline{E}\right\rangle \geq\frac{1}{2}\left\langle \mathbb{C}^V_{\mathrm{KUBC}}\,\overline{E},\overline{E}\right\rangle . \tag{50}$$

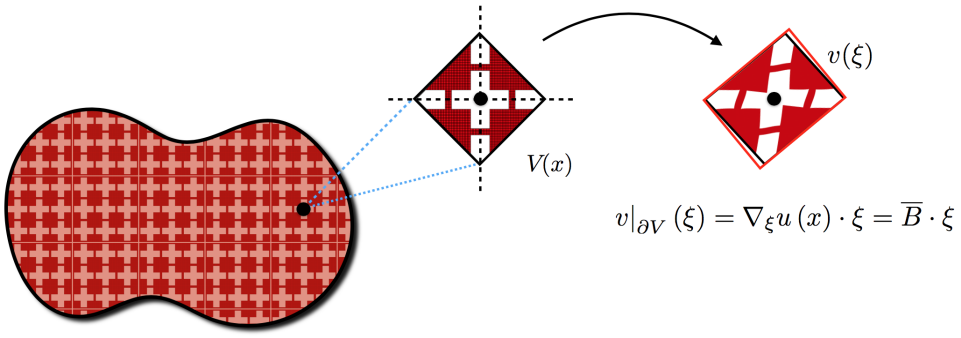

Figure 8: Affine Dirichlet loading (KUBC) of the unit-cell $V(x)$. The macroscopic deformation state $\nabla_\xi u\left(x\right)=\overline{B}$ defines a microscopic Dirichlet boundary value problem on the boundary of the microvolume $V(x)$ attached to each macroscopic material point $x\in\Omega$. Here, we show the superposition of simple shear and elongation.

$$\begin{aligned}\int_{\xi\in\partial V}\left\langle u\left(\xi\right),\sigma\left(\xi\right)\cdot n\right\rangle_{\mathbb{R}^3}dS_V &= \int_{\xi\in\partial V}\left\langle \sigma^T\left(\xi\right)\cdot u\left(\xi\right),n\right\rangle_{\mathbb{R}^3}dS_V=\int_{\xi\in V}\mathrm{div}\left(\sigma^T\cdot u\right)dV=\int_{\xi\in V}\mathrm{div}\left(\sigma\cdot u\right)dV\\ &=\int_{\xi\in V}\left\langle \nabla u,\sigma\right\rangle_{\mathbb{R}^{3\times3}}+\left\langle u,\underbrace{\mathrm{Div}\,\sigma}_{=0}\right\rangle dV=\int_{\xi\in V}\left\langle \sigma\left(\xi\right),\varepsilon\left(\xi\right)\right\rangle dV.\end{aligned} \tag{47}$$

On the other hand, for KUBC, we have $u|_{\partial V}=\overline{B}\cdot\xi$ and

$$\begin{aligned}\int_{\xi\in\partial V}\left\langle u\left(\xi\right),\sigma\left(\xi\right)\cdot n\right\rangle_{\mathbb{R}^3}dS_V &= \int_{\xi\in\partial V}\left\langle \overline{B}\cdot\xi,\sigma\left(\xi\right)\cdot n\right\rangle_{\mathbb{R}^3}dS_V=\int_{\xi\in V}\mathrm{div}\left(\sigma^T\cdot\left(\overline{B}\cdot\xi\right)\right)dV\\ &=\int_{\xi\in V}\mathrm{div}\left(\sigma\cdot\left(\overline{B}\cdot\xi\right)\right)dV=\int_{\xi\in V}\left\langle \nabla\left[\overline{B}\cdot\xi\right],\sigma\right\rangle+\left\langle \overline{B}\cdot\xi,\underbrace{\mathrm{Div}\,\sigma}_{=0}\right\rangle dV\\ &=\int_{\xi\in V}\left\langle \overline{B},\sigma\right\rangle dV=\left\langle \overline{B},\int_{\xi\in V}\sigma\,dV\right\rangle=\left|V\right|\left\langle \overline{B},\frac{1}{\left|V\right|}\int_{\xi\in V}\sigma\,dV\right\rangle=\left|V\right|\left\langle \mathrm{sym}\,\overline{B},\overline{\sigma}\right\rangle .\end{aligned} \tag{48}$$

Since $\mathrm{sym}\,\overline{B}=\overline{E}=\overline{\varepsilon}$, see (41), taking (47) and (48) together we obtain

$$\left\langle \overline{\sigma},\overline{\varepsilon}\right\rangle =\frac{1}{\left|V\right|}\int_{\xi\in V}\left\langle \sigma\left(\xi\right),\varepsilon\left(\xi\right)\right\rangle dV.$$

[14]The Hill-Mandel lemma implies that for KUBC (among others) it holds that,

$$\left\langle \overline{\sigma},\overline{\varepsilon}\right\rangle =\frac{1}{\left|V\right|}\int_{\xi\in V}\left\langle \sigma\left(\xi\right),\varepsilon\left(\xi\right)\right\rangle d\xi,\quad\mathrm{div}\,\sigma\left(\xi\right)=0,\quad u|_{\partial V}=\overline{B}\cdot\xi,$$

where $\overline{\varepsilon},\overline{\sigma}$ are the mean strain and stress, respectively.

Let us assume that on the fine scale we have the linear elastic constitutive law $\sigma\left(\xi\right)=\mathbb{C}\left(\xi\right)\varepsilon\left(\xi\right)$, where $\mathbb{C}\left(\xi\right)$ is uniformly positive definite. Then the equilibrium equation $\mathrm{div}\left(\mathbb{C}\left(\xi\right)\varepsilon\left(\xi\right)\right)=0$, $u|_{\partial V}\left(\xi\right)=\overline{B}\cdot\xi$ has a unique (inhomogeneous) solution $\widehat{u}\left(\xi\right)$, such that $\varepsilon\left(\xi\right)=\mathrm{sym}\,\nabla\widehat{u}\left(\xi\right)$ depends linearly on $\overline{E}=\mathrm{sym}\,\overline{B}$. Thus, the stress $\widehat{\sigma}\left(\xi\right)=\mathbb{C}\left(\xi\right)\varepsilon\left(\xi\right)$ depends also linearly on $\overline{E}$. On the other hand, it follows by partial integration that $\overline{\varepsilon}=\overline{E}$ see (41), and moreover, that the mean stress $\overline{\sigma}=\frac{1}{\left|V\right|}\int_{\xi\in V}\sigma\left(\xi\right)d\xi$ depends also linearly on $\overline{E}$. This means that there exists a mapping $\mathbb{C}^V_{\mathrm{KUBC}}$ such that $\overline{\sigma}=\mathbb{C}^V_{\mathrm{KUBC}}\,\overline{E}$. Therefore we must have

$$\frac{1}{2}\left\langle \mathbb{C}^V_{\mathrm{KUBC}}\,\overline{E},\overline{E}\right\rangle =\inf\left(\frac{1}{\left|V\right|}\int_{\xi\in V}\frac{1}{2}\left\langle \mathbb{C}\left(\xi\right)\left(\mathrm{sym}\nabla_\xi v\left(\xi\right)+\overline{E}\right),\mathrm{sym}\nabla_\xi v\left(\xi\right)+\overline{E}\right\rangle d\xi\;\Big|\; v\in\mathcal{C}^\infty_0\left(V(x),\mathbb{R}^3\right)\right).$$

In our given periodic arrangement there are many different possibilities to choose unit-cells, see Fig. 5. In the following we use an **extended Neumann's principle** [71], suitably adapted to our setting:

Extended Neumann's principle

The invariance group of every stiffness tensor of the relaxed micromorphic model should contain the maximal invariance group of the periodic metamaterial.

Applying this principle, the number of candidate unit-cells V in (49) is reduced to the 4 unit-cells from Fig. 6 showing tetragonal symmetry[15]. Finally, we determine the tensor $\mathbb{C}_{\text{micro}}$ in (46) by requiring

$$\forall\, \overline{E} \in \operatorname{Sym}(3) \;:\; \left\langle \mathbb{C}_{\text{micro}}\, \overline{E}, \overline{E} \right\rangle \geq \left\langle \mathbb{C}^V_{\text{KUBC}}\, \overline{E}, \overline{E} \right\rangle \tag{51}$$

for all 4 unit cells and in addition, any other possible tensor $\mathbb{C}^*_{\text{micro}}$, verifying (51) should satisfy

$$\left\langle \mathbb{C}^*_{\text{micro}}\, \overline{E}, \overline{E} \right\rangle \geq \left\langle \mathbb{C}_{\text{micro}}\, \overline{E}, \overline{E} \right\rangle .$$

This will define $\mathbb{C}_{\text{micro}}$ unambiguously[16]. The calculation of $\mathbb{C}^V_{\text{KUBC}}$ is then done in the FEM - framework as shown in Table 3 for all possible unit-cells V representing tetragonal symmetry.

In order to distill the missing information on $\mathbb{C}_{\text{micro}}$ in (51), we proceed as follows. Our goal is to find a positive definite tensor $\mathbb{C}_{\text{micro}}$ which is the least upper bound of the stiffness of the underlying microstructure. Since the fitting will be done in the 2D-case, we may turn to the planar Voigt representation and the inequality condition (51) can be restated as

$$\forall\, (x,y,z)^T \in \mathbb{R}^3 \;:\; \left\langle \begin{pmatrix} 2\widehat{\mu}+\widehat{\lambda} & \widehat{\lambda} & 0 \\ \widehat{\lambda} & 2\widehat{\mu}+\widehat{\lambda} & 0 \\ 0 & 0 & \widehat{\mu}^* \end{pmatrix}_{\mathbb{C}_{\text{micro}}} \begin{pmatrix} x \\ y \\ z \end{pmatrix}, \begin{pmatrix} x \\ y \\ z \end{pmatrix} \right\rangle \geq \left\langle \begin{pmatrix} 2\mu+\lambda & \lambda & 0 \\ \lambda & 2\mu+\lambda & 0 \\ 0 & 0 & \mu^* \end{pmatrix}_{\mathbb{C}^V_{\text{KUBC}}} \begin{pmatrix} x \\ y \\ z \end{pmatrix}, \begin{pmatrix} x \\ y \\ z \end{pmatrix} \right\rangle, \tag{52}$$

where (x,y,z) represents $\left(\overline{E}_{11}, \overline{E}_{22}, \overline{E}_{12}\right)$. We denote the four KUBC-entries as $\mu_i, \lambda_i, \mu_i^*,\ i = 1,2,3,4$, respectively. The question is how to obtain the values $\widehat{\mu}, \widehat{\lambda}, \widehat{\mu}^*$ such that

$$\left\langle \begin{pmatrix} 2\widehat{\mu}+\widehat{\lambda} & \widehat{\lambda} & 0 \\ \widehat{\lambda} & 2\widehat{\mu}+\widehat{\lambda} & 0 \\ 0 & 0 & \widehat{\mu}^* \end{pmatrix}_{\mathbb{C}_{\text{micro}}} \begin{pmatrix} x \\ y \\ z \end{pmatrix}, \begin{pmatrix} x \\ y \\ z \end{pmatrix} \right\rangle \geq \left\langle \begin{pmatrix} 2\mu_i+\lambda_i & \lambda_i & 0 \\ \lambda_i & 2\mu_i+\lambda_i & 0 \\ 0 & 0 & \mu_i^* \end{pmatrix} \begin{pmatrix} x \\ y \\ z \end{pmatrix}, \begin{pmatrix} x \\ y \\ z \end{pmatrix} \right\rangle, \qquad i = 1,2,3,4 \tag{53}$$

is always verified. Since μ^* sits on the diagonal, we must necessarily have that

$$\mu^* \geq \mu_i^* \qquad \forall\, i = 1,2,3,4. \tag{54}$$

Therefore, the problem is reduced to the 2×2 block

$$\forall\, (x,y)^T \in \mathbb{R}^2 \;:\; \left\langle \begin{pmatrix} 2\widehat{\mu}+\widehat{\lambda} & \widehat{\lambda} \\ \widehat{\lambda} & 2\widehat{\mu}+\widehat{\lambda} \end{pmatrix} \begin{pmatrix} x \\ y \end{pmatrix}, \begin{pmatrix} x \\ y \end{pmatrix} \right\rangle \geq \left\langle \begin{pmatrix} 2\mu_i+\lambda_i & \lambda_i \\ \lambda_i & 2\mu_i+\lambda_i \end{pmatrix} \begin{pmatrix} x \\ y \end{pmatrix}, \begin{pmatrix} x \\ y \end{pmatrix} \right\rangle, \quad i = 1,2,3,4. \tag{55}$$

According to the Sylvester-criterion for the difference of positive definite tensors (see the Appendix 11.4), we must have $\widehat{\mu} \geq \mu_i$ and $\widehat{\mu} + \widehat{\lambda} \geq \mu_i + \lambda_i$ for $i = 1,2,3,4$. We choose

$$\begin{aligned} \widehat{\mu} &:= \max_i \{\mu_i\}, & \widehat{\mu}^* &:= \max_i \{\mu_i^*\}, \\ \widehat{\mu} + \widehat{\lambda} &:= \max_i \{\mu_i + \lambda_i\}, & \widehat{\lambda} &:= \max_i \{\mu_i + \lambda_i\} - \widehat{\mu}. \end{aligned} \tag{56}$$

[15] Consider any other unit-cell. The stiffness tensor $\mathbb{C}_{\text{micro}}$ determined from (49) will not be tetragonal. The square unit-cell candidates are restricted to sidelength $a\sqrt{2}$, which is done in view of the maximal stiffness, since larger cells become less stiff.

[16] Considering the Voigt upper bound as representing the maximal microscopic stiffness is not useful for two reasons:

First, $\mathbb{C}_{\text{Voigt}}$ will be isotropic and lose the information of the geometry of the microstructure. Second, the actual deformation in the microstructure will never exhibit constant strain.

This determines μ, μ^*, λ uniquely. We have picked the highlighted values in Table 3 for $\mathbb{C}_{\text{micro}}$ in (33).

Note again that for PBCs, the geometry of the unit-cell does not matter as far as the macroscopic stiffness $\mathbb{C}_{\text{macro}}$ is concerned. In contrast, it is well known that, under affine Dirichlet conditions (see Fig. 8) the size and geometry of the unit-cell critically matters [30, 35].

Some further remarks are in order. Our approach is invariant under considering $L_c \to \infty$ and stable under perturbation of the affine boundary conditions into

$$u|_{\partial V}(x+\xi) = \overline{B} \cdot \xi + \varepsilon\, g(\xi)\,.$$

The latter with non-affine $g(\xi)$ will only induce a slight inhomogeneity of the solution on the coarse scale, the identification procedure remaining the same.

In contrast, if we consider the relaxed micromorphic model with full gradient contribution as a representative of the classical Mindlin-Eringen micromorphic approach (using ∇P instead of $\operatorname{Curl} P$), then (43) will turn into

$$\inf_{u}\left\{\int_{\xi\in V}\frac{1}{2}\left\langle \mathbb{C}_{\text{micro}}\operatorname{sym}\nabla_\xi u(x+\xi), \operatorname{sym}\nabla_\xi u(x+\xi)\right\rangle + L_c^2\left\|D_\xi^2\,\widetilde{u}\left(\frac{\xi}{\varepsilon}\right)\right\|^2 d\xi \;\middle|\; u|_{\xi\in\partial V}(x+\xi) = \overline{B}\cdot\xi + \varepsilon\, g(\xi)\right\} \tag{57}$$

which is singular for $L_c \to \infty$ and non-zero, non-affine $g(\xi)$. Now, in (57) it is not possible to separate the effects of curvature and strain over the unit-cell, as done in (49). This implies that fittings for $\mathbb{C}_{\text{micro}}$ based on (57) would be correlated to fittings of the characteristic length scale L_c. The obtained values for $\mathbb{C}_{\text{micro}}$ would be length scale dependent and would therefore not qualify as true material parameters. This observation points to the special role played by $\operatorname{Curl} P$ as the unique curvature measure in the relaxed micromorphic model. Nevertheless, static identification procedures similar to the problematic (57) have been carried out for the description of periodic composites as an equivalent couple stress continuum in [13] or a Cosserat medium in [26].

The salient features of our novel approach of parameter identification are:

- if the unit-cell is homogeneous (no contrast of material parameters), then $\mathbb{C}_{\text{micro}} = \mathbb{C}_{\text{macro}}$, $\mathbb{C}_e = +\infty$ and the relaxed micromorphic model automatically turns into classical linear elasticity with stiffness $\mathbb{C}_{\text{macro}}$ while the classical Mindlin-Eringen model would turn into a second gradient formulation.
- $\mathbb{C}_{\text{micro}}$ represents the stiffest possible linear elastic response of any admissible tetragonal unit-cell under affine Dirichlet boundary conditions.
- Both $\mathbb{C}_{\text{micro}}$ and $\mathbb{C}_{\text{macro}}$ are readily available by numerical homogenization FEM-calculations on the unit-cell level as shown before.
- Both $\mathbb{C}_{\text{micro}}$ and $\mathbb{C}_{\text{macro}}$ can be determined independently of the characteristic length-scale L_c of the relaxed micromorphic model (it remains to be seen whether L_c scales with the size of the assumed unit-cell).
- For large rigid inclusions in the unit-cell, we have in the limit of infinite rigidity that $\mathbb{C}_{\text{micro}} \to +\infty$, reducing the relaxed micromorphic model effectively to a Cosserat model (a model with "rigid microstructure").

8 Fitting material parameters and analysis of dispersion curves

In this section we will show how:

- thanks to the general anisotropic micro-macro homogenization formula developed in [8] it is possible to establish a functional dependence between the components of the tensors $\mathbb{C}_e$ and $\mathbb{C}_{\text{micro}}$ appearing in the relaxed micromorphic model and those of the elastic macroscopic elasticity tensor $\mathbb{C}_{\text{macro}}$ of the effective (Cauchy) relaxed micromorphic limit model when considering the tetragonal case. Since $\mathbb{C}_{\text{micro}}$ and $\mathbb{C}_{\text{macro}}$ are known from static arguments, $\mathbb{C}_e$ can be readily computed,
- the calculation of the cut-off frequencies provides the possibility to obtain four extra relations between the micro elastic parameters and the micro inertia terms, thus finally allowing the computation of the micro inertiae and of the Cosserat couple modulus μ_c.

8.1 Micro-macro homogenization formula

We now particularize the tensorial micro-macro homogenization formulas obtained in [8, 49, 50] for the general anisotropic framework to the tetragonal case. To this aim, we start counting the parameters of the relaxed micromorphic model for the tetragonal case, which are

$$(\mu_e, \lambda_e, \mu_e^*, \mu_c, \mu_{\text{micro}}, \lambda_{\text{micro}}, \mu^*_{\text{micro}}, \mu_{\text{macro}}, \lambda_{\text{macro}}, \mu^*_{\text{macro}}, L_c, \alpha_1, \alpha_2, \alpha_3, \alpha_1^*)$$

for the potential part of the energy and

$$(\rho, \eta_1, \eta_2, \eta_3, \eta_1^*, \overline{\eta}_1, \overline{\eta}_2, \overline{\eta}_3, \overline{\eta}_1^*)$$

for the kinetic one, then we use the fundamental homogenization formula found in [8]. In [8] it is shown that in the limit $L_c \to 0$ it is possible to homogenize the relaxed micromorphic model to a Cauchy one whose elastic (macroscopic) stiffness $\mathbb{C}_{\text{macro}}$ is linked to the relaxed micromorphic material parameters, $\mathbb{C}_{\text{micro}}, \mathbb{C}_e$ by the relation

$$\begin{aligned} &\mathbb{C}_{\text{macro}} = \mathbb{C}_{\text{micro}} \left(\mathbb{C}_{\text{micro}} + \mathbb{C}_e\right)^{-1} \mathbb{C}_e \\ \iff \quad &\mathbb{C}_e = \mathbb{C}_{\text{micro}} \left(\mathbb{C}_{\text{micro}} - \mathbb{C}_{\text{macro}}\right)^{-1} \mathbb{C}_{\text{macro}}, \end{aligned} \tag{58}$$

which, in our tetragonal case, gives the identities

$$\begin{aligned} &\mu_{\text{macro}} = \frac{\mu_e\, \mu_{\text{micro}}}{\mu_e + \mu_{\text{micro}}}, \qquad 2\mu_{\text{macro}} + 3\lambda_{\text{macro}} = \frac{(2\mu_e + 3\lambda_e)\,(2\mu_{\text{micro}} + 3\lambda_{\text{micro}})}{2\,(\mu_e + \mu_{\text{micro}}) + 3\,(\lambda_e + \lambda_{\text{micro}})}, \qquad \mu^*_{\text{macro}} = \frac{\mu_e^*\, \mu^*_{\text{micro}}}{\mu_e^* + \mu^*_{\text{micro}}}, \\ &\qquad\qquad\qquad\qquad\qquad\qquad \iff \\ &\mu_e = \frac{\mu_{\text{macro}}\, \mu_{\text{micro}}}{\mu_{\text{micro}} - \mu_{\text{macro}}}, \qquad 2\mu_e + 3\lambda_e = \frac{(2\mu_{\text{macro}} + 3\lambda_{\text{macro}})\,(2\mu_{\text{micro}} + 3\lambda_{\text{micro}})}{(2\mu_{\text{micro}} + 3\lambda_{\text{micro}}) - (2\mu_{\text{macro}} + 3\lambda_{\text{macro}})}, \qquad \mu_e^* = \frac{\mu^*_{\text{macro}}\, \mu^*_{\text{micro}}}{\mu^*_{\text{micro}} - \mu^*_{\text{macro}}}. \end{aligned} \tag{59}$$

Equations (59) give the explicit relations between the parameters of the tetragonal relaxed micromorphic model and the corresponding macroscopic parameters of the Cauchy model seen as a limiting case of the relaxed micromorphic model when $L_c \to 0$.

The importance of this micro-macro homogenization formula can hardly be overestimated. Indeed, it allows for calibrating the a priori unknown material parameters of the linear relaxed micromorphic model $\mathbb{C}_e$ against the in principle known and measurable macroscopic response $\mathbb{C}_{\text{macro}}$ and microscopic response $\mathbb{C}_{\text{micro}}$. In our case, $\mathbb{C}_{\text{macro}}$ has been obtained via numerical homogenization of periodic media (see Section 7.1). On the other hand, $\mathbb{C}_{\text{macro}}$ can be equivalently determined from a comparison with the Bloch-Floquet analysis as it will be shown in the Appendix 11.6. More precisely, we will show how the macroscopic parameters $\mu_{\text{macro}}, \lambda_{\text{macro}}$ and μ^*_{macro} can be directly related to the slopes of the acoustic branches of a Cauchy continuum with tetragonal symmetry, and this will allow the determination of the macro parameters for the given metamaterial. We will check that the macro parameters obtained with the two methods turn out to be the same.

The clear physical interpretation of the micro stiffnesses $\mathbb{C}_{\text{micro}}$, on the other hand, is more complicated. Indeed, we know that such micro stiffnesses must be related to the mechanical properties of the unit-cell and true experimental static tests should be run on a specimen composed by a single unit-cell in order to obtain their values. As we showed in Section 7.2, different stiffnesses of the unit-cell can be obtained when changing the representative unit-cell for the same metamaterial. However, we established rigorously that the elastic parameters of the stiffest response on the microscale must be chosen as $\mathbb{C}_{\text{micro}}$.

Once the macro and micro parameters $\mathbb{C}_{\text{macro}}$ and $\mathbb{C}_{\text{micro}}$ have been determined, the micro-macro homogenization formula (58) allows us to uniquely determine the stiffness $\mathbb{C}_e$ which realizes the transition between the macro and micro scale. In particular, for the considered tetragonal metamaterial, and considering the values of $\mathbb{C}_{\text{macro}}$ and $\mathbb{C}_{\text{micro}}$ given in Tables 2 and 3 respectively, the values of $\mathbb{C}_e$ given in Table 4 can be easily computed through the homogenization formula (59).

λ_e	μ_e	μ_e^*
[GPa]	[GPa]	[GPa]
-0.11	17.34	0.67

Table 4: Obtained numerical values for the parameters related to the transition scale. The tensor $\mathbb{C}_e$ remains positive definite.

8.2 Cut offs for the optic branches

Thanks to the determination of $\mathbb{C}_{\text{macro}}$ and $\mathbb{C}_{\text{micro}}$ based on the static arguments presented in Section 7 and that of $\mathbb{C}_e$ through formula (58), only the Cosserat couple modulus μ_c remains to be determined as far as the purely elastic parameters are concerned. On the other hand, all the micro inertiae $\eta_1, \eta_1^*, \eta_2, \eta_3, \overline{\eta}_1, \overline{\eta}_1^*, \overline{\eta}_2, \overline{\eta}_3$ appearing in the kinetic energy (10) remain to be determined as well. To this aim we consider the so-called cut-off frequencies. Solving the equation $\det \widetilde{D} = 0$ imposing that $k = 0$, we find the following characteristic frequencies:

$$\omega_r = \sqrt{\frac{\mu_c}{\eta_2}}, \qquad \omega_s = \sqrt{\frac{\mu_e + \mu_{\text{micro}}}{\eta_1}}, \qquad \omega_s^* = \sqrt{\frac{\mu_e^* + \mu_{\text{micro}}^*}{\eta_1^*}}, \qquad \omega_p = \sqrt{\frac{\mu_e + \mu_{\text{micro}} + \lambda_e + \lambda_{\text{micro}}}{\eta_1 + \eta_3}}. \tag{60}$$

Such characteristic frequencies correspond to the starting point ($k = 0$) of the dispersion curves and are known as cut-off frequencies. They are independent of the wave direction.

The simple fact of imposing that such characteristic frequencies are equal to the numerical values of the cut-offs calculated via the Bloch-Floquet analysis (see Fig.(2)) allows us to establish specific relations for computing some of the parameters of the relaxed micromorphic model which are still free. In particular, as we will show in the next Section, the last three formulas of equation (60) enable us to compute η_1, η_1^* and η_3.

8.3 Fitting of the parameters on the dispersion curves

In this Section we show the fitting procedure that we used to calibrate the remaining free parameters of our relaxed micromorphic model on the metamaterial introduced in Section 5. To do so, we denote by $\overline{\omega}_r, \overline{\omega}_s, \overline{\omega}_p$ and $\overline{\omega}_s^*$ the numerical values of the cut-offs calculated by the Bloch-Floquet analysis. Moreover, we also denote by $\overline{a}_{\text{L}}$ and $\overline{a}_{\text{T}}$ the numerical values of the slopes of the tangents to the acoustic curves obtained via the Bloch-Floquet analysis. Note again that the third (out-of-plane) acoustic branch is not present in this case since we implemented a Bloch-Floquet analysis of a fully 2D metamaterial. In Fig. 9 we identify such numerical quantities. We explicitly remark that if the numerical values of the cut-off frequencies directly allow the computation of some micro inertiae, the identification of the numerical value of the slopes is not essential for the calibration procedure, given that the purely elastic parameters have already been determined. Nevertheless, as we will show in Appendix 11.6 the numerical determination of the slopes of the acoustic curves allows on the one hand to provide an alternative method for the computation of the macro parameters $\mathbb{C}_{\text{macro}}$ and, on the other hand, to clearly connect the relaxed micromorphic model to the corresponding equivalent Cauchy homogenized continuum.

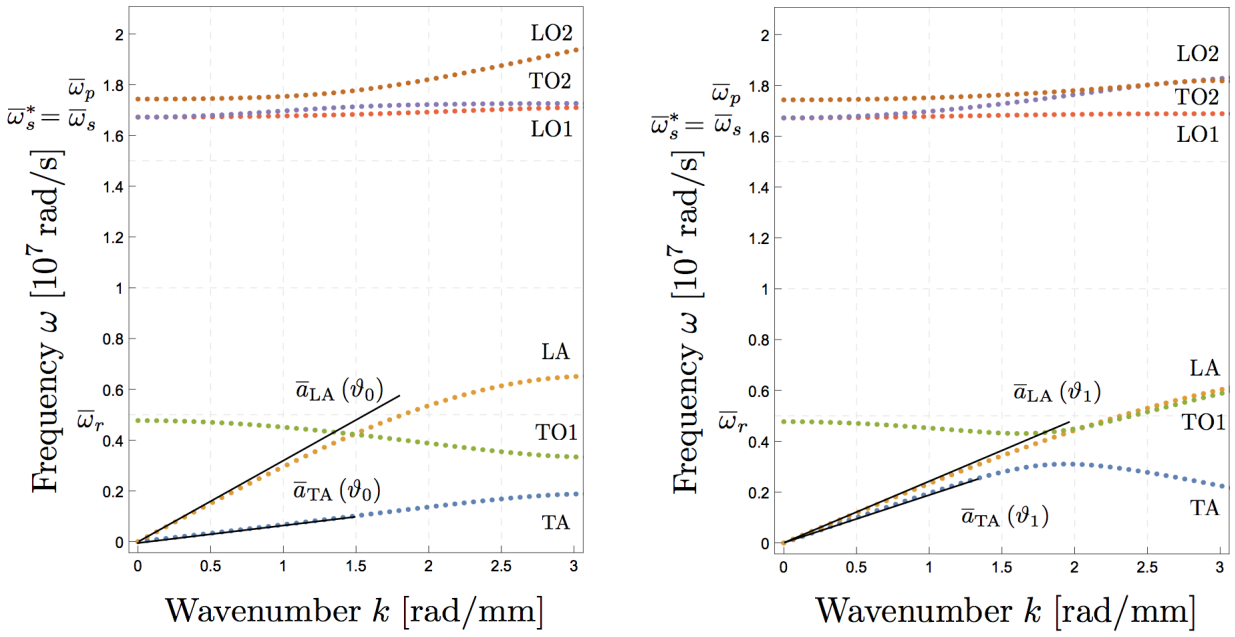

Figure 9: Dispersion curves of the selected metamaterial and identification of the key numerical quantities needed for the fitting procedure. The cut off frequency $\omega_r, \omega_s, \omega_s^*$ and ω_p are direction independent, while the tangents to the acoustic curves $\overline{a}_{\mathrm{TA}}$ and $\overline{a}_{\mathrm{LA}}$ depend on the direction of wave propagation.

The numerical values of the cut-off frequencies corresponding to Fig. 9 are given in Table 5.

$\overline{\omega}_r$	$\overline{\omega}_s$	$\overline{\omega}_s^*$	$\overline{\omega}_p$
[rad/s]	[rad/s]	[rad/s]	[rad/s]
$0.4 \cdot 10^7$	$1.68 \cdot 10^7$	$1.68 \cdot 10^7$	$1.75 \cdot 10^7$

Table 5: Numerical values of the cut-offs for the considered metamaterial.

At this point, replacing in the last three equations (60) the values of the cut-off frequencies given in Table 5 as well as the values of the elastic parameters given in Tables 3 and 4, we can uniquely determine η_1, η_1^* and η_3, obtaining the values in Table 6.

η_1	η_3	η_1^*
[kg/m]	[kg/m]	[kg/m]
$9.3 \cdot 10^{-5}$	$0.95 \cdot 10^{-5}$	$3.19 \cdot 10^{-5}$

Table 6: Numerical values for micro inertia parameters.

The parameters of the relaxed micromorphic model which remain free after these considerations are $\eta_2, \overline{\eta}_1, \overline{\eta}_2, \overline{\eta}_3, \overline{\eta}_1^*$. To complete the fitting procedure, we start slowly increasing these free parameters, starting from zero, so as to optimally fit dispersion curves of Fig. 9 both for $\vartheta = 0$ and $\vartheta = \pi/4$. The order with which the free inertia parameters are increased is related to the effect that such parameters have on the dispersion curves. More particularly:

- η_2 and $\overline{\eta}_2$ have an effect on the acoustic curves LA and TA and are adjusted to best fit such curves,
- the remaining parameters $\overline{\eta}_1, \overline{\eta}_1^*, \overline{\eta}_3$ are eventually increased only for fine-tuning the fitting. Their effect is mainly visible for higher wavenumber (smaller wavelength).

As for the characteristic length L_c, we set here $L_c = 0$. Nevertheless, we know that a non-vanishing L_c is a crucial point for a finer fitting of the dispersion curves. On the other hand, this task is really delicate and we need to postpone it to a further work where a micro-inertia related to Curl $P_{,t}$ will also be introduced.

Summarizing the results obtained up to now, we show in Table 7 the values for the inertiae and in Table 8 a summary of all the elastic parameters computed before.

ρ	η_1	η_2	η_3	η_1^*	$\overline{\eta}_1$	$\overline{\eta}_2$	$\overline{\eta}_3$	$\overline{\eta}_1^*$
$\left[\text{kg/m}^3\right]$	[kg/m]	[kg/m]	[kg/m]	[kg/m]	[kg/m]	[kg/m]	[kg/m]	[kg/m]
1485	$9.3 \cdot 10^{-5}$	$1 \cdot 10^{-7}$	$0.95 \cdot 10^{-5}$	$3.19 \cdot 10^{-5}$	$4.8 \cdot 10^{-5}$	0	0	0

Table 7: Summary of the numerical values for inertia parameters.

λ_e	μ_e	μ_e^*	λ_{micro}	μ_{micro}	μ_{micro}^*	μ_c	λ_{macro}	μ_{macro}	μ_{macro}^*
[GPa]	[GPa]	[GPa]	[GPa]	[GPa]	[GPa]	[GPa]	[GPa]	[GPa]	[GPa]
-0.11	17.34	0.67	5.27	8.93	8.33	$1.85 \cdot 10^{-3}$	1.74	5.89	0.62

Table 8: Summary of the numerical values for the elastic parameters of the tetragonal relaxed micromorphic model in 2D. The macroscopic parameters of the resulting homogenized metamaterial are also provided in the last Table. The values related to $\mathbb{C}_e$ still define a positive definite tensor.

In Fig. 10 we show the obtained fitting for $\vartheta = 0$ and $\vartheta = \pi/4$.

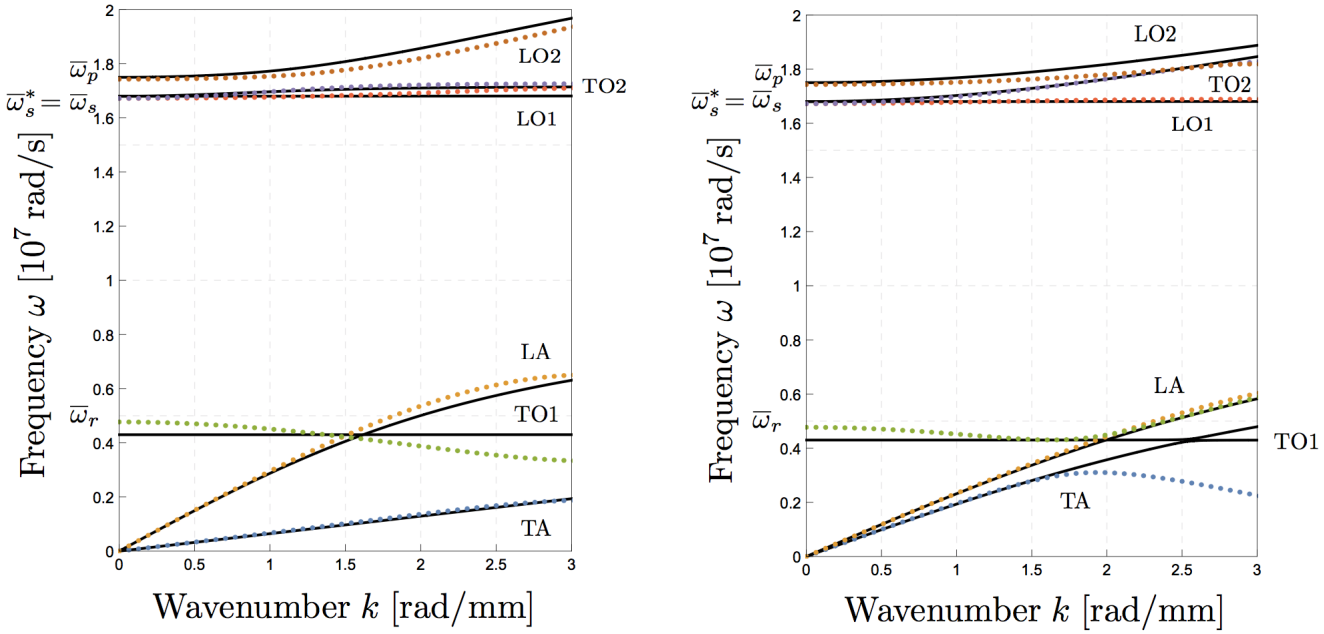

Figure 10: Comparison between our relaxed micromorphic continuum model and the COMSOL® one. In (a) we plot the dispersion branches for $\widehat{\boldsymbol{k}} = (1, 0, 0)$ and in (b) for $\widehat{\boldsymbol{k}} = \left(\sqrt{2}/2, \sqrt{2}/2, 0\right)$. Dotted lines represent COMSOL® dispersion curves, continuous lines represent the dispersion curves obtained with the relaxed micromorphic model. The two directions $\widehat{\boldsymbol{k}}$ are used in the fitting procedure.

The result is quite satisfactory for a wide range of wavelengths. The only relevant differences can be found in the curve TO_1 both for $\vartheta = 0$ and $\vartheta = \pi/4$ and TA at $\vartheta = \pi/4$. This discrepancy is mainly due to the fact that at present the relaxed micromorphic model is not yet able to give rise to decreasing dispersion curves. Such possibility will be taken into account in future work by adding suitably non-local terms in the kinetic energy and considering $L_c > 0$.

At this point we want to strongly remark that the parameter calibration that we present in Section 7 and 8 is the most natural and simple approach imaginable using enriched continuum models. Indeed, the elastic parameters

are calibrated on simple mechanical tests on both macro and micro specimens of the considered metamaterial. On the other hand, dynamical parameters (micro-inertiae) are determined by imposing simple relations on the cut-off frequencies. After that, very few parameters remain free and they are slowly varied to improve the fitting of the dispersion curves at higher wavenumbers (small wavelengths). We can hence strongly claim that we are providing a transparent and efficient characterization of the considered mechanical metamaterial by means of an enriched continuum model.

Our method is physics-based and it is far-away from parameter fittings that are often provided when dealing with the superposition of generalized continuum models to phenomenological data: we do not need to calibrate a huge number of parameters by using "ad hoc" optimization methods, we just obtain the fitting as a simple consequence of our mechanical observations.

We also remark that slight differences can be found in the fitting for some of the higher optic curves when considering high wavenumbers (wavelength smaller than twice the unit-cell), while in general most of the dispersion curves fit well the overall behavior also for wavelength which go down to the size of the unit-cell. We will show in further works that generalizing the expression of the kinetic energy will allow to obtain an even better fitting for the whole considered range of wavelengths.

9 Predictive analysis of dispersion and anisotropy in tetragonal metamaterials

In this Section we show the capability of the anisotropic relaxed micromorphic model to describe complex phenomena in specific metamaterials.

We have already seen in Section 5 that the metamaterial targeted in this paper has a tetragonal symmetry. Moreover, in Sections 7 and 8 we have developed the procedure allowing to calibrate the material parameters of the relaxed micromorphic model on the considered metamaterial.

In the present Section, we show that the relaxed micromorphic model, as calibrated on the considered tetragonal metamaterial, is able to simultaneously reproduce very complex observable macroscopic phenomena, namely

- the dispersive behavior both for the acoustic and the optic curves,
- anisotropic (tetragonal) mechanical behavior of the considered metamaterial for the first six modes.

The first characteristic, i.e. the dispersive behavior of the metamaterial, has already been underlined in the previous Section when noticing that the dispersion curves are not straight lines, but curves. This means that the speed of propagation of each mode is not a constant (as is the case in classical Cauchy continua) but varies when changing the wavelength of the travelling wave. We show again in this Section how the dispersive behavior of the considered metamaterial can be highlighted by introducing the concept of phase velocity. The **phase velocity** is defined as the ratio $\omega(k)/k$ and, in dispersive media, changes when changing the wavenumber (or equivalently the wavelength).

The phase velocity also changes when changing the direction of propagation of the travelling wave if the considered medium is not isotropic. Both such features of the phase velocity are easily understandable since:

- the speed of propagation of waves reasonably changes when the travelling wave reaches a wavelength which is comparable to the characteristic size of the underlying microstructure. Such wavelength are easily attainable for the most common metamaterials for which the microstructure has typically the size of millimeters or more,
- if the medium is anisotropic, i.e. if its deformation response varies when varying the direction of application of the external load, it is clear that the speed of propagation of waves inside the medium changes as well when changing the direction of propagation of the travelling wave itself.

We can simultaneously show both such characteristics (anisotropy and dispersion) by looking at the polar plots of the phase velocity $\omega(k)/k$ for each mode and for different values of the wavenumber k and of the angle ϑ giving the direction of propagation of the travelling wave.

We start presenting the case of a classical tetragonal non-dispersive Cauchy medium (see Fig. 11).

In Fig. 11 we show the polar plots of the phase velocity ω/k for the tetragonal Cauchy continuum which is obtained as a limiting case of the relaxed micromorphic model as fitted on the considered tetragonal metamaterial (see Sections 7.1 and 11.6). More particularly, Fig. 11 shows that:

1. the two acoustic modes which are described by the Cauchy theory do not describe dispersion. In fact, since in Cauchy theory the dispersion curve is a straight line, once fixed the value of k, the phase velocity ω/k takes

limit macroscopic Cauchy model

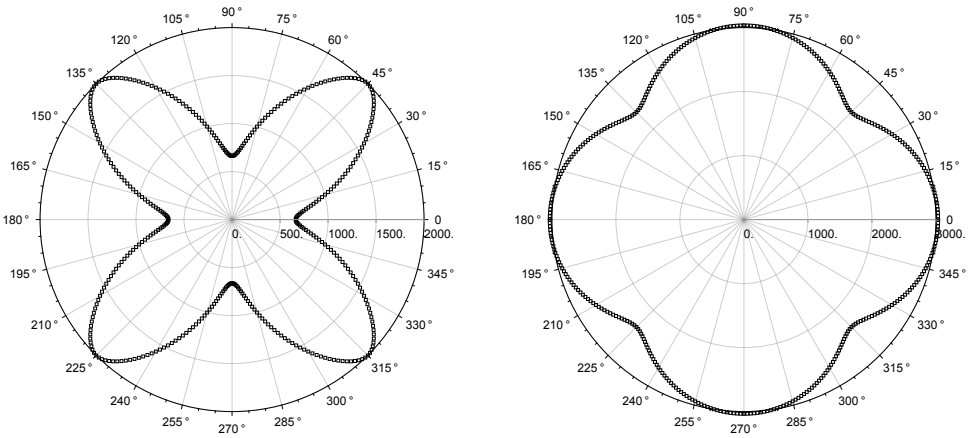

TA **LA**

Figure 11: Polar plots of the phase velocity ω/k for the two acoustic modes of the equivalent tetragonal Cauchy medium, the elastic parameters of which are related to those of the relaxed micromorphic model through formulas (59) and using the values given in Table 9. In each plot, each radial line from zero indicates the direction of propagation of the travelling wave and the length of any segment going from zero to a point of the curve is the measure of the phase velocity ω/k in the considered direction.

a constant value for any chosen value of k. It is for this reason that, in Cauchy media, we find only one curve in the polar plot of the phase velocity.

2. Cauchy theory can only describe the first two acoustic modes without any possibility of describing higher modes.

According to these observations, it becomes clear that a Cauchy theory is too restrictive for describing the rich behavior of metamaterials.

As already remarked, second gradient theories could somewhat improve the description of the dispersive behaviors with respect to the Cauchy theory, but in any case only the first 2 modes could be analyzed in the 2D case.

As far as the relaxed micromorphic model is concerned, we will show in the remainder of this Section that it is able to describe:

- not only the first two, but also other modes related to higher frequencies,
- anisotropy, not only for the first two, but also for the other modes,
- dispersion for all the considered modes (here the first 6).

We can start remarking from Fig. 12 that the transverse acoustic mode is perfectly described for lower values of k (external curve), while some differences with the Bloch-Floquet analysis of the metamaterial arise for higher values of k (more internal curves).

The larger difference can be detected for waves travelling at 45°. This is coherent with Fig. 10(b) in which it can be easily seen that the transverse wave TA calculated via the relaxed micromorphic model starts diverging from the one calculated via the Block-Floquet analysis when increasing the value of k. This means that, as far as the transverse acoustic mode TA is concerned, its description via the relaxed micromorphic model is less accurate when considering propagation at 45° and higher wavenumbers (smaller wavelengths). As a matter of fact, the description of the TA mode at 45° starts being less accurate for wavelengths twice the characteristic size of the unit-cell and smaller[17].

[17]One could argue that an effective medium model like the relaxed micromorphic model should only be operative in describing the response for wavelength larger than a certain threshold, like e.g. 4 times the unit-cell. This is not our point of view. We are optimistic to calibrate the relaxed micromorphic model up to wavelength comparable to the chosen size of the unit-cell used in the static homogenization for $\mathbb{C}_{\text{micro}}$.

This lack of accuracy for small wavelengths is not present for the longitudinal acoustic mode LA for which the relaxed micromorphic model describes well the behavior of the LA curve for all directions of propagation and for wavelengths which become very small and even comparable to the size of the unit-cell.

The behavior of the curve TO_1 has to be considered carefully. Indeed, we fitted our relaxed micromorphic model to the TO_1 dispersion curve with an almost horizontal curve. We are hence able to recover for this mode the average dispersive behavior, but not the true patterns of the phase velocity which show anisotropic behaviors for higher wavenumbers (smaller wavelengths). This behavior will be improved in further works when the non-locality of the matematerial will be considered by considering $L_c > 0$ and by adding a term $\operatorname{Curl} P_{,t}$ in the kinetic energy.

We also recall that the relaxed micromorphic model is able to catch some other essential features of the description of the considered metamaterial, such as the presence of band-gaps (see Fig.10).

Based on some preliminary studies, we already know that the typical decreasing behavior of the TO_1 curve obtained via the Bloch-Floquet analysis can be described by the relaxed micromorphic model if we allow it to include non local effects. In other words, if we consider the case $L_c > 0$, a better and finer fitting of the TO_1 curve could be obtained. Nevertheless, the study of this additional case deserves extra attention since an extra micro-inertia term involving $\operatorname{Curl} P_{,t}$ should also be considered. We will hence treat such complete non-local cases in further works, building on the results presented here.

In Fig. 13 we can see that the relaxed micromorphic model describes almost perfectly both dispersion and anisotropy for the higher optic modes.

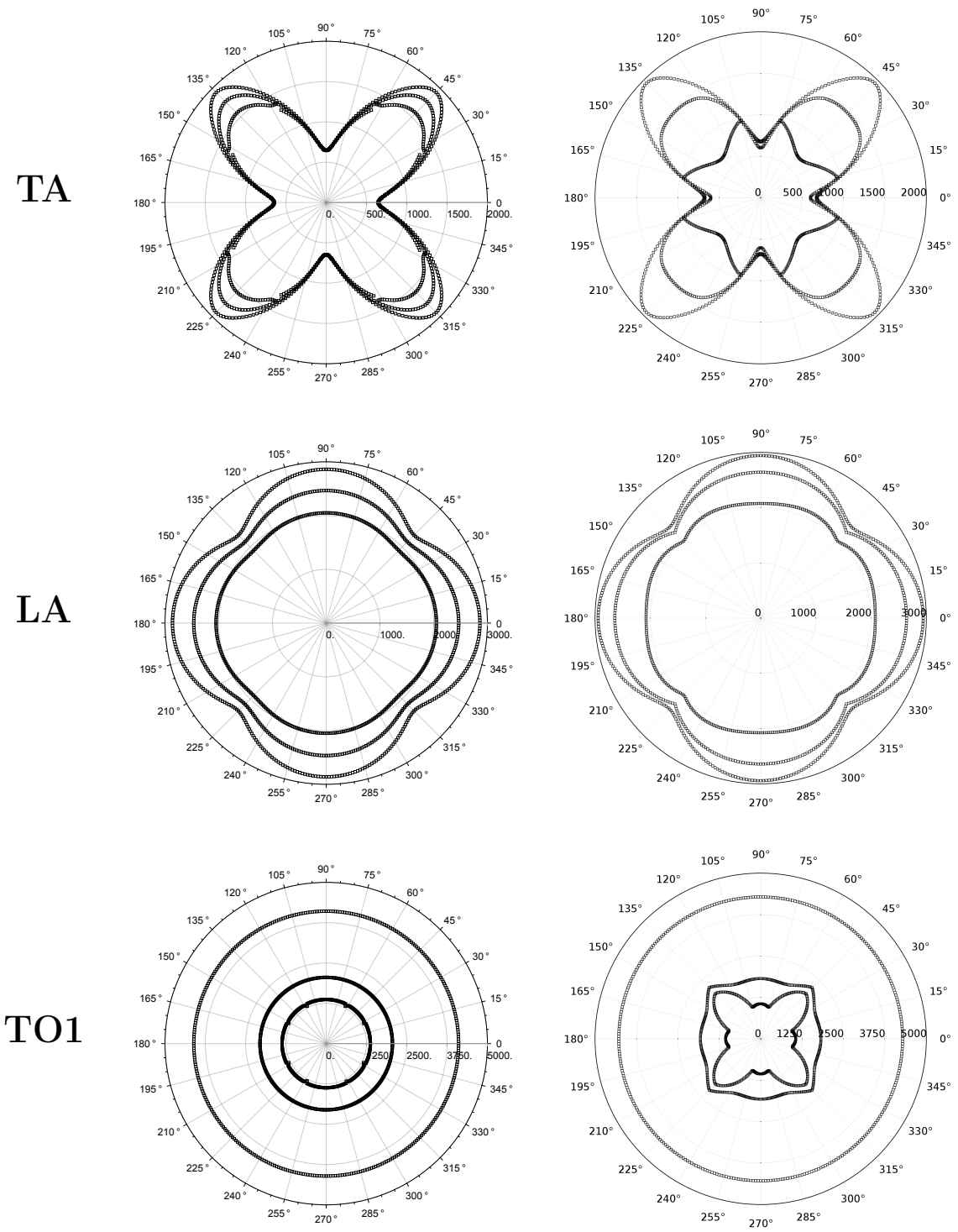

Figure 12: Phase velocity as a function of the direction of wave propagation $\widehat{\boldsymbol{k}}$ for the first three modes as calculated with the relaxed micromorphic model (left) and with the Bloch-Floquet analysis (right). The plotted curves have been calculated for the values of the wave number equal to $\pi, \dfrac{2\pi}{3}, \dfrac{\pi}{3}\,\dfrac{[\text{rad}]}{[\text{mm}]}$. For any curve, the distance from the center of the circle to a point of the curve itself gives the value of the phase velocity ω/k. More external curves are relative to lower values of k, while the curves become closer to the origin when increasing the value of k. The most internal curve corresponds to a wavelength comparable to the unit-cell.

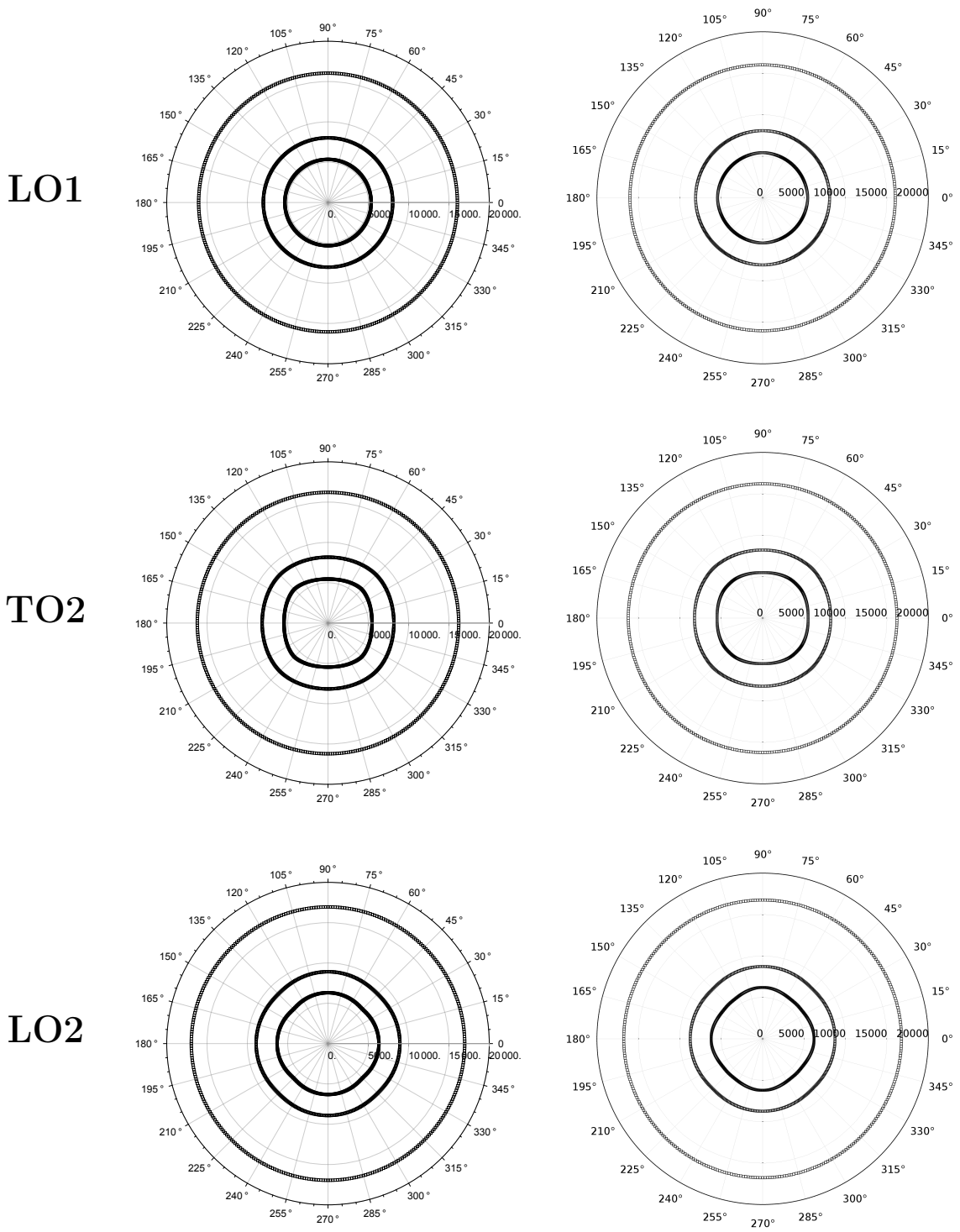

Figure 13: Phase velocity as a function of the direction of wave propagation $\widehat{\boldsymbol{k}}$ for higher modes as calculated with the relaxed micromorphic model (left) and with the Bloch-Floquet analysis (right). The plotted curves have been calculated for the values of the wave number equal to π, $\frac{2\pi}{3}$, $\frac{\pi}{3}$ $\frac{[\text{rad}]}{[\text{mm}]}$. For any curve, the distance from the center of the circle to a point of the curve itself gives the value of the phase velocity ω/k. More external curves are relative to lower values of k, while the curves become closer to the origin when increasing the value of k. The most internal curve corresponds to a wavelength comparable to the unit-cell.

10 Conclusion and further perspectives

In this paper we have particularized the general anisotropic relaxed micromorphic model developed in [8] to the case of tetragonal symmetry. We show that this particular symmetry class allows us to describe the anisotropic behavior of a band-gap metamaterial with specific tetragonal microstructure.

We explicitly show the true advantage of using the relaxed micromorphic model [8] in describing the mechanical behavior of metamaterials by introducing only standard fourth order elasticity tensors (in Voigt-notation) as it is the case for classical elasticity. This efficient theoretical framework allows us to avoid unnecessary complexifications related e.g. to the introduction of elastic tensors of order higher than four, as it is the case for higher gradient elasticity (see e.g. [6, 56, 57]). Indeed, the study of the anisotropy classes of the tensors appearing in the relaxed micromorphic model follows the classical lines and does not require any extra development.

Once it has been established that the selected metamaterial has a tetragonal symmetry, we particularize the anisotropic relaxed micromorphic model to this case. As a second step, we set up a fitting procedure to determine the values of the parameters of the relaxed micromorphic model by i) computing the purely elastic parameters via suitably conceived static tests and ii) obtaining the values of dynamical parameters by superimposing the dispersion curves obtained with the relaxed micromorphic model to the corresponding ones obtained with a classical Bloch-Floquet analysis. The relaxed micromorphic model is a "macroscopic continuum" homogenized model which is able to reproduce the response of the selected metamaterial with only few material parameters which do not depend on frequency. We have mathematically justified that the tensor $\mathbb{C}_{\text{micro}}$ can be identified with the Löwner-half-order matrix-supremum of suitable stiffness tensors on the microscale. To our understanding this identification is entirely new. In contrast, $\mathbb{C}_{\text{macro}}$ follows from standard periodic homogenization and determines the mesoscale elasticity tensor $\mathbb{C}_e$ via the micro-macro homogenization formula (58)

$$\mathbb{C}_e = \mathbb{C}_{\text{micro}} \left(\mathbb{C}_{\text{micro}} - \mathbb{C}_{\text{macro}}\right)^{-1} \mathbb{C}_{\text{macro}}.$$

In this micro-macro homogenization formula we need to have that $\mathbb{C}_{\text{micro}} - \mathbb{C}_{\text{macro}}$ is positive definite (and therefore invertible). For this, consider

$$\begin{aligned}
&|V(x)| \frac{1}{2} \left\langle \left(\mathbb{C}_{\text{micro}} - \mathbb{C}_{\text{macro}}\right) \overline{E}, \overline{E} \right\rangle \geq |V(x)| \frac{1}{2} \left\langle \left(\mathbb{C}^V_{\text{KUBC}} - \mathbb{C}_{\text{macro}}\right) \overline{E}, \overline{E} \right\rangle \qquad (61)\\
&= \inf \left\{ \int_{\xi \in V(x)} \frac{1}{2} \left\langle \mathbb{C}(\xi) \left(\text{sym}\nabla_\xi v(\xi) + \overline{E}\right), \text{sym}\nabla_\xi v(\xi) + \overline{E} \right\rangle d\xi \;\middle|\; v \in \mathcal{C}_0^\infty \left(V(x), \mathbb{R}^3\right) \right\} \\
&\qquad - \inf \left\{ \int_{\xi \in V(x)} \frac{1}{2} \left\langle \mathbb{C}(\xi) \left(\text{sym}\nabla_\xi v(\xi) + \overline{E}\right), \text{sym}\nabla_\xi v(\xi) + \overline{E} \right\rangle d\xi \;\middle|\; v \in \mathcal{C}^\infty \left(V(x), \mathbb{R}^3\right) \text{ is periodic} \right\} \\
&=: Q\left(\overline{E}, \overline{E}\right).
\end{aligned}$$

By compactness it would be sufficient for strict positive definiteness of $\mathbb{C}_{\text{micro}} - \mathbb{C}_{\text{macro}}$ that $Q\left(\overline{E}, \overline{E}\right) > 0 \; \forall \overline{E} \in \text{Sym}(3)$. Although it is easy to see that $Q\left(\overline{E}, \overline{E}\right) \geq 0$ in general, it remains to investigate under which assumptions on the geometry and material of the unit-cell this property can be established for other metamaterials. This will be subject of further research.

We did not yet approach the determination of the static curvature parameters, i.e. the characteristic length scale L_c (11). This will be greatly facilitated in future works since we already know the size-independent material parameters $\mathbb{C}_{\text{micro}}$ and $\mathbb{C}_{\text{macro}}$. It suffices then, in principle, to perform a range of inhomogeneous boundary value problems which activate the curvature terms of the relaxed micromorphic model in order to fit L_c, $\mathbb{L}$ and $\mathbb{L}_c$ via the Hill-Mandel energy equivalence condition.

The advantage of our continuum model can be found in the perspective of modeling metamaterials in a simplified framework with transparent mechanical interpretation and thus by so providing a concrete possibility for the design of the relatively complex metastructures by means of the use of a relatively simplified model.

Moreover, the fact that such an enriched continuum model is available allows us to simplify the study of other problems that would be otherwise difficult to treat, such as, e.g., the study of interfaces between different anisotropic metamaterials.

The pertinence of the proposed model is shown not only on the dispersion curves but also on the polar plots of the phase velocity which are in good agreement with the analogous results obtained by means of the discrete approach. The few differences that can be found between the discrete and the continuum model are limited to few

modes and to high wavenumbers (small wavelengths). Such differences will be treated in future works in which the role of the non-local inertia terms will be investigated together with the case of non-vanishing characteristic length $L_c > 0$.

Future investigations will also focus on the mechanical characterization of a larger class of band-gap metamaterials with the final aim of the FE-implementation of morphologically complex band-gap metastructures.

Finally, the application of the relaxed micromorphic model to more complex metamaterials including e.g. piezoelectric effects will also be investigated.

Acknowledgements

The work of I.D. Ghiba was supported by a grant of the "Alexandru Ioan Cuza" University of Iasi, within the Research Grants program, Grant UAIC, code GI-UAIC-2017-10.

11 Appendix

11.1 Variation of the kinetic energy

$$\begin{aligned}
\delta\int_0^T\int_\Omega J\left(u_{,t},\nabla u_{,t},P_{,t}\right)dm\,dt &= \delta\int_0^T\int_\Omega \frac{1}{2}\Big(\left\langle \rho\, u_{,t},u_{,t}\right\rangle + \left\langle \mathbb{J}_{\text{micro}}\,\text{sym}\,P_{,t},\text{sym}\,P_{,t}\right\rangle + \left\langle \mathbb{J}_c\,\text{skew}\,P_{,t},\text{skew}\,P_{,t}\right\rangle\\
&\quad + \left\langle \mathbb{T}\,\text{sym}\,\nabla u_{,t},\text{sym}\,\nabla u_{,t}\right\rangle + \left\langle \mathbb{T}_c\,\text{skew}\,\nabla u_{,t},\text{skew}\,\nabla u_{,t}\right\rangle\Big)dm\,dt\\
&= \underbrace{\rho\int_0^T\int_\Omega \left\langle u_{,t},\delta u_{,t}\right\rangle dm\,dt}_{\mathsf{K}_1} + \underbrace{\int_0^T\int_\Omega \left\langle \mathbb{J}_{\text{micro}}\,\text{sym}\,P_{,t},\text{sym}\,\delta P_{,t}\right\rangle dm\,dt}_{\mathsf{K}_2}\\
&\quad + \underbrace{\int_0^T\int_\Omega \left\langle \mathbb{J}_c\,\text{skew}\,P_{,t},\text{skew}\,\delta P_{,t}\right\rangle dm\,dt}_{\mathsf{K}_3} + \underbrace{\int_0^T\int_\Omega \left\langle \mathbb{T}\,\text{sym}\,\nabla u_{,t},\text{sym}\,\nabla\delta u_{,t}\right\rangle dm\,dt}_{\mathsf{K}_4}\\
&\quad + \underbrace{\int_0^T\int_\Omega \left\langle \mathbb{T}_c\,\text{skew}\,\nabla u_{,t},\text{skew}\,\nabla\delta u_{,t}\right\rangle dm\,dt}_{\mathsf{K}_5}.
\end{aligned}$$

Integrations by parts:

$$\begin{aligned}
\mathsf{K}_1 &= \rho\int_0^T\int_\Omega \frac{d}{dt}\left\langle u_{,t},\delta u\right\rangle dm\,dt - \rho\int_0^T\int_\Omega \left\langle u_{,tt},\delta u\right\rangle dm\,dt\\
&= \rho\int_0^T \frac{d}{dt}\left(\int_\Omega \left\langle u_{,t},\delta u\right\rangle dm\right)dt - \rho\int_0^T\int_\Omega \left\langle u_{,tt},\delta u\right\rangle dm\,dt\\
&= \rho\int_{\Omega\times\{T\}} \left\langle u_{,t}\left(x,T\right),\delta u\left(x,T\right)\right\rangle dm\,dt - \rho\int_{\Omega\times\{0\}} \left\langle u_{,t}\left(x,0\right),\delta u\left(x,0\right)\right\rangle dm\,dt - \rho\int_0^T\int_\Omega \left\langle u_{,tt},\delta u\right\rangle dm\,dt.
\end{aligned}$$

$$\begin{aligned}
\mathsf{K}_2 &= \int_0^T\int_\Omega \frac{d}{dt}\left\langle \mathbb{J}_{\text{micro}}\,\text{sym}\,P_{,t},\text{sym}\,\delta P\right\rangle dm\,dt - \int_0^T\int_\Omega \left\langle \mathbb{J}_{\text{micro}}\,\text{sym}\,P_{,tt},\text{sym}\,\delta P\right\rangle dm\,dt\\
&= \int_0^T \frac{d}{dt}\left(\int_\Omega \left\langle \mathbb{J}_{\text{micro}}\,\text{sym}\,P_{,t},\delta P\right\rangle dm\right)dt - \int_0^T\int_\Omega \left\langle \mathbb{J}_{\text{micro}}\,\text{sym}\,P_{,tt},\delta P\right\rangle dm\,dt\\
&= \int_{\Omega\times\{T\}} \left\langle \mathbb{J}_{\text{micro}}\,\text{sym}\,P_{,t}\left(x,T\right),\delta P\left(x,T\right)\right\rangle dm - \int_{\Omega\times\{0\}} \left\langle \mathbb{J}_{\text{micro}}\,\text{sym}\,P_{,t}\left(x,0\right),\delta P\left(x,0\right)\right\rangle dm\\
&\quad - \int_0^T\int_\Omega \left\langle \mathbb{J}_{\text{micro}}\,\text{sym}\,P_{,tt},\delta P\right\rangle dm\,dt.
\end{aligned}$$

$$\begin{aligned}
\mathsf{K}_3 &= \int_0^T\int_\Omega \frac{d}{dt}\left\langle \mathbb{J}_c\,\text{skew}\,P_{,t},\text{skew}\,\delta P\right\rangle dm\,dt - \int_0^T\int_\Omega \left\langle \mathbb{J}_c\,\text{skew}\,P_{,tt},\text{skew}\,\delta P\right\rangle dm\,dt\\
&= \int_0^T \frac{d}{dt}\left(\int_\Omega \left\langle \mathbb{J}_c\,\text{skew}\,P_{,t},\delta P\right\rangle dm\right)dt - \int_0^T\int_\Omega \left\langle \mathbb{J}_c\,\text{skew}\,P_{,tt},\delta P\right\rangle dm\,dt\\
&= \int_{\Omega\times\{T\}} \left\langle \mathbb{J}_c\,\text{skew}\,P_{,t}\left(x,T\right),\delta P\left(x,T\right)\right\rangle dm - \int_{\Omega\times\{0\}} \left\langle \mathbb{J}_c\,\text{skew}\,P_{,t}\left(x,0\right),\delta P\left(x,0\right)\right\rangle dm - \int_0^T\int_\Omega \left\langle \mathbb{J}_c\,\text{skew}\,P_{,tt},\delta P\right\rangle dm\,dt.
\end{aligned}$$

$$
\begin{aligned}
\mathsf{K}_4 &= \int_0^T\!\!\int_\Omega \langle \mathbb{T}\,\mathrm{sym}\,\nabla u_{,t}, \nabla\delta u_{,t}\rangle\, dm\, dt \\
&= \int_0^T\!\!\int_{\partial\Omega} \langle (\mathbb{T}\,\mathrm{sym}\,\nabla u_{,t})\cdot n, \delta u_{,t}\rangle\, dm dt - \int_0^T\!\!\int_\Omega \langle \mathrm{Div}\,(\mathbb{T}\,\mathrm{sym}\,\nabla u_{,t}), \delta u_{,t}\rangle\, dm\, dt \\
&= \int_{\partial\Omega\times\{T\}} \langle (\mathbb{T}\,\mathrm{sym}\,\nabla u_{,t}\,(x,T))\cdot n, \delta u_{,t}\,(x,T)\rangle\, dm - \int_{\partial\Omega\times\{0\}} \langle (\mathbb{T}\,\mathrm{sym}\,\nabla u_{,t}\,(x,0))\cdot n, \delta u_{,t}\,(x,0)\rangle\, dm \\
&\quad - \int_0^T\!\!\int_{\partial\Omega} \langle (\mathbb{T}\,\mathrm{sym}\,\nabla u_{,tt})\cdot n, \delta u\rangle\, dm\, dt \\
&\quad - \left(\int_0^T\!\!\int_\Omega \frac{d}{dt}\langle \mathrm{Div}\,(\mathbb{T}\,\mathrm{sym}\,\nabla u_{,t}), \delta u\rangle\, dm\, dt - \int_0^T\!\!\int_\Omega \langle \mathrm{Div}\,(\mathbb{T}\,\mathrm{sym}\,\nabla u_{,tt}), \delta u\rangle\, dm\, dt\right).
\end{aligned}
$$

$$
\begin{aligned}
\mathsf{K}_5 &= \int_0^T\!\!\int_\Omega \langle \mathbb{T}_c\,\mathrm{skew}\,\nabla u_{,t}, \nabla\delta u_{,t}\rangle\, dm\, dt \\
&= \int_0^T\!\!\int_{\partial\Omega} \langle (\mathbb{T}_c\,\mathrm{skew}\,\nabla u_{,t})\cdot n, \delta u_{,t}\rangle\, dm dt - \int_0^T\!\!\int_\Omega \langle \mathrm{Div}\,(\mathbb{T}_c\,\mathrm{skew}\,\nabla u_{,t}), \delta u_{,t}\rangle\, dm\, dt \\
&= \int_{\partial\Omega\times\{T\}} \langle (\mathbb{T}_c\,\mathrm{skew}\,\nabla u_{,t}\,(x,T))\cdot n, \delta u_{,t}\,(x,T)\rangle\, dm - \int_{\partial\Omega\times\{0\}} \langle (\mathbb{T}_c\,\mathrm{skew}\,\nabla u_{,t}\,(x,0))\cdot n, \delta u_{,t}\,(x,0)\rangle\, dm \\
&\quad - \int_0^T\!\!\int_{\partial\Omega} \langle (\mathbb{T}_c\,\mathrm{skew}\,\nabla u_{,tt})\cdot n, \delta u\rangle\, dm\, dt \\
&\quad - \left(\int_0^T\!\!\int_\Omega \frac{d}{dt}\langle \mathrm{Div}\,(\mathbb{T}_c\,\mathrm{skew}\,\nabla u_{,t}), \delta u\rangle\, dm\, dt - \int_0^T\!\!\int_\Omega \langle \mathrm{Div}\,(\mathbb{T}_c\,\mathrm{skew}\,\nabla u_{,tt}), \delta u\rangle\, dm\, dt\right)
\end{aligned}
$$

So considering only the bulk parts, we find for the kinetic energy

$$
\int_0^T\!\!\int_\Omega \left(\langle -\rho u_{,tt} + \mathrm{Div}\,(\mathbb{T}\,\mathrm{sym}\,\nabla u_{,tt} + \mathbb{T}_c\,\mathrm{skew}\,\nabla u_{,tt}), \delta u\rangle - \langle \mathbb{J}_{\mathrm{micro}}\,\mathrm{sym}\,P_{,tt} + \mathbb{J}_c\,\mathrm{skew}\,P_{,tt}, \delta P\rangle\right) dm\, dt.
$$

11.2 Variation of the potential energy

$$
\begin{aligned}
\delta\int_0^T\!\!\int_\Omega W(\nabla u, P, \mathrm{Curl}\,P)\, dm\, dt = {}& \underbrace{\delta\int_0^T\!\!\int_\Omega \frac{1}{2}\langle \mathbb{C}_e\,\mathrm{sym}\,(\nabla u - P), \mathrm{sym}\,(\nabla u - P)\rangle\, dm\, dt}_{\mathsf{P}_1} \\
&+ \underbrace{\delta\int_0^T\!\!\int_\Omega \frac{1}{2}\langle \mathbb{C}_{\mathrm{micro}}\,\mathrm{sym}\,P, \mathrm{sym}\,P\rangle\, dm\, dt}_{\mathsf{P}_2} \\
&+ \underbrace{\delta\int_0^T\!\!\int_\Omega \frac{1}{2}\langle \mathbb{C}_c\,\mathrm{skew}\,(\nabla u - P), \mathrm{skew}\,(\nabla u - P)\rangle\, dm\, dt}_{\mathsf{P}_3} \\
&+ \underbrace{\delta\int_0^T\!\!\int_\Omega \frac{L_c^2}{2}\langle \mathbb{L}\,\mathrm{sym}\,\mathrm{Curl}\,P, \mathrm{sym}\,\mathrm{Curl}\,P\rangle\, dm\, dt}_{\mathsf{P}_4} \\
&+ \underbrace{\delta\int_0^T\!\!\int_\Omega \frac{L_c^2}{2}\langle \mathbb{L}_c\,\mathrm{skew}\,\mathrm{Curl}\,P, \mathrm{skew}\,\mathrm{Curl}\,P\rangle\, dm\, dt}_{\mathsf{P}_5}.
\end{aligned}
$$

Integration by parts:

$$
\begin{aligned}
\mathsf{P}_1 &= \frac{1}{2}\int_0^T\!\!\int_\Omega \left(\langle \mathbb{C}_e\,\mathrm{sym}\,(\nabla\delta u - \delta P), \mathrm{sym}\,(\nabla u - P)\rangle + \langle \mathbb{C}_e\,\mathrm{sym}\,(\nabla u - P), \mathrm{sym}\,(\nabla\delta u - \delta P)\rangle\right) dm\, dt \\
(\text{sym of } \mathbb{C}_e) \rightsquigarrow &= \int_0^T\!\!\int_\Omega \langle \mathbb{C}_e\,\mathrm{sym}\,(\nabla u - P), \mathrm{sym}\,(\nabla\delta u - \delta P)\rangle\, dm\, dt = \int_0^T\!\!\int_\Omega \langle \mathbb{C}_e\,\mathrm{sym}\,(\nabla u - P), \nabla\delta u - \delta P\rangle\, dm\, dt \\
&= \int_0^T\!\!\int_\Omega \langle \mathbb{C}_e\,\mathrm{sym}\,(\nabla u - P), \nabla\delta u\rangle\, dm\, dt - \int_0^T\!\!\int_\Omega \langle \mathbb{C}_e\,\mathrm{sym}\,(\nabla u - P), \delta P\rangle\, dm\, dt \\
&= \int_0^T\!\!\int_\Omega \mathrm{div}\,((\mathbb{C}_e\,\mathrm{sym}\,(\nabla u - P))\cdot\delta u)\, dm\, dt - \int_0^T\!\!\int_\Omega \langle \mathrm{Div}\,(\mathbb{C}_e\,\mathrm{sym}\,(\nabla u - P)), \delta u\rangle\, dm\, dt \\
&\quad - \int_0^T\!\!\int_\Omega \langle \mathbb{C}_e\,\mathrm{sym}\,(\nabla u - P), \delta P\rangle\, dm\, dt \\
&= \int_0^T\!\!\int_{\partial\Omega} \langle (\mathbb{C}_e\,\mathrm{sym}\,(\nabla u - P))\cdot n, \delta u\rangle\, dm\, dt - \int_0^T\!\!\int_\Omega \langle \mathrm{Div}\,(\mathbb{C}_e\,\mathrm{sym}\,(\nabla u - P)), \delta u\rangle\, dm\, dt \\
&\quad - \int_0^T\!\!\int_\Omega \langle \mathbb{C}_e\,\mathrm{sym}\,(\nabla u - P), \delta P\rangle\, dm\, dt.
\end{aligned}
$$

In an analogous way we have

$$\mathsf{P}_2 = \frac{1}{2}\int_0^T\!\!\int_\Omega \left(\langle \mathbb{C}_{\text{micro}}\,\text{sym}\,\delta P, \text{sym}\,P\rangle + \langle \mathbb{C}_{\text{micro}}\,\text{sym}\,P, \text{sym}\,\delta P\rangle\right) dm\,dt$$

$$(\text{sym of } \mathbb{C}_{\text{micro}}) \rightsquigarrow = \int_0^T\!\!\int_\Omega \langle \mathbb{C}_{\text{micro}}\,\text{sym}\,P, \text{sym}\,\delta P\rangle\, dm\,dt = \int_0^T\!\!\int_\Omega \langle \mathbb{C}_{\text{micro}}\,\text{sym}\,P, \delta P\rangle\, dm\,dt.$$

Variation of P_3:

$$\begin{aligned}
\mathsf{P}_3 &= \frac{1}{2}\,\delta \int_0^T\!\!\int_\Omega \langle \mathbb{C}_c\,\text{skew}\left(\nabla u - P\right), \text{skew}\left(\nabla u - P\right)\rangle\, dm\,dt\\
(\text{sym of } \mathbb{C}_c) \rightsquigarrow &= \int_0^T\!\!\int_\Omega \langle \mathbb{C}_c\,\text{skew}\left(\nabla u - P\right), \text{skew}\left(\nabla \delta u - \delta P\right)\rangle\, dm\,dt\\
&= \int_0^T\!\!\int_\Omega \langle \mathbb{C}_c\,\text{skew}\left(\nabla u - P\right), \nabla \delta u - \delta P\rangle\, dm\,dt\\
&= \int_0^T\!\!\int_\Omega \langle \mathbb{C}_c\,\text{skew}\left(\nabla u - P\right), \nabla \delta u\rangle\, dm\,dt - \int_0^T\!\!\int_\Omega \langle \mathbb{C}_c\,\text{skew}\left(\nabla u - P\right), \delta P\rangle\, dm\,dt\\
&= \int_0^T\!\!\int_{\partial\Omega} \langle (\mathbb{C}_c\,\text{skew}\left(\nabla u - P\right))\cdot n, \delta u\rangle\, dm\,dt - \int_0^T\!\!\int_\Omega \langle \text{Div}\left(\mathbb{C}_c\,\text{skew}\left(\nabla u - P\right)\right), \delta u\rangle\, dm\,dt\\
&\quad - \int_0^T\!\!\int_\Omega \langle \mathbb{C}_c\,\text{skew}\left(\nabla u - P\right), \delta P\rangle\, dm\,dt,
\end{aligned}$$

For P_4 we find

$$\begin{aligned}
\mathsf{P}_4 &= \frac{L_c^2}{2}\,\delta \int_0^T\!\!\int_\Omega \langle \mathbb{L}\,\text{sym Curl}\,P, \text{sym Curl}\,P\rangle\, dm\,dt\\
(\text{sym of } \mathbb{L}) \rightsquigarrow &= L_c^2 \int_0^T\!\!\int_\Omega \langle \mathbb{L}\,\text{sym Curl}\,P, \text{sym Curl}\,\delta P\rangle\, dm\,dt\\
&= L_c^2 \int_0^T\!\!\int_\Omega \langle \mathbb{L}\,\text{sym Curl}\,P, \text{Curl}\,\delta P\rangle\, dm\,dt\\
&= L_c^2 \int_0^T\!\!\int_\Omega \sum_{i=1}^3 \left\langle \left(\mathbb{L}\,\text{sym Curl}\,P\right)_i, \left(\text{Curl}\,\delta P\right)_i\right\rangle_{\mathbb{R}^3} dm\,dt\\
&= L_c^2 \int_0^T\!\!\int_\Omega \sum_{i=1}^3 \left\langle \left(\mathbb{L}\,\text{sym Curl}\,P\right)_i, \text{curl}\left(\delta P\right)_i\right\rangle_{\mathbb{R}^3} dm\,dt\\
&= L_c^2 \int_0^T\!\!\int_\Omega \sum_{i=1}^3 \left(\text{div}\left(\left(\mathbb{L}\,\text{sym Curl}\,P\right)_i \times \text{curl}\left(\delta P\right)_i\right) + \left\langle \text{curl}\left(\mathbb{L}\,\text{sym Curl}\,P\right)_i, \left(\delta P\right)_i\right\rangle_{\mathbb{R}^3}\right) dm\,dt\\
&= L_c^2 \sum_{i=1}^3 \int_0^T\!\!\int_{\partial\Omega} \left\langle \left(\left(\mathbb{L}\,\text{sym Curl}\,P\right)_i \times \text{curl}\left(\delta P\right)_i\right), n\right\rangle dm\,dt\\
&\quad + L_c^2 \int_0^T\!\!\int_\Omega \langle \text{Curl}\left(\mathbb{L}\,\text{sym Curl}\,P\right), \delta P\rangle_{\mathbb{R}^{3\times 3}}\, dm\,dt.
\end{aligned}$$

For the P_5 part we have

$$\begin{aligned}
\mathsf{P}_5 &= \frac{L_c^2}{2}\,\delta \int_0^T\!\!\int_\Omega \langle \mathbb{L}_c\,\text{skew Curl}\,P, \text{skew Curl}\,P\rangle\, dm\,dt\\
(\text{sym of } \mathbb{L}_c) \rightsquigarrow &= L_c^2 \int_0^T\!\!\int_\Omega \langle \mathbb{L}_c\,\text{skew Curl}\,P, \text{skew Curl}\,\delta P\rangle\, dm\,dt\\
&= L_c^2 \int_0^T\!\!\int_\Omega \langle \mathbb{L}_c\,\text{skew Curl}\,P, \text{Curl}\,\delta P\rangle\, dm\,dt\\
&= L_c^2 \int_0^T\!\!\int_\Omega \sum_{i=1}^3 \left\langle \left(\mathbb{L}_c\,\text{skew Curl}\,P\right)_i, \left(\text{Curl}\,\delta P\right)_i\right\rangle_{\mathbb{R}^3} dm\,dt\\
&= L_c^2 \int_0^T\!\!\int_\Omega \sum_{i=1}^3 \left\langle \left(\mathbb{L}_c\,\text{skew Curl}\,P\right)_i, \text{curl}\left(\delta P\right)_i\right\rangle_{\mathbb{R}^3} dm\,dt\\
&= L_c^2 \int_0^T\!\!\int_\Omega \sum_{i=1}^3 \left(\text{div}\left(\left(\mathbb{L}_c\,\text{skew Curl}\,P\right)_i \times \text{curl}\left(\delta P\right)_i\right) + \left\langle \text{curl}\left(\mathbb{L}_c\,\text{skew Curl}\,P\right)_i, \left(\delta P\right)_i\right\rangle_{\mathbb{R}^3}\right) dm\,dt\\
&= L_c^2 \sum_{i=1}^3 \int_0^T\!\!\int_{\partial\Omega} \left\langle \left(\left(\mathbb{L}_c\,\text{skew Curl}\,P\right)_i \times \text{curl}\left(\delta P\right)_i\right), n\right\rangle dm\,dt\\
&\quad + L_c^2 \int_0^T\!\!\int_\Omega \langle \text{Curl}\left(\mathbb{L}_c\,\text{skew Curl}\,P\right), \delta P\rangle_{\mathbb{R}^{3\times 3}}\, dm\,dt.
\end{aligned}$$

11.3 Components of the matrix

We give the explicit expression of the matrix $\widetilde{D} \in \mathbb{R}^{6\times 6}$ for the plane problem: we denote with $\widetilde{D}_i$, $i = 1, \ldots, 6$ the columns of the matrix.

$$\widetilde{D}_1 = \begin{pmatrix} \frac{1}{4}k^2\left(-\omega^2\left(4\left(2\bar{\eta}_1+\bar{\eta}_3\right)\cos^2\vartheta+\sin^2\vartheta\left(\bar{\eta}_2+4\bar{\eta}_s\right)\right)+4\,\sin^2\vartheta\left(\mu_c+\mu_e^*\right)+4\cos^2\vartheta\left(\lambda_e+2\,\mu_e\right)\right)-\omega^2\varrho \\ \frac{1}{4}\,k^2\sin\vartheta\,\cos\vartheta\left(\omega^2\left(\bar{\eta}_2-4\left(\bar{\eta}_3+\bar{\eta}_s\right)\right)-4\left(\mu_c+\lambda_e+\mu_e^*\right)\right) \\ k\,\cos\vartheta\left(\lambda_e+2\mu_e\right) \\ k\,\sin\vartheta\left(\mu_c+\mu_e^*\right) \\ k\,\sin\vartheta\left(\mu_e^*-\mu_c\right) \\ k\,\lambda_e\cos\vartheta \end{pmatrix},$$

$$\widetilde{D}_2 = \begin{pmatrix} \frac{1}{4}k^2\sin\vartheta\cos\vartheta\left(\omega^2\left(\bar{\eta}_2-4\left(\bar{\eta}_3+\bar{\eta}_s\right)\right)-4\mu_c+4\lambda_e+4\mu_{\rm es}\right) \\ \frac{1}{4}k^2\left(-\omega^2\left(4\left(2\bar{\eta}_1+\bar{\eta}_3\right)\sin^2\vartheta+\cos^2\vartheta\left(\bar{\eta}_2+4\bar{\eta}_s\right)\right)+4\,\cos^2\vartheta\left(\mu_c+\mu_e^*\right)+4\,\sin^2\vartheta\left(\lambda_e+2\mu_e\right)\right)-\rho\omega^2 \\ k\,\lambda_e\sin\vartheta \\ k\,\cos\vartheta\left(\mu_e^*-\mu_c\right) \\ k\,\cos\vartheta\left(\mu_c+\mu_e^*\right) \\ k\,\sin\vartheta\left(\lambda_e+2\mu_e\right) \end{pmatrix},$$

$$\widetilde{D}_3 = \begin{pmatrix} -k\cos\vartheta\left(\lambda_e+2\mu_e\right) \\ -k\lambda_e\sin\vartheta \\ -k^2L_c^2\sin^2\vartheta-\lambda_e-2\left(\mu_e+\mu_{\rm micro}\right)+\left(2\eta_1+\eta_3\right)\omega^2-\lambda_{\rm micro} \\ k^2L_c^2\sin\vartheta\cos\vartheta \\ 0 \\ -\lambda_e+\eta_3\omega^2-\lambda_{\rm micro} \end{pmatrix},$$

$$\widetilde{D}_4 = \begin{pmatrix} -k\,\sin\vartheta\left(\mu_c+\mu_e^*\right) \\ k\,\cos\vartheta\left(\mu_c-\mu_e^*\right) \\ k^2L_c^2\,\sin\vartheta\,\cos\vartheta \\ -k^2L_c^2\cos^2\vartheta-\mu_c-\mu_e^*-\mu_{\rm micro}^*+\omega^2\left(\eta_2+\eta_s\right) \\ \mu_c-\mu_e^*-\mu_{\rm micro}^*+\omega^2\left(\eta_s-\eta_2\right) \\ 0 \end{pmatrix},$$

$$\widetilde{D}_5 = \begin{pmatrix} k\,\sin\vartheta\left(\mu_c-\mu_e^*\right) \\ -k\,\cos\vartheta\left(\mu_c+\mu_e^*\right) \\ 0 \\ \mu_c-\mu_e^*-\mu_{\rm micro}^*+\omega^2\left(\eta_s-\eta_2\right) \\ -k^2L_c^2\sin^2\vartheta-\mu_c-\mu_e^*-\mu_{\rm micro}^*+\omega^2\left(\eta_2+\eta_s\right) \\ k^2L_c^2\sin\vartheta\,\cos\vartheta \end{pmatrix},$$

$$\widetilde{D}_6 = \begin{pmatrix} -k\,\lambda_e\cos\vartheta \\ -k\,\sin\vartheta\left(\lambda_e+2\mu_e\right) \\ -\lambda_e+\eta_3\,\omega^2-\lambda_{\rm micro} \\ 0 \\ k^2L_c^2\,\sin\vartheta\,\cos\vartheta \\ -k^2L_c^2\,\cos^2\vartheta-\lambda_e-2\left(\mu_e+\mu_{\rm micro}\right)+\left(2\eta_1+\eta_3\right)\omega^2-\lambda_{\rm micro} \end{pmatrix}.$$

11.4 Silvester's criterium

We are looking to find a condition between two pairs of Lamé coefficients (λ, μ) and $(\tilde{\lambda}, \tilde{\mu})$ such that

$$f_{(\lambda,\mu)}(x,y) \geq f_{(\tilde{\lambda},\tilde{\mu})}(x,y) \qquad \forall\ (x,y) \in \mathbb{R}^{2\times 2}, \tag{62}$$

where

$$f_{(\lambda,\mu)}(x,y) = (\lambda+2\,\mu)\,x^2+2\,\lambda\,x\,y+(\lambda+2\,\mu)\,y^2 = \left\langle \begin{pmatrix} \lambda+2\,\mu & \lambda \\ \lambda & \lambda+2\,\mu \end{pmatrix}\begin{pmatrix} x \\ y \end{pmatrix}, \begin{pmatrix} x \\ y \end{pmatrix}\right\rangle, \tag{63}$$

$$f_{(\tilde{\lambda},\tilde{\mu})}(x,y) = (\tilde{\lambda}+2\,\tilde{\mu})\,x^2+2\,\tilde{\lambda}\,x\,y+(\tilde{\lambda}+2\,\tilde{\mu})\,y^2 = \left\langle \begin{pmatrix} \tilde{\lambda}+2\,\tilde{\mu} & \tilde{\lambda} \\ \tilde{\lambda} & \tilde{\lambda}+2\,\tilde{\mu} \end{pmatrix}\begin{pmatrix} x \\ y \end{pmatrix}, \begin{pmatrix} x \\ y \end{pmatrix}\right\rangle.$$

Therefore, the question may be reformulated as, find the relation between (λ, μ) and $(\tilde{\lambda}, \tilde{\mu})$ such that

$$\left\langle \left[\begin{pmatrix} \lambda+2\,\mu & \lambda \\ \lambda & \lambda+2\,\mu \end{pmatrix} - \begin{pmatrix} \tilde{\lambda}+2\,\tilde{\mu} & \tilde{\lambda} \\ \tilde{\lambda} & \tilde{\lambda}+2\,\tilde{\mu} \end{pmatrix}\right]\begin{pmatrix} x \\ y \end{pmatrix}, \begin{pmatrix} x \\ y \end{pmatrix}\right\rangle \geq 0, \qquad \forall\ (x,y) \in \mathbb{R}^{2\times 2}, \tag{64}$$

i.e. the difference matrix

$$\begin{pmatrix} \lambda+2\,\mu & \lambda \\ \lambda & \lambda+2\,\mu \end{pmatrix} - \begin{pmatrix} \tilde{\lambda}+2\,\tilde{\mu} & \tilde{\lambda} \\ \tilde{\lambda} & \tilde{\lambda}+2\,\tilde{\mu} \end{pmatrix} \tag{65}$$

is positive definite. We write the condition (62) in the form

$$\left[(\lambda+2\,\mu)-(\tilde{\lambda}+2\,\tilde{\mu})\right]x^2+2\left[\lambda-\tilde{\lambda}\right]x\,y+\left[(\lambda+2\,\mu)-(\tilde{\lambda}+2\,\tilde{\mu})\right]y^2 \geq 0 \qquad \forall\ (x,y) \in \mathbb{R}^2.$$

By applying the Silvester's criterion, we find that this is possible if and only if

$$(\lambda + 2\,\mu) - (\tilde{\lambda} + 2\,\tilde{\mu}) \geq 0, \qquad [(\lambda + 2\,\mu) - (\tilde{\lambda} + 2\,\tilde{\mu})]^2 - [\lambda - \tilde{\lambda}]^2 \geq 0, \tag{66}$$

conditions which are equivalent to

$$\lambda + 2\,\mu \geq \tilde{\lambda} + 2\,\tilde{\mu}, \qquad (\lambda + 2\,\mu) - (\tilde{\lambda} + 2\,\tilde{\mu}) \geq \lambda - \tilde{\lambda} \geq -[(\lambda + 2\,\mu) - (\tilde{\lambda} + 2\,\tilde{\mu})], \tag{67}$$

and, further, to

$$\lambda + 2\,\mu \geq \tilde{\lambda} + 2\,\tilde{\mu}, \qquad (\lambda + 2\,\mu) - (\tilde{\lambda} + 2\,\tilde{\mu}) \geq \lambda - \tilde{\lambda}, \qquad \lambda - \tilde{\lambda} \geq -[(\lambda + 2\,\mu) - (\tilde{\lambda} + 2\,\tilde{\mu})]. \tag{68}$$

These inequalities are equivalent to

$$\mu \geq \tilde{\mu}, \qquad \lambda + 2\,\mu \geq \tilde{\lambda} + 2\,\tilde{\mu}, \qquad \lambda + \mu \geq \tilde{\lambda} + \tilde{\mu}, \tag{69}$$

and the non-redundant inequalities to be satisfied, are

$$\mu \geq \tilde{\mu}, \qquad \lambda + \mu \geq \tilde{\lambda} + \tilde{\mu}. \tag{70}$$

11.5 Our view on classical homogenization

A philosophical reflection is indispensable at this point: what is the most effective way to find a homogenized model which is able to account for the mechanical behavior of anisotropic elastic metamaterials at a macroscopic scale? In the best possible situation, we would like to be able to start from the specific characteristics of the metamaterial's microstructure and set up a rigorous and simple procedure that, without the need of introducing cumbersome hypotheses, leads us to the desired homogenized (effective) model. Moreover, we would like the obtained model to be able to describe all the main characteristics of the metamaterial's behavior (degree of anisotropy, dispersion, band-gap properties, etc...) at the macroscopic scale.

It is highly unlikely that such a definitive answer can come from standard homogenization methods. Homogenization techniques can, at the present state of knowledge, be used to get some important indications, such as the anisotropic behavior of the wave speed of the first two modes (see e.g. [64]) or the fact that enriched continuum models of the micromorphic type emerge as a result of the homogenization of metamaterials with internal resonances [59, 65], and provide an interpretation of the vibration modes for relatively large wavelength as associated to the characteristics of the underlying microstructure [7, 11, 12, 17].

But it is unlikely, if not entirely inconceivable, to think that such homogenization techniques can give a complete and definitive answer about the "right" homogenized model that has to be used to simultaneously describe, among others:

- the anisotropic deformation response of metamaterials,
- the dependence of the dispersion curves on the direction of wave propagation, not only for the first acoustic modes, but also for the optic modes at higher frequencies,
- the "eventually anisotropic" properties of the band-gap,
- a still accurate description of the dispersive behavior of the metamaterial, even for small wavelengths which become comparable to the size of the unit-cell.

Our answer to this difficult and intricate question is in line with Truesdell and Noll's remark [70, p. 350, footnote 3]. It is our firm belief that the answer must be searched in the field of enriched (micromorphic) continuum mechanics and the attention must be switched from "which homogenization technique should be used" to "which enriched macroscopic continuum model should be used" to describe the desired properties of the considered metamaterials at the engineering scale.

In some sense, we are entering in the same controversial discussions that characterized the history of the theory of elasticity for several decades[18] (from the late 1600s when Hooke's law was experimentally discovered, to the first half of the 19^{th} century when the general governing equations for macroscopic elastic isotropic solids were finally obtained).

Throughout these years the question was that of establishing the form of the differential equations governing the macroscopic deformation of an elastic solid in such a way that the experimental evidence could be successfully explained. For years, arguments based on molecular hypotheses where carried out, trying to derive the equations of elasticity by imposing the balance of interactions among molecules constituting the considered solid. Among the most prominent supporters of this "molecular" viewpoint were Navier, Poisson and Saint-Venant, sometimes accompanied by Cauchy and Lamé (who also adopted different methodologies). The big problem of this molecular approach was that a consensus could never be found on the general form that the equation of elasticity for solids should have. For a long time the discussion was centered about the question whether the behavior of an isotropic solid should be governed by 1 (rari-constant theory) or 2 (multi-constant theory) elastic constants and whether the behavior of a completely anisotropic solid should count 15 or 21 elastic coefficients.

The results obtained by the application of molecular methods always featured one constant in the isotropic case and 15 constants in the completely anisotropic one.

The second viewpoint concerning the way of deriving the equations of elasticity was supported by Green (see [38]) who proposed in 1837 to derive the equations of elasticity by finding the minimum of the strain energy density of the solid. He considered for the strain energy density a quadratic form in the strain, which is equivalent to say that he considered a linear stress-strain relationship. This constitutive assumption was in line with Hooke's one-dimensional law and all other experimental evidence suggesting proportionality between stress and strain in the regime of infinitesimal deformations.

With this simple argument Green was able to set up the equations of elasticity in the form that we know today, featuring 2 elastic constants in the isotropic case and 21 in the completely anisotropic one.

He did not need any argument concerning the interactions among molecules to obtain this result which only relied on the macroscopic observation that stress and strain are related in a linear fashion.

[18] See [38] for a complete treatise on the historical dissertation presented here.

The lesson that we retain from this series of events is that the mechanical behavior of materials depends on their interior molecular arrangement, but we do not necessarily need to know details about such molecular distributions if our aim is that of mastering the behavior of materials at the macroscopic scale. A simple observation of the stress-strain response at the macroscopic scale may be sufficient to obtain the correct answer about the macroscopic equations of motion for elastic solids.

In recent times, we are observing an explosion of research efforts based on the detailed calculation of systems composed by larger and larger number of particles. More than once, some of the authors assisted to discussions according to which it is not worth to study continuum models because of the future availability of quantum computers which will allow arbitrarily large sets of particles to be considered. We strongly disagree with this point of view since this would be equivalent to claiming that it is useless to continue teaching the theory of elasticity given that such computers will allow for the design of engineering structures by taking into account all the constituting atoms. The simple fact that airplanes fly and bridges stand up is a testament to the theory of elasticity, showing all its charm in its astonishing simplicity.

We completely share the viewpoint of Green and, in this paper, we start giving our answer concerning the fundamental question of finding the set of differential equations that governs the motion of metamaterials at the macroscopic scale.

11.6 Equivalent dynamical determination of the macroscopic stiffness $\mathbb{C}_{\text{macro}}$

In this Section, we show how the macroscopic parameters previously obtained by simple static arguments can be equivalently computed using the slopes of the acoustic dispersion curves close to the origin. This equivalent method is very useful to make a strong connection between the relaxed micromorphic model and classical elasticity, but it does not add any extra feature to the fitting procedure presented in the main body.

11.6.1 Tangents in zero to the acoustic branches

Let us consider the "macroscopic" Cauchy partial differential system of equations (since this is linear elasticity with elastic stiffness tensor $\mathbb{C}_{\text{macro}}$)

$$\rho\, u_{,tt} - \text{Div}\left(\mathbb{C}_{\text{macro}}\, \text{sym}\, \nabla u\right) = 0 \tag{71}$$

which is the limiting case of the relaxed micromorphic model. In this classical case, it is possible to obtain an analytical expression for the dispersion curves. In order to do so, we make the plane wave ansatz for u, i.e., we assume that there exist $\widetilde{u} \in \mathbb{R}^3$ and a function[19] $\phi \in \mathcal{C}^2(\mathbb{R}, \mathbb{R})\,,\ s \mapsto \phi(s)$ with somewhere non-vanishing second derivative, such that

$$u(x,t) = \widetilde{u}\, \phi\left(\langle \boldsymbol{k}, x\rangle - \omega\, t\right).$$

Setting $s(x,t) := \langle \boldsymbol{k}, x\rangle - \omega\, t$, $\left(s \in \mathcal{C}^\infty\left(\overline{\Omega} \times [0,T], \mathbb{R}\right)\right)$ we calculate the space and time derivatives of u:

$$u_{i,j} = \widetilde{u}_i\, \frac{\partial}{\partial x_j}\phi\left(s(x,t)\right) = \widetilde{u}_i\, \frac{d\phi}{ds}\ \left(s(x,t)\right) \frac{\partial}{\partial x_j}\left(\langle \boldsymbol{k}, x\rangle - \omega\, t\right) = \widetilde{u}_i\, k_j\, \frac{d\phi}{ds}, \tag{72}$$

$$u_{,t} = \widetilde{u}\, \frac{d}{dt}\phi\left(s(x,t)\right) = \widetilde{u}\, \frac{d}{dt}\phi\left(s(x,t)\right) = \widetilde{u}\, \frac{d}{ds}\phi\left(s(x,t)\right) \frac{d}{dt}\left(\langle \boldsymbol{k}, x\rangle - \omega\, t\right) = -\,\omega\, \widetilde{u}\, \frac{d\phi}{ds},$$

$$u_{,tt} = \widetilde{u}\, \frac{d^2}{dt^2}\phi\left(s(x,t)\right) = \widetilde{u}\, \frac{d^2}{ds^2}\phi\left(s(x,t)\right) \left(\frac{d}{dt}\left(\langle \boldsymbol{k}, x\rangle - \omega\, t\right)\right)^2 = \omega^2\, \widetilde{u}\, \frac{d^2\phi}{ds^2}. \tag{73}$$

From (72), we derive

$$\text{sym}\, \nabla u = \frac{d\phi}{ds}\ \text{sym}\ \left(\widetilde{u} \otimes \boldsymbol{k}\right),$$

and thus

$$\mathbb{C}_{\text{macro}}\, \text{sym}\, \nabla u = \frac{d\phi}{ds}\, \mathbb{C}_{\text{macro}}\, \text{sym}\ \left(\widetilde{u} \otimes \boldsymbol{k}\right). \tag{74}$$

We calculate the divergence of (74):

$$\begin{aligned}
\text{Div}\left(\mathbb{C}_{\text{macro}}\, \text{sym}\, \nabla u\right) &= \text{Div}\left(\frac{d\phi}{ds}\, \mathbb{C}_{\text{macro}}\, \text{sym}\ \left(\widetilde{u} \otimes \boldsymbol{k}\right)\right) \quad \text{or equivalently in index notation} \\
&= \frac{\partial}{\partial x_j}\left[\frac{d\phi}{ds}\left(s(x,t)\right)\ \left(\mathbb{C}_{\text{macro}}\right)_{ijmn} \frac{1}{2}\left(\widetilde{u}_m k_n + \widetilde{u}_n k_m\right)\right] \\
&= \frac{d}{ds}\frac{d\phi}{ds}\left(s(x,t)\right) \frac{\partial}{\partial x_j}\left(\langle \boldsymbol{k}, x\rangle - \omega\, t\right)\ \left(\mathbb{C}_{\text{macro}}\right)_{ijmn} \frac{1}{2}\left(\widetilde{u}_m k_n + \widetilde{u}_n k_m\right) \\
&= \frac{d^2\phi}{ds^2}\, k_j\, \left(\mathbb{C}_{\text{macro}}\right)_{ijmn} \frac{1}{2}\left(\widetilde{u}_m k_n + \widetilde{u}_n k_m\right) \\
&= \frac{d^2\phi}{ds^2}\left(\mathbb{C}_{\text{macro}}\right)_{ijmn} k_j\, \frac{1}{2}\left(\widetilde{u}_m k_n + \widetilde{u}_n k_m\right) = \frac{d^2\phi}{ds^2}\, \mathbb{C}_{\text{macro}}\left(\boldsymbol{k} \otimes \text{sym}\left(\widetilde{u} \otimes \boldsymbol{k}\right)\right).
\end{aligned} \tag{75}$$

In this way, entering (73) and (75) in (71) we find

$$\rho\, \omega^2\, \frac{d^2\phi}{ds^2}\, \widetilde{u} = \frac{d^2\phi}{ds^2}\, \mathbb{C}_{\text{macro}}\left(\boldsymbol{k} \otimes \text{sym}\left(\widetilde{u} \otimes \boldsymbol{k}\right)\right) \quad \Longleftrightarrow \quad \left(\rho\, \omega^2\, \widetilde{u} - \mathbb{C}_{\text{macro}}\left(\boldsymbol{k} \otimes \text{sym}\left(\widetilde{u} \otimes \boldsymbol{k}\right)\right)\right) \frac{d^2\phi}{ds^2} = 0. \tag{76}$$

Thanks to the hypothesis that $\frac{d^2\phi}{ds^2}$ is somewhere non-vanishing, equation (76) is verified for all $s \in \mathbb{R}$ if and only if

$$\rho\, \omega^2\, \widetilde{u} - \mathbb{C}_{\text{macro}}\left(\boldsymbol{k} \otimes \text{sym}\left(\widetilde{u} \otimes \boldsymbol{k}\right)\right) = 0. \tag{77}$$

[19] for example e^s, $\cos s$, $\sin s$.

In order to calculate the dispersion relations, it is useful to rewrite the term $\mathbb{C}_{\text{macro}}\left(\boldsymbol{k}\otimes\text{sym}\left(\widetilde{u}\otimes\boldsymbol{k}\right)\right)$ as follows.

Firstly, from the symmetries of $\mathbb{C}_{\text{macro}}$, we remark that

$$\begin{aligned}\left(\mathbb{C}_{\text{macro}}\left(\boldsymbol{k}\otimes\text{sym}\left(\widetilde{u}\otimes\boldsymbol{k}\right)\right)\right)_i &= \left(\mathbb{C}_{\text{macro}}\right)_{ijmn}k_j\,\frac{1}{2}\left(\widetilde{u}_m k_n+\widetilde{u}_n k_m\right)\\ &= \frac{1}{2}\left[\left(\mathbb{C}_{\text{macro}}\right)_{ijmn}k_j\widetilde{u}_m k_n+\left(\mathbb{C}_{\text{macro}}\right)_{ijmn}k_j\widetilde{u}_n k_m\right]\\ &= \frac{1}{2}\left[\left(\mathbb{C}_{\text{macro}}\right)_{ijmn}k_j\widetilde{u}_m k_n+\left(\mathbb{C}_{\text{macro}}\right)_{ijnm}k_j\widetilde{u}_n k_m\right]=\left(\mathbb{C}_{\text{macro}}\right)_{ijmn}k_j\widetilde{u}_m k_n.\end{aligned}\tag{78}$$

We find

$$\left(\mathbb{C}_{\text{macro}}\left(\boldsymbol{k}\otimes\widetilde{u}\otimes\boldsymbol{k}\right)\right)_i=\left(\mathbb{C}_{\text{macro}}\right)_{ijmn}k_j\widetilde{u}_m k_n=\left[\left(\mathbb{C}_{\text{macro}}\right)_{ijmn}k_j k_n\right]\widetilde{u}_m.\tag{79}$$

Using eq. (78) together with (79), and remembering that $\boldsymbol{k}=k\,\widehat{\boldsymbol{k}}$ with $k=\left\|\boldsymbol{k}\right\|\in\mathbb{R}^+$ and $\widehat{\boldsymbol{k}}=\boldsymbol{k}/k$, we can finally rewrite eq. (77) as

$$\rho\,\omega^2\underbrace{\widetilde{u}}_{=\mathbb{1}\cdot\widetilde{u}}-\mathbb{C}_{\text{macro}}\left(\boldsymbol{k}\otimes\text{sym}\left(\widetilde{u}\otimes\boldsymbol{k}\right)\right)=0\qquad\Longleftrightarrow\qquad\left(\rho\,\omega^2\,\delta_{im}-k^2\,\left(\mathbb{C}_{\text{macro}}\right)_{ijmn}\widehat{k}_j\widehat{k}_n\right)\widetilde{u}_m=0.\tag{80}$$

The equation (80) is an eigenvalues problem for the linear application $k^2\,\left(\mathbb{C}_{\text{macro}}\right)_{ijmn}\widehat{k}_j\widehat{k}_n$ (which is the acoustic tensor). The stated problem admits non-trivial solutions if and only if the determinant of $\rho\,\omega^2\,\delta_{im}-k^2\,\left(\mathbb{C}_{\text{macro}}\right)_{ijmn}\widehat{k}_j\widehat{k}_n$ is zero. In this way, we are interested in looking for couples (k,ω) such that

$$\det\left(\rho\,\omega^2\,\delta_{im}-k^2\,\left(\mathbb{C}_{\text{macro}}\right)_{ijmn}\widehat{k}_j\widehat{k}_n\right)=0.\tag{81}$$

Moreover, we are interested in studying this problem as a function of the direction of propagation $\widehat{\boldsymbol{k}}$ of the wave. In order to do this, it is convenient to introduce spherical coordinates for the wave vector $\widehat{\boldsymbol{k}}\in\mathbb{S}^2$ (the unit sphere in $\mathbb{R}^3$):

$$k_1=\sin\varphi\,\cos\vartheta,\qquad k_2=\sin\varphi\,\sin\vartheta,\qquad k_3=\cos\varphi,\tag{82}$$

where $\vartheta\in[0,2\pi)$ is the polar angle and $\varphi\in[0,\pi]$ is the azimuthal angle. For the problem in the $(x_1,x_2,0)$ plane, the angle φ is $\pi/2$, so

$$k_1=\cos\vartheta,\qquad k_2=\sin\vartheta,\qquad k_3=0,\tag{83}$$

and

$$\widehat{\boldsymbol{k}}\otimes\widehat{\boldsymbol{k}}=\begin{pmatrix}\cos^2\vartheta & \cos\vartheta\,\sin\vartheta & 0\\ \cos\vartheta\,\sin\vartheta & \sin^2\vartheta & 0\\ 0 & 0 & 0\end{pmatrix}.$$

Let us now consider the Voigt representation of the tensor $\mathbb{C}_{\text{macro}}$ in the case of the tetragonal symmetry

$$\widetilde{\mathbb{C}}_{\text{macro}}=\begin{pmatrix}2\mu_{\text{macro}}+\lambda_{\text{macro}} & \lambda_{\text{macro}} & \lambda^*_{\text{macro}} & 0 & 0 & 0\\ \lambda_{\text{macro}} & 2\mu_{\text{macro}}+\lambda_{\text{macro}} & \lambda^*_{\text{macro}} & 0 & 0 & 0\\ \lambda^*_{\text{macro}} & \lambda^*_{\text{macro}} & (\widetilde{\mathbb{C}}_{\text{macro}})_{33} & 0 & 0 & 0\\ 0 & 0 & 0 & (\widetilde{\mathbb{C}}_{\text{macro}})_{44} & 0 & 0\\ 0 & 0 & 0 & 0 & (\widetilde{\mathbb{C}}_{\text{macro}})_{44} & 0\\ 0 & 0 & 0 & 0 & 0 & \mu^*_{\text{macro}}\end{pmatrix}.$$

A direct calculation gives

$$\left(\mathbb{C}_{\text{macro}}\right)_{ijmn}\widehat{k}_j\widehat{k}_n=\begin{pmatrix}\mu^*_{\text{macro}}\,\sin^2\vartheta+\cos^2\vartheta\,(\lambda_{\text{macro}}+2\mu_{\text{macro}}) & \cos\vartheta\,\sin\vartheta\,(\mu^*_{\text{macro}}+\lambda_{\text{macro}}) & 0\\ \cos\vartheta\,\sin\vartheta\,(\mu^*_{\text{macro}}+\lambda_{\text{macro}}) & \cos^2\vartheta\mu^*_{\text{macro}}+\sin^2\vartheta\,(\lambda_{\text{macro}}+2\mu_{\text{macro}}) & 0\\ 0 & 0 & \left(\widetilde{\mathbb{C}}_{\text{macro}}\right)_{44}\end{pmatrix},$$

thus, for $\rho\,\omega^2\,\delta_{im}-k^2\,\left(\mathbb{C}_{\text{macro}}\right)_{ijmn}\widehat{k}_j\widehat{k}_n$, we find

$$\begin{pmatrix}\rho\omega^2-k^2\left(\mu^*_{\text{macro}}\sin^2\vartheta+\cos^2\vartheta\,(\lambda_{\text{macro}}+2\mu_{\text{macro}})\right) & -k^2\cos\vartheta\,\sin\vartheta\,(\mu^*_{\text{macro}}+\lambda_{\text{macro}}) & 0\\ -k^2\cos\vartheta\,\sin\vartheta\,(\mu^*_{\text{macro}}+\lambda_{\text{macro}}) & \rho\omega^2-k^2\left(\mu^*_{\text{macro}}\cos^2\vartheta+\sin^2\vartheta\,(\lambda_{\text{macro}}+2\mu_{\text{macro}})\right) & 0\\ 0 & 0 & \rho\omega^2-\left(\widetilde{\mathbb{C}}_{\text{macro}}\right)_{44}k^2\end{pmatrix}.$$

In this way we can compute

$$\begin{aligned}&\det\left(\rho\,\omega^2\,\delta_{im}-k^2\,\left(\mathbb{C}_{\text{macro}}\right)_{ijmn}\widehat{k}_j\widehat{k}_n\right)=\\ &\quad=\left(\rho\,\omega^2-\left(\widetilde{\mathbb{C}}_{\text{macro}}\right)_{44}k^2\right)\Big[\left(\rho\,\omega^2-k^2\left(\cos^2\vartheta\,(\lambda_{\text{macro}}+2\mu_{\text{macro}})+\mu^*_{\text{macro}}\sin^2\vartheta\right)\right)\\ &\qquad\left(\rho\,\omega^2-k^2\left(\sin^2\vartheta\,(\lambda_{\text{macro}}+2\mu_{\text{macro}})+\mu^*_{\text{macro}}\cos^2\vartheta\right)\right)-k^4\sin^2\vartheta\cos^2\vartheta\,(\lambda_{\text{macro}}+\mu^*_{\text{macro}})^{\,2}\Big].\end{aligned}\tag{84}$$

The dispersion curves for the classical limit Cauchy model are obtained solving the equation (81), or equivalently (84), with respect to ω^2. We call $\left\{\pm\,\omega_{\text{macro},i}\left(k,\vartheta\right)\right\}_{i=1}^3$ the dispersion curves for the Cauchy continuum obtained by solving (81) for the special tetragonal case given in (84). A direct calculation shows that the positive solutions $\left\{\omega_{\text{macro},i}\left(k,\vartheta\right)\right\}_{i=1}^3$ of (81) for the tetragonal case are three straight lines in the (ω,k) plane with slopes (here, and only here, we use the abbreviations $\mu_M=\mu_{\text{macro}}$, $\lambda_M=\lambda_{\text{macro}}$, $\mu^*_M=\mu^*_{\text{macro}}$):

$$a_{\text{LA}}=\sqrt{\frac{\lambda_M+\mu^*_M+2\mu_M+\sqrt{2\cos(4\vartheta)\,(\lambda_M+\mu_M)\left(\mu_M-\mu^*_M\right)+2\lambda_M\mu_M+\lambda_M^2+\mu_M^{*2}-2\mu_M\mu^*_M+2\mu_M^2}}{2\rho}},\tag{85}$$

$$a_{\text{TA}}=\sqrt{\frac{\lambda_M+\mu^*_M+2\mu_M-\sqrt{2\cos(4\vartheta)\,(\lambda_M+\mu_M)\left(\mu_M-\mu^*_M\right)+2\lambda_M\mu_M+\lambda_M^2+\mu_M^{*2}-2\mu_M\mu^*_M+2\mu_M^2}}{2\rho}},$$

$$a_{\text{TA3}}=\sqrt{\frac{\left(\widetilde{\mathbb{C}}_{\text{macro}}\right)_{44}}{\rho}}\qquad\text{(absent in the plain strain case)}.\tag{86}$$

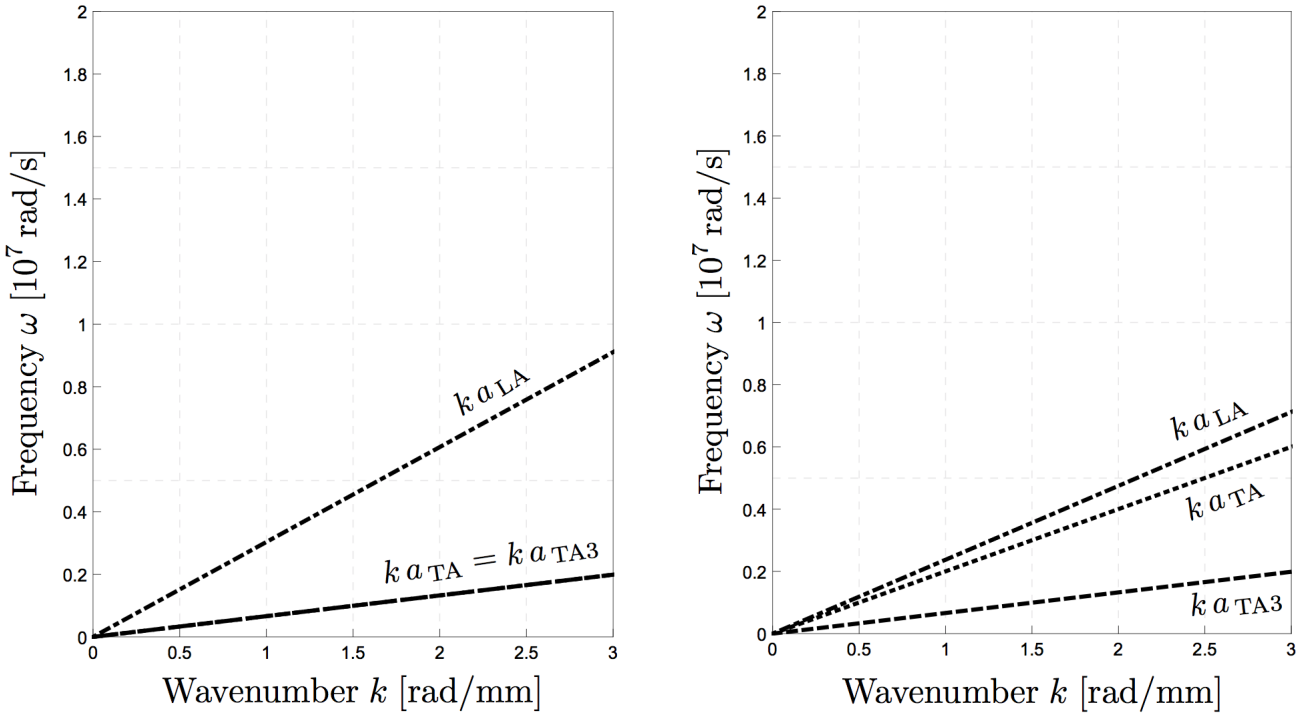

(a) (b)

Figure 14: Dispersion branches for the limiting tetragonal Cauchy continuum with $\widehat{\boldsymbol{k}} = (1,0,0)$ (Fig. (a)) and $\widehat{\boldsymbol{k}} = \left(\sqrt{2}/2, \sqrt{2}/2, 0\right)$ (Fig. (b)).

Note the complete absence of the Cosserat couple modulus μ_c in the latter formulas.

Such dispersion curves are called (in-plane) longitudinal-acoustic (LA), (in-plane) transverse-acoustic (TA) and (out-of-plane) transverse acoustic (TA3). Since in this paper we are interested only in vibrations in the $(x_1, x_2, 0)$ plane, the third acoustic line with slope a_{TA3} will not be considered for the fitting procedure since it corresponds to out-of-plane vibrations.

One remarkable property of the relaxed micromorphic model is that the slopes of its acoustic curves close to the origin, are exactly given by the slopes of the acoustic lines (85) of the equivalent Cauchy continuum. More precisely, the slopes at zero of the acoustic branches of the dispersion curves as obtained via the relaxed micromorphic model can be computed by means of equations (85) when using the identities (59).

11.6.2 Dynamical calculation of the macroscopic stiffness $\mathbb{C}_{\mathbf{macro}}$

Based on the results of Section 11.6.1, we can compute the numerical values of the macroscopic parameters $\mu_{\mathrm{macro}}, \lambda_{\mathrm{macro}}$ and μ^*_{macro} which represent the measure of the macroscopic stiffness of the considered tetragonal metamaterial. To this aim, considering the two directions of propagation $\vartheta_0 = 0$ and $\vartheta_1 = \pi/4$, we set up the following system of algebraic equations:

$$\begin{aligned}
a_{\mathrm{LA}}\left(\vartheta_0, \lambda_{\mathrm{macro}}, \mu_{\mathrm{macro}}, \mu^*_{\mathrm{macro}}\right) &= \sqrt{\frac{2\mu_{\mathrm{macro}} + \lambda_{\mathrm{macro}}}{\rho}} = \overline{a}_{\mathrm{LA}}\left(\vartheta_0\right), \\
a_{\mathrm{LA}}\left(\vartheta_1, \lambda_{\mathrm{macro}}, \mu_{\mathrm{macro}}, \mu^*_{\mathrm{macro}}\right) &= \sqrt{\frac{\mu_{\mathrm{macro}} + \mu^*_{\mathrm{macro}} + \lambda_{\mathrm{macro}}}{\rho}} = \overline{a}_{\mathrm{LA}}\left(\vartheta_1\right), \\
a_{\mathrm{TA}}\left(\vartheta_0, \lambda_{\mathrm{macro}}, \mu_{\mathrm{macro}}, \mu^*_{\mathrm{macro}}\right) &= \sqrt{\frac{\mu^*_{\mathrm{macro}}}{\rho}} = \overline{a}_{\mathrm{TA}}\left(\vartheta_0\right), \\
a_{\mathrm{TA}}\left(\vartheta_1, \lambda_{\mathrm{macro}}, \mu_{\mathrm{macro}}, \mu^*_{\mathrm{macro}}\right) &= \sqrt{\frac{\mu_{\mathrm{macro}}}{\rho}} = \overline{a}_{\mathrm{TA}}\left(\vartheta_1\right).
\end{aligned} \tag{87}$$

This system of algebraic equations counts 4 equations and the unknowns. We use the first 3 equations to calculate the unknowns $\lambda_{\mathrm{macro}}, \mu_{\mathrm{macro}}, \mu^*_{\mathrm{macro}}$ and then plug the found values in the fourth equation.

If our hypothesis according to which the metamaterial we are considering has a tetragonal symmetry is correct, the fourth equation has to be automatically satisfied. This is indeed the case.

The numerical values of the macroscopic parameters which are found with the described procedure are given in Table 9.

Bloch - Floquet			periodic homogenization		
λ_{macro}	μ_{macro}	μ^*_{macro}	λ_{macro}	μ_{macro}	μ^*_{macro}
[GPa]	[GPa]	[GPa]	[GPa]	[GPa]	[GPa]
1.77	5.95	0.65	1.74	5.89	0.62

Table 9: Left: numerical values of the macroscopic parameters of the relaxed micromorphic model as obtained via the dynamical fitting and Bloch-Floquet analysis. Right: for comparison the values obtained by periodic homogenization.

We remark that these macroscopic parameters are almost equivalent to those computed by FE-analysis and shown in Table 2.

References

[1] Assyr Abdulle. Analysis of a heterogeneous multiscale FEM for problems in elasticity. *Mathematical Models and Methods in Applied Sciences*, 16(04):615–635, 2006.

[2] Assyr Abdulle. The finite element heterogeneous multiscale method: a computational strategy for multiscale PDEs. *GAKUTO International Series Mathematical Sciences and Applications*, 31(EPFL-ARTICLE-182121):135–184, 2009.

[3] Tryfon Antonakakis, Richard Craster, and Sebastien Guenneau. High-frequency homogenization of zero-frequency stop band photonic and phononic crystals. *New Journal of Physics*, 15(10):103014, 2013.

[4] Mario N. Armenise, Carlo E. Campanella, Caterina Ciminelli, Francesco Dell'Olio, and Vittorio M. N. Passaro. Phononic and photonic band gap structures: Modelling and applications. *Physics Procedia*, 3(1):357–364, 2010.

[5] Nicolas Auffray. On the algebraic structure of isotropic generalized elasticity theories. *Mathematics and Mechanics of Solids*, 20(5):565–581, 2015.

[6] Nicolas Auffray, Hung Le Quang, and Qi-Chang He. Matrix representations for 3d strain-gradient elasticity. *Journal of the Mechanics and Physics of Solids*, 61(5):1202–1223, 2013.

[7] Jean-Louis Auriault and Claude Boutin. Long wavelength inner-resonance cut-off frequencies in elastic composite materials. *International Journal of Solids and Structures*, 49(23):3269–3281, 2012.

[8] Gabriele Barbagallo, Angela Madeo, Marco Valerio d'Agostino, Rafael Abreu, Ionel-Dumitrel Ghiba, and Patrizio Neff. Transparent anisotropy for the relaxed micromorphic model: macroscopic consistency conditions and long wave length asymptotics. *International Journal of Solids and Structures*, 120:7–30, 2017.

[9] Alain Bensoussan, Jacques-Louis Lions, and George Papanicolaou. *Asymptotic Analysis for Periodic Structures*, volume 5. North-Holland Publishing Company Amsterdam, 1978.

[10] Felix Bloch. Über die Quantenmechanik der Elektronen in Cristallgittern. *Zeitschrift für Physik A Hadrons and Nuclei*, 52(7):555–600, 1929.

[11] Claude Boutin and Stéphane Hans. Homogenisation of periodic discrete medium: Application to dynamics of framed structures. *Computers and Geotechnics*, 30(4):303–320, 2003.

[12] Claude Boutin, Antoine Rallu, and Stéphane Hans. Large scale modulation of high frequency waves in periodic elastic composites. *Journal of the Mechanics and Physics of Solids*, 70:362–381, 2014.

[13] Frederic Bouyge, Iwona Jasiuk, Stéphane Boccara, and Martin Ostoja-Starzewski. A micromechanically based couple-stress model of an elastic orthotropic two-phase composite. *European Journal of Mechanics-A/Solids*, 21(3):465–481, 2002.

[14] Bernhard Burgeth, Martin Welk, Christian Feddern, and Joachim Weickert. Mathematical morphology on tensor data using the Löwner ordering. In *Visualization and Processing of Tensor Fields*, pages 357–368. Springer, 2006.

[15] Youping Chen and James D. Lee. Connecting molecular dynamics to micromorphic theory. (I). Instantaneous and averaged mechanical variables. *Physica A: Statistical Mechanics and its Applications*, 322:359–376, 2003.

[16] Youping Chen and James D. Lee. Determining material constants in micromorphic theory through phonon dispersion relations. *International Journal of Engineering Science*, 41(8):871–886, 2003.

[17] Céline Chesnais, Claude Boutin, and Stéphane Hans. Wave propagation and non-local effects in periodic frame materials: Generalized continuum mechanics. *Mathematics and Mechanics of Solids*, 20(8):929–958, 2015.

[18] Bernard Dacorogna. *Direct Methods in the Calculus of Variations*, volume 78. Springer, 2007.

[19] Marco Valerio d'Agostino, Gabriele Barbagallo, Ionel-Dumitrel Ghiba, Rafael Abreu, Angela Madeo, and Patrizio Neff. A panorama of dispersion curves for the isotropic weighted relaxed micromorphic model. *Zeitschrift für Angewandte Mathematik und Mechanik*, 97(11):1436–1481, 2017.

[20] Francesco dell'Isola, Angela Madeo, and Luca Placidi. Linear plane wave propagation and normal transmission and reflection at discontinuity surfaces in second gradient 3D continua. *Zeitschrift für Angewandte Mathematik und Mechanik*, 92(1):52–71, 2012.

[21] Weinan E and Bjorn Engquist. The heterogeneous multiscale methods. *Communications in Mathematical Sciences*, 1(1):87–132, 2003.

[22] Bernhard Eidel and Andreas Fischer. The heterogeneous multiscale finite element method for the homogenization of linear elastic solids and a comparison with the FE^2 method. *Computer Methods in Applied Mechanics and Engineering*, 329:332–368, 2018.

[23] Ahmed Cemal Eringen. *Microcontinuum field theories*. Springer-Verlag, New York, 1999.

[24] Claudio Findeisen, Jörg Hohe, Muamer Kadic, and Peter Gumbsch. Characteristics of mechanical metamaterials based on buckling elements. *Journal of the Mechanics and Physics of Solids*, 102:151–164, 2017.

[25] Gaston Floquet. Sur les equations differentielles lineaires. *Ann. Ecole Normale Supérieure*, 12(1883):47–88, 1883.

[26] Samuel Forest. Aufbau und Identifikation von Stoffgleichungen für höhere Kontinua mittels Homogenisierungsmethoden. *Technische Mechanik*, 19(4):297–306, 1999.

[27] Samuel Forest. Homogenization methods and mechanics of generalized continua - part 2. *Theoretical and Applied Mechanics*, 28-29(28-29):113–144, 2002.

[28] Samuel Forest and Duy Khanh Trinh. Generalized continua and non-homogeneous boundary conditions in homogenisation methods. *Zeitschrift für Angewandte Mathematik und Mechanik*, 91(2):90–109, 2011.

[29] Ionel-Dumitrel Ghiba, Patrizio Neff, Angela Madeo, Luca Placidi, and Giuseppe Rosi. The relaxed linear micromorphic continuum: existence, uniqueness and continuous dependence in dynamics. *Mathematics and Mechanics of Solids*, 20(10):1171–1197, 2014.

[30] Sergej Hazanov and Christian Huet. Order relationships for boundary conditions effect in heterogeneous bodies smaller than the representative volume. *Journal of the Mechanics and Physics of Solids*, 42(12):1995–2011, 1994.

[31] Rodney Hill. Elastic properties of reinforced solids: some theoretical principles. *Journal of the Mechanics and Physics of Solids*, 11(5):357–372, 1963.

[32] Rodney Hill. On constitutive macro-variables for heterogeneous solids at finite strain. 326(1565):131–147, 1972.

[33] Scott J. Hollister and Noboru Kikuchi. A comparison of homogenization and standard mechanics analyses for periodic porous composites. *Computational Mechanics*, 10(2):73–95, 1992.

[34] Muneo Hori and Sia Nemat-Nasser. *Micromechanics: Overall Properties of Heterogeneous Materials*, volume 37. Elsevier, 2013.

[35] Christian Huet. Application of variational concepts to size effects in elastic heterogeneous bodies. *Journal of the Mechanics and Physics of Solids*, 38(6):813–841, 1990.

[36] Geralf Hütter. Homogenization of a Cauchy continuum towards a micromorphic continuum. *Journal of the Mechanics and Physics of Solids*, 99:394–408, 2017.

[37] Min Kyung Lee, Pyung Sik Ma, Il Kyu Lee, Hoe Woong Kim, and Yoon Young Kim. Negative refraction experiments with guided shear-horizontal waves in thin phononic crystal plates. *Applied Physics Letters*, 98(1):011909, 2011.

[38] Augustus Edward Hough Love. A treatise on the mathematical theory of elasticity. *Cambridge University Press*, 2013.

[39] Angela Madeo, Gabriele Barbagallo, Marco Valerio d'Agostino, Luca Placidi, and Patrizio Neff. First evidence of non-locality in real band-gap metamaterials: determining parameters in the relaxed micromorphic model. *Proceedings of the Royal Society A: Mathematical, Physical and Engineering Sciences*, 472(2190):20160169, 2016.

[40] Angela Madeo, Manuel Collet, Marco Miniaci, Kévin Billon, Morvan Ouisse, and Patrizio Neff. Modeling phononic crystals via the weighted relaxed micromorphic model with free and gradient micro-inertia. *Journal of Elasticity*, pages 1–25, 2017.

[41] Angela Madeo, Patrizio Neff, Elias C. Aifantis, Gabriele Barbagallo, and Marco Valerio d'Agostino. On the role of micro-inertia in enriched continuum mechanics. *Proc. R. Soc. A*, 473(2198):20160722, 2017.

[42] Angela Madeo, Patrizio Neff, Marco Valerio d'Agostino, and Gabriele Barbagallo. Complete band gaps including non-local effects occur only in the relaxed micromorphic model. *Comptes Rendus Mécanique*, 344(11):784–796, 2016.

[43] Angela Madeo, Patrizio Neff, Ionel-Dumitrel Ghiba, Luca Placidi, and Giuseppe Rosi. Band gaps in the relaxed linear micromorphic continuum. *Zeitschrift für Angewandte Mathematik und Mechanik*, 95(9):880–887, 2014.

[44] Angela Madeo, Patrizio Neff, Ionel-Dumitrel Ghiba, Luca Placidi, and Giuseppe Rosi. Wave propagation in relaxed micromorphic continua: modeling metamaterials with frequency band-gaps. *Continuum Mechanics and Thermodynamics*, 27(4-5):551–570, 2015.

[45] Angela Madeo, Patrizio Neff, Ionel-Dumitrel Ghiba, and Giussepe Rosi. Reflection and transmission of elastic waves in non-local band-gap metamaterials: a comprehensive study via the relaxed micromorphic model. *Journal of the Mechanics and Physics of Solids*, 95:441–479, 2016.

[46] Jean Mandel. Plasticité classique et viscoplasticité. International Centre for Mechanical Sciences. Courses and Lectures, 1971.

[47] Jean-Claude Michel, Hervé Moulinec, and Pierre M. Suquet. Effective properties of composite materials with periodic microstructure: a computational approach. *Computer Methods in Applied Mechanics and Engineering*, 172(1-4):109–143, 1999.

[48] Raymond David Mindlin. Micro-structure in linear elasticity. *Archive for Rational Mechanics and Analysis*, 16(1):51–78, 1964.

[49] Patrizio Neff. On material constants for micromorphic continua. In *Trends in Applications of Mathematics to Mechanics, STAMM Proceedings, Seeheim*, pages 337–348. Shaker–Verlag, 2004.

[50] Patrizio Neff and Samuel Forest. A geometrically exact micromorphic model for elastic metallic foams accounting for affine microstructure. Modelling, existence of minimizers, identification of moduli and computational results. *Journal of Elasticity*, 87(2-3):239–276, 2007.

[51] Patrizio Neff, Ionel-Dumitrel Ghiba, Markus Lazar, and Angela Madeo. The relaxed linear micromorphic continuum: well-posedness of the static problem and relations to the gauge theory of dislocations. *The Quarterly Journal of Mechanics and Applied Mathematics*, 68(1):53–84, 2014.

[52] Patrizio Neff, Ionel-Dumitrel Ghiba, Angela Madeo, Luca Placidi, and Giuseppe Rosi. A unifying perspective: the relaxed linear micromorphic continuum. *Continuum Mechanics and Thermodynamics*, 26(5):639–681, 2014.

[53] Patrizio Neff, Angela Madeo, Gabriele Barbagallo, Marco Valerio d'Agostino, Rafael Abreu, and Ionel-Dumitrel Ghiba. Real wave propagation in the isotropic-relaxed micromorphic model. *Proceedings of the Royal Society A: Mathematical, Physical and Engineering Sciences*, 473(2197):20160790, 2017.

[54] Sia Nemat-Nasser and Ankit Srivastava. Overall dynamic constitutive relations of layered elastic composites. *Journal of the Mechanics and Physics of Solids*, 59(10):1953–1965, 2011.

[55] Sia Nemat-Nasser, John R. Willis, Ankit Srivastava, and Alireza V. Amirkhizi. Homogenization of periodic elastic composites and locally resonant sonic materials. *Physical Review B*, 83(10):104103, 2011.

[56] Marc Olive and Nicolas Auffray. Symmetry classes for even-order tensors. *Mathematics and Mechanics of Complex Systems*, 1(2):177–210, 2013.

[57] Marc Olive and Nicolas Auffray. Symmetry classes for odd-order tensors. *Zeitschrift für Angewandte Mathematik und Mechanik*, 94(5):421–447, 2014.

[58] Scott Pecullan, Leonid Gibiansky, and Salvatore Torquato. Scale effects on the elastic behavior of periodic and hierarchical two-dimensional composites. *Journal of the Mechanics and Physics of Solids*, 47(7):1509–1542, 1999.

[59] Kim Pham, Varvara G. Kouznetsova, and Marc G. D. Geers. Transient computational homogenization for heterogeneous materials under dynamic excitation. *Journal of the Mechanics and Physics of Solids*, 61(11):2125–2146, 2013.

[60] Luca Placidi, Giuseppe Rosi, Ivan Giorgio, and Angela Madeo. Reflection and transmission of plane waves at surfaces carrying material properties and embedded in second-gradient materials. *Mathematics and Mechanics of Solids*, 19(5):555–578, 2014.

[61] Giuseppe Rosi and Nicolas Auffray. Anisotropic and dispersive wave propagation within strain-gradient framework. *Wave Motion*, 63:120–134, 2016.

[62] Giuseppe Rosi, Luca Placidi, and Nicolas Auffray. On the validity range of strain-gradient elasticity: a mixed static-dynamic identification procedure. *arXiv preprint arXiv:1707.06801*, 2017.

[63] Jörg Schröder. A numerical two-scale homogenization scheme: the FE^2-method. In Jörg Schröder and Klaus Hackl, editors, *Plasticity and beyond: microstructures, crystal-plasticity and phase transitions*, volume 550, pages 1–64. Springer, 2014.

[64] Alessandro Spadoni, Massimo Ruzzene, Stefano Gonella, and Fabrizio Scarpa. Phononic properties of hexagonal chiral lattices. *Wave motion*, 46(7):435–450, 2009.

[65] Ashwin Sridhar, Varvara G. Kouznetsova, and Marc G. D. Geers. Homogenization of locally resonant acoustic metamaterials towards an emergent enriched continuum. *Computational Mechanics*, 57(3):423–435, 2016.

[66] Walter Steurer and Daniel Sutter-Widmer. Photonic and phononic quasicrystals. *Journal of Physics D: Applied Physics*, 40(13):229–247, 2007.

[67] Pierre M. Suquet. Local and global aspects in the mathematical theory of plasticity. *Plasticity today*, pages 279–309, 1985.

[68] Pierre M. Suquet. Effective properties of nonlinear composites. In *Continuum Micromechanics*, pages 197–264. Springer, 1997.

[69] Duy Khanh Trinh, Ralf Janicke, Nicolas Auffray, Stefan Diebels, and Samuel Forest. Evaluation of generalized continuum substitution models for heterogeneous materials. *International Journal for Multiscale Computational Engineering*, 10(6), 2012.

[70] A. Clifford Truesdell and Walter Noll. The Non-Linear Field Theories of Mechanics. In *The non-linear field theories of mechanics*, pages 1–579. Springer, 2004.

[71] Woldemar Voigt. *Lehrbuch der Krystallphysik:(mit Ausschluss der Krystalloptik)*. BG Teubner, 1910.

[72] Tarek I. Zohdi. Homogenization methods and multiscale modeling. *Encyclopedia of Computational Mechanics*, 2004.